POLITECNICO DI MILANO

Facoltà di Ingegneria Industriale

Corso di Laurea in
Ingegneria Aeronautica

The combustion of metallic nano-particles: Iron and Aluminum as possible candidates for metallic fuel in an internal combustion engine

Relatore: Prof. Aldo COGHE

Co-relatore: Prof. Santiago MOLINA

Tesi di Laurea di:

Giada MALANDRA Matr. 754706

Anno Accademico 2011 - 2012

Acknowledgement

First of all I would like to thank Professor Coghe for his help and support in developing this thesis, even if I drawn it up abroad.
Furthermore, I am grateful to all the staff of CMT for the months spent in Valencia; I would like to thank Professor Santiago Molina for giving me the possibility of working for COMETNANO project and also for allowing me to take part into the meeting with the other European partners.

Clearly, I would like to thank my family for supporting me during this years and for all the sacrifices done by my parents to give me the possibility of becoming the person I am today.

Finally, I want to thank all my friends: without you, life would not be the same!!

Index

List of figures

List of tables

Abstract

This work is focused on the combustion of metallic nano-particles under an air flow, with the aim of using them as potential fuels for Internal Combustion Engines (ICEs). This thesis is part of an European Project, called COMETNANO: it is an EU-funded, 3-years project, focusing on the evaluation of metallic nano-particles as fuel. It is an integrated approach studying the synthesis of metallic nano-particles, their controlled combustion under realistic conditions and the recycling of such spent fuels by renewable means.
In particular, this work is focused on the investigation of different kinds of nano-particles in a cylinder chamber, in order to test their behavior during combustion under engine conditions: the approach is both quantitative (measurements of pressure and luminous intensity) and qualitative and supported by a video-optical system. Following this, data resulting from tests are post-processed to obtain important information on the way in which these particles burn.

The nano-particles investigated are different in type and dimension:

- Iron: 25 – 50 – 70 - 85 nm
- Aluminum: 18 – 85 nm

The tests show that iron gives better opportunities to reach the aim of this project.

Moreover, in accordance with project aim, a study on NO_x emissions was carried out: a set of tests on iron and aluminum under different operating conditions was performed and the exhausted gas analyzed. The results clearly show that NO's concentration is the only one detected, although its value is very small.

Finally, it has been presented an investigation on regenerated nano-particles; in fact, one of COMETNANO main goal was the possibility to re-use burnt nano-powders after a regeneration process. Consequently, after the realization of a suitable method for their production, their combustion behavior was tested and compared with the original particles.

Key words: Cometnano, nano-particles, metallic fuel, internal combustion engine, NO_x emissions, regeneration.

Sommario

Questo lavoro di tesi si inserisce all'interno di un progetto europeo, noto con il nome di COMETNANO, incentrato sullo studio di differenti nano particelle metalliche, con l'obiettivo di poterle utilizzare come possibile combustibile per motori a combustione interna.
In particolare, lo studio qui riportato, è focalizzato sull'indagine sperimentale della combustione in aria di nano particelle di Alluminio e Ferro, al fine di verificarne le possibili idoneità come combustibili.
L'analisi realizzata prevede sia uno studio quantitativo dei dati di pressione e intensità luminosa raccolti durante la fase di combustione, sia un'analisi qualitativa tramite approccio ottico.

Questo progetto, della durata di tre anni, è stato suddiviso tra differenti istituti/centri di ricerca situati in quattro Paesi europei:

- CMT : Centro Motores Termicos – Università politecnica di Valencia
- APTL/CERTH: Aerosol and Particle Technology Laboratory (Grecia)
- AEIFOROS Metal Processing S.A. (Grecia)
- AMR: Advanced Materials Resources (U.K)
- IM/CNR: Istituto Motori (Italia)

Ciascuno di questi istituti ha focalizzato la propria attenzione su alcuni aspetti precisi: in particolare, molti dei mesi iniziali sono stati spesi nella scelta del tipo di metallo da utilizzare, per la mancanza di dati riguardanti le caratteristiche di combustione in aria.
Il progetto di tesi svolto, riguarda l'ultimo semestre dei tre anni di lavoro di COMETNANO e pertanto, si incentra soprattutto sull'analisi delle caratteristiche di combustione delle nano particelle selezionate nei mesi di studio precedenti: in particolare le indagini svolte han permesso di selezionare Alluminio e Ferro come i metalli maggiormente idonei per gli scopi previsti. Tuttavia, un ruolo fondamentale risulta essere svolto dal diametro delle nano particelle: pertanto si è scelto di realizzare l'analisi sperimentale prendendo in considerazione le seguenti tipologie di nano polveri:

- Alluminio: 18 – 85 nm
- Ferro: 25 – 50 – 70 – 85 nm.

I passi realizzati in questo studio riguardano innanzitutto prove di combustione eseguite tramite opportuno apparato sperimentale: tale strumentazione consta di un cilindro utilizzato come camera di combustione, dotato di due finestre ottiche per la realizzazione di un'analisi qualitativa della combustione attraverso filmato completo registrato da videocamera ad alta velocità. Il tutto è collegato alla bombola d'aria tramite due accessi: uno necessario per inserire l'aria direttamente all'interno della camera di combustione, e l'altro connesso al sistema di iniezione. All'interno della camera è presente un riscaldatore in grado di portare la temperatura fino a 800°C, la quale è controllata tramite due termocoppie.
Infine la linea sperimentale è fornita di un sensore di pressione per il sistema di iniezione, un piezo-resistivo per la pressione media e, in ultimo, un sensore piezoelettrico per la misura della pressione istantanea.
L'obiettivo dei test è quello di valutare l'andamento della pressione e dell'intensità luminosa: per quanto riguarda la pressione è sufficiente collegare gli appositi sensori ad un oscilloscopio, passando per un amplificatore di segnale. Invece, nel caso della luminosità, sono previsti due approcci: uno tramite utilizzo di un fotodiodo e l'altro attraverso videocamera Photron, in grado di riprodurre tramite tecnica ottica l'intera combustione.

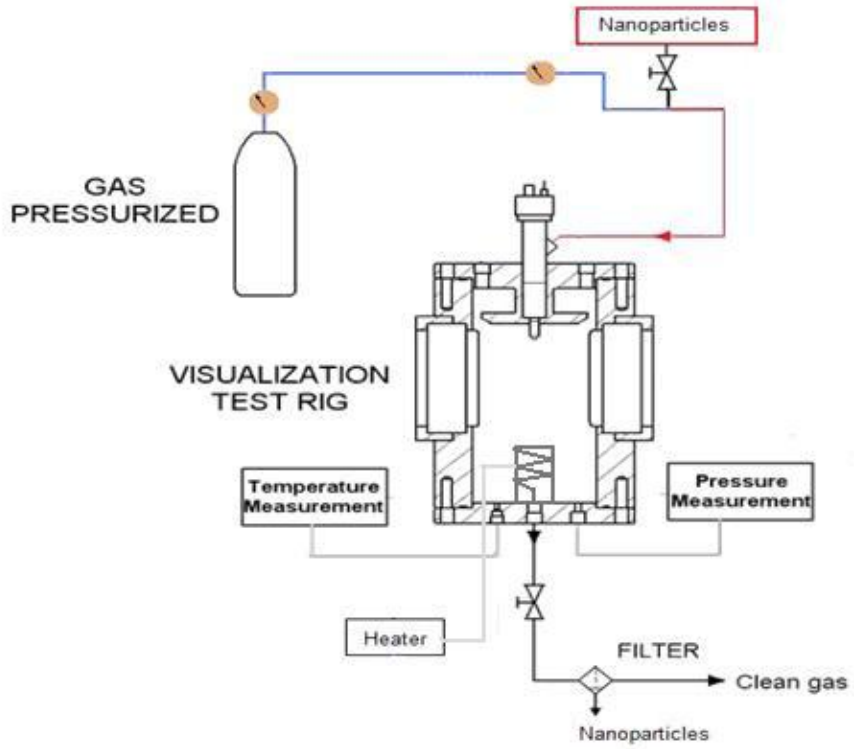

Come si evince dalla figura sopra riportata, il sistema di iniezione delle nano particelle è collegato alla bombola di gas pressurizzato e alla camera di combustione: è costituito da un serbatoio dove vengono inserite le polveri e collegato tramite una valvola di non ritorno all'ugello di iniezione in camera.

Per le prove di combustione viene seguita una procedura messa a punto con l'obiettivo di garantire che le condizioni operative siano sempre le medesime in ogni prova. In particolare il procedimento consiste nei seguenti passi:

1. Riempimento della camera di combustione con aria fino a raggiungere una pressione di 8 bar.
2. Innalzamento della temperatura interna fino a 200°C e mantenimento della stessa per almeno 10 minuti in modo da garantirne l'uniformità.
3. Aggiustamento della pressione a 10 bar tramite valvola.
4. Riscaldamento dell'aria interna alla camera a 700 °C.
5. Apertura del sistema di iniezione e inserimento manuale delle polveri.
6. Chiusura dell'interno sistema e posizionamento dell'elettrovalvola.
7. Spegnimento del riscaldatore e avvio del test tramite segnale di trigger.
8. Svuotamento della camera e attesa fino a che la temperatura non torna ad assestarsi intorno a valori di temperatura ambiente.

I test sono realizzati alle condizioni operative di:

- Pressione iniziale: 10 e 15 bar
- Temperatura finale: 700 e 750°C
- Quantità di nanopolveri: 30 mg.

I risultati, per quanto riguarda l'andamento della pressione, mostrano un ΔP rispetto ai test senza nano particelle maggiore per Al 85nm e per Ferro 70 nm a 10 bar; comportamento che trova riscontro anche nel caso di pressione iniziale pari a 15 bar. Anche le informazioni fornite dal fotodiodo mostrano una maggiore luminosità per le specie sopra citate.
Successivamente, a causa della rottura del sistema di iniezione, la sostituzione dello stesso ha richiesto una nuova esecuzione dei test: questa volta si è deciso di concentrarsi solo sulle polveri di ferro e anche in questo caso le nano particelle di 70 nm di diametro hanno mostrato le caratteristiche migliori. Da notare che le polveri da 70 nm utilizzate in questo progetto sono state appositamente prodotte da APTL e istituto NEO dopo aver messo a punto opportune procedure di sintesi: in particolare quelle prodotte da NEO han mostrato migliori caratteristiche di combustione. Per quanto concerne le polveri

commerciali (25 – 50 – 85 nm), le migliori sono risultate quelle con un diametro di 50 nm.

Come precedentemente riportato, oltre all'analisi quantitativa, è stata condotta anche un'indagine qualitativa con l'obiettivo di stabilire cosa accade all'interno del cilindro e in particolare come e dove la combustione ha luogo.
Per tale analisi si è utilizzata la tecnica ottica Schlieren, basata sul cambiamento dell'indice di rifrazione della luce a contatto con un corpo, e le cui informazioni vengono raccolte tramite videocamera photron. Tale approccio ha permesso di ottenere non solo il video completo della combustione ma anche, tramite analisi dei singoli frame, una mappa rappresentante la dislocazione della combustione all'interno del cilindro anche dal punto di vista temporale durante la durata del test.
I risultati ottenuti, per pressioni iniziali pari sia a 10 che 15 bar e temperatura a 700°C, mostrano una combustione più diffusa all'interno del cilindro per il ferro rispetto all'alluminio; in particolare, in accordo con i risultati precedentemente evidenziati, il ferro con dimensioni di 70 nm realizza una combustione non solo più diffusa ma anche più duratura nel tempo. Per quanto riguarda l'alluminio, i dati risultano piuttosto contrastanti a causa della stretta dipendenza delle proprietà di combustione di quest'ultimo dalle condizioni operative.
Terminata tale analisi e visti i risultati ottenuti, si è deciso di realizzare un'altra indagine riguardante lo studio delle emissioni di inquinanti e in particolare la valutazione delle quantità di NO emesse; si è scelto di valutare soltanto le polveri di ferro con 70 nm di diametro prodotte da NEO, ovvero quelle che han mostrato i risultati migliori durante l'analisi di pressione e luminosità. I test vengono svolti con la medesima procedura dei precedenti ma al termine, i gas prodotti vengono raccolti all'interno di un'apposita borsa collegata al filtro d'uscita. Tali gas sono stati poi analizzati tramite l'analizzatore di gas di scarico Horiba, il quale ha fornito un'indicazione della quantità di NO prodotta. Le basse quantità di polveri inserite durante la combustione hanno creato alcuni problemi durante l'analisi realizzata dalla strumentazione Horiba, tuttavia, in generale, i risultati si sono dimostrati in linea con le aspettative. In particolare, si nota che:

- all'aumentare della quantità di polveri inserite (30 – 50 – 70 mg), la produzione di NO aumenta
- a pari quantità di polveri inserite in camera di combustione, all'aumentare della temperatura di esercizio (700 – 750 °C) gli ossidi di azoto prodotti risultano maggiori
- l'utilizzo dell'alluminio favorisce la formazione di NO.

La parte terminale di questo lavoro si occupa di un altro degli obiettivi principali di COMETNANO, ovvero la possibilità di rigenerare gli ossidi prodotti durante la combustione allo scopo di riutilizzarli per successive combustioni. A tal proposito sia APTL che NEO hanno studiato e realizzato una procedura per la rigenerazione degli ossidi di ferro: la polvere così rigenerata è stata sottoposta a test di combustione con la medesima procedura riportata precedentemente. Quello che si evince dai risultati è che gli ossidi rigenerati mostrano buone capacità di combustione fino alla seconda rigenerazione: a partire dalla terza le caratteristiche decadono sensibilmente apportando sempre più un minore incremento di pressione. La motivazione può risiedere nel fatto che, a partire dalla terza rigenerazione, la struttura delle nano particelle si modifica a tal punto da non consentire più buone capacità di combustione, come confermato da analisi al microscopio. Un altro motivo può essere legato ad un'incompleta rigenerazione degli ossidi e quindi all'inserimento all'interno della camera di combustione di una quantità mista di polveri rigenerate e ossidi.
È quindi sicuramente necessario migliorare la procedura di rigenerazione al fine di valutare quali siano gli effettivi benefici apportati dalla rigenerazione e se, la messa a punto su grande scala di tale procedura sia realmente vantaggiosa.
Per quanto riguarda l'alluminio invece, è stata studiata una procedura per realizzare nano polveri a partire da particelle micrometriche: tale procedimento ha permesso la realizzazione di nanoAl altamente energetico che ha mostrato le migliori capacità di combustione, a confronto con le polveri commerciali indagate precedentemente.

A conclusione di questo lavoro, è quindi possibile evidenziare alcune considerazioni:

- l'alluminio presenta un maggior contenuto energetico che favorisce un maggior incremento di pressione; tuttavia la combustione avviene senza problemi solo con temperature superiori a 700 °C.
- il ferro risulta essere più affidabile come possibile combustibile metallico poiché non richiede particolari condizioni di temperatura o pressione per realizzare una combustione completa.
- Per quanto riguarda l'influenza del diametro delle particelle, tra quelle commerciali, 50 nm è la dimensione che favorisce le migliori prestazioni; tuttavia, le particelle con diametro di 70 nm prodotte sia da NEO che da APTL risultano essere quelle con attitudini migliori alla combustione.
- Per quanto riguarda le emissioni prodotte, l'unico dato rilevabile è la quantità di NO, che pur essendo minima, rispetta comunque l'andamento atteso dalla teoria: incremento di NO all'aumentare della temperatura e della quantità di polveri combuste.

- In accordo con la teoria, l'alluminio, che per bruciare necessita di temperature superiori, produce anche una quantità maggiore di NO.
- Infine, dallo studio degli ossidi rigenerati è emerso che, dopo la seconda rigenerazione, la struttura delle polveri si modifica a tal punto da non apportare più benefici alla combustione; altro motivo può risiedere nel fatto che la procedura di rigenerazione messa a punto, non garantisca che tutti gli ossidi siano effettivamente rigenerati, inficiando di conseguenza le successive combustioni.

Il progetto COMETNANO ha fornito sicuramente interessanti informazioni riguardo l'utilizzo di nano polveri metalliche come possibili combustibili per motori a combustione interna. In particolare è emerso che il ferro, pur disponendo di un quantitativo energetico minore rispetto all'alluminio, risulta comunque più affidabile e permette una combustione completa senza richiedere particolari condizioni operative.
Infine, resta da approfondire l'influenza del diametro sulla combustione, in particolare le differenze strutturali tra le polveri commerciali e quelle prodotte dalle procedure messe a punto da APTL e NEO.
Per concludere, nell'ottica di poter sostituire in futuro i comuni combustibili con quelli metallici, è assolutamente indispensabile approfondire l'aspetto della rigenerazione, per rendere gli ossidi combusti riutilizzabili per il maggior numero di volte possibile.

Parole chiave: Cometnano, nanoparticelle, combustibile metallico, motore a combustione interna, emissioni di NO_x, rigenerazione.

Chapter 1

Introduction

COMETNANO is an EU-funded, 3-year project focusing on the evaluation of metallic nano-particles as potential fuels for Internal Combustion Engines (ICEs).

The project provides different topics:

- The production of tailor-made fuel nano-particles with controllable regression rate
- The use of an environmental-friendly way for the recycling of burned residual particles, employing 100% renewable energy technology
- The introduction of required modifications, based on the existing mature technology of conventional ICEs, for the definition of the first metal-fuelled ICE
- The investigation of any potential environmental and health dangers of the new technology and the design of abatement measures.

These fields of investigation are divided between four different Nations cooperating to reach the aim of this project. In particular, there are:

- CMT – Motores Termicos , Universidad Politecnica of Valencia
- APTL/CERTH: Aerosol and Particle Technology Laboratory (Greece)
- AEIFOROS Metal Processing S.A. (Greece)
- AMR: Advanced Materials Resources (U.K)
- IM/CNR: Istituto Motori (Italy)

Each partner is principally focused on one topic, linked to each others; the activities are divided into 36 months, that is the project overall duration.

1.1 A brief explanation

This thesis concerns the last year of the project and its attention is concentrated, in particular, on the combustion behavior's evaluation for different nano-particles under ICE conditions and the measurement of emissions delivered during the combustion process; following, combustion analysis are concentrated on the use of regenerated nano-powders, produced by the method obtained during the previous years of this project.

The use of nano-particles as fuel is not so simply for several reasons. First of all, their ignition is difficult; however, after ignition, combustion process goes on in an uncontrollable way, developing very high temperatures and making the whole process unsuitable for ICE applications. Indeed, the recent studies on nano-powders manufacturing, show that increased reactivity and controllability of powder in the nano-scale regime, is ascribed to their substantially high surface area.
The project started with the choice of suitable metals: this activity went on more than six months and is based on the knowledge of metal properties and characteristics. In particular the attention is focused on the energy released by metals during combustion, but also on their cost and availability.
In fact, limited reserves of liquid fossil fuel, air pollution and increased atmospheric carbon dioxide level delivered by burning fossil fuels are the main drivers for finding alternative energy carriers and energy transfer systems for transportation. The clusters of metallic nano-particles should be a heat source to propel vehicles: with the fuel tank of the same size, a vehicle feeded with iron as fuel will cover a distance two times greater than the one covered by a car with gasoline and aluminum three times greater.
It is possible to make a comparison between iron and Hydrogen or a conventional liquid hydrocarbon as source of energy: first of all, metallic fuel shows greater energy capacity per volumetric unit, lower predisposition to form explosive fuel/air mixture and doesn't require any special storage conditions. In addition, iron nano-particles should be stored and transported at ambient temperatures and pressures, further more there is the possibility of regenerating burnt nano-particles with the aim to use them again in a new combustion process: in this way, there is no production of waste material.

Despite of the abovementioned advantages, metallic fuels present also disadvantages:

- Iron energy content per unit weight is approximately one fifth of that of hydrocarbon fuels, even if the weight is less than most proposed hydrogen storage systems of comparable energy content

- Outside the high-temperature zone of combustion, the metal oxide condenses and solidifies, forming solid agglomerations that are deposited on the walls of a combustion chamber and other parts of the engine.
- Metal combustion high temperature contributes to the formation of NO_x, increasing atmospheric pollution.

1.2 Aim of this work

As regards what abovementioned about nano-particles, the aim of this work, realized at UPV between the 1st of October and the 1st of April, is to test the use of chosen metals as engine's fuel. The nano-particles investigated are different to understand which present the best attitudes for the finality of the project. Tests have been carried out in different conditions and the results show important information about combustion's behavior and main properties, like pressure, luminosity and temperature. The approach is both quantitative, with pressure and luminosity analysis, and qualitative, with the help of a video-optical system.
An important aspect that is also necessary to determine, is the evaluation of NO_x emissions: in fact, the use of metallic fuels as a new source of energy is not positive if the combustion process releases a huge quantity of pollutants. To carry out this investigation, other tests have been carried out using the same procedure of the previous ones but, at the end, exhausted gas are collected and analyzed by suitable devices.
Finally, the last part of this project, is focused on regenerated nano-particles: as regards Iron, the available particles have been regenerated from one to six times; on the contrary, as concerns Aluminum, only one time. The aim is to evaluate their combustion behavior under the same operating conditions using for original nano-powders; the most important information is the pressure increment, as it represents powders energy content.

1.3 Plan of presentation

This thesis is articulated in the following chapters:

- Chapter 2: it is presented a general description of COMETNANO project; in particular, the steps made in the previous years are explained.
- Chapter 3: this chapter is focused on main properties and behavior of different metals, with reference to their main characteristic.

- Chapter 4: in this chapter there is an explanation of tests rig used for the experiments and the description of the procedure for their realization.
- Chapter 5: The results of combustion tests in terms of pressure and luminosity are reported; there is also the comparison between different kinds of nano-powders.
- Chapter 6: In the first part there is a brief explanation regarding NO_x emissions; the second part shows the results of tests carried out in different operating conditions.
- Chapter 7: This chapter is focused on optical technique: after a brief explanation about their main properties and uses, the results showing the characteristic of nano-powders combustion are pointed out.
- Chapter 8 : In this chapter, the topic is the regeneration of burnt nano-particles: following an introduction about methods to regenerate these nano-particles, it is possible to find the results concerning pressure increment obtained from tests carried out; furthermore, it will be stressed the comparison between these results and those obtained with combustion of original powders.
- Chapter 9: this chapter includes the conclusions of the work and, in additions, a mention to some future developments.

Chapter 2

General description of the project

COMETNANO Project is the first one that investigates the opportunity to use metallic powders as fuel for internal combustion engine; for this reason there are not many studies that should be used as a point of reference. Moreover, the results obtained during this project are important but they are only a first step in order to achieve the required aim.

In particular, this project specific target is to systematically investigate the feasibility and propose ways of employing metallic nano-particles as potential replacement of traditional fuel for internal combustion engine. The importance of nano-powders use is that they produce more energy than conventional fuel and, at the same time, they don't produce pollution if the temperature of combustion is not so high; in fact the only combustion products are metal oxides, having the peculiarity of being re-used for a second combustion.

In fact, one of the aim of this project is to find a way to recycle metal oxides: in that case, in a possible future application, they will be retained in the vehicle and their weight doesn't decrease as happens when petrol is used: it's not necessary, or is enough to add a small quantity of new metal in the cycle.

Another important point is to consider the required modifications of a conventional engine to perform the injection of the nano-particles and the filter's system to collect the products of combustion; in particular, the idea for the collector/filter consists in a tank with two compartments, separated by a movable separator: metal fuel and metal oxides need to be stored into separate chambers. During combustion, the quantity of nano-fuel decreases and the amount of oxides increases accordingly; so the movable separator provides the necessary space for burned particles.

2.1 A brief chronology

The project has a total duration of three years and this thesis work covers only the last six months: this means that a lot of steps have been done during the previous years. The following pages will show a brief explanation of the steps reached in the first two years by Cometnano's partners.

2.1.1 First semester

In the first six months, each institute starts a series of activities.
First of all, attention was focused on the choice of metals: a lot of studies and researches in literature were done in order to find data about combustion in a cylinder chamber, focusing on the heat change between powder and ambient air, and in the kinetic and diffusive process.
At the same time, a CFD simulation of injection system is started, as the test rig for the *shock tube tests* is prepared for the future experiments.
A lot of time was spent searching and studying possible techniques for the production of iron nano-particles: a lot of lab-scale experiments were carried out in order to determine parameters leading on their synthesis process. The goal was determined at approximately 50 nm, and initially, had been used aqueous solutions of iron nitrate; as it is possible to see in the following image, the particles present a hollow structure, with an external dense layer of 2-4 nm of thickness.

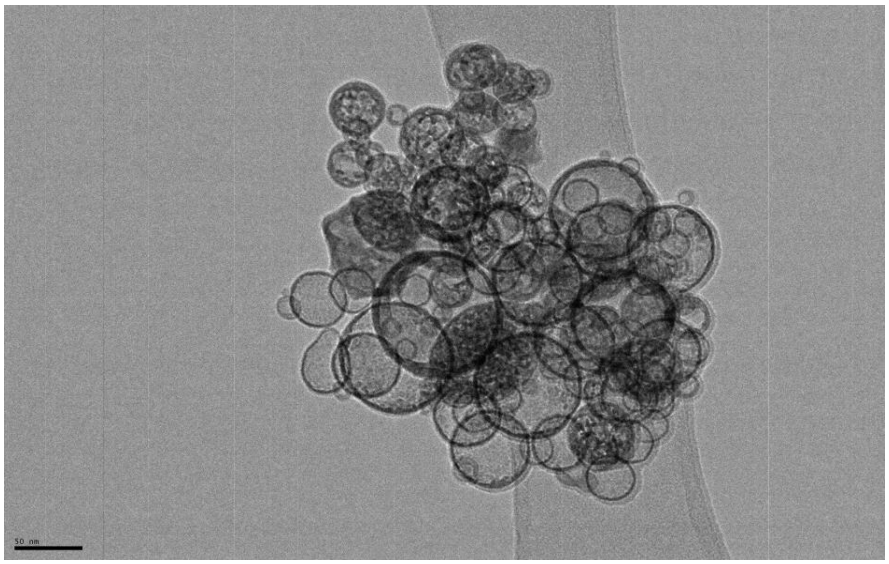

Figure 1: TEM image of the ASP- synthesized iron oxide [1]

Moreover, attention was focused on the determination of the appropriate conditions for the reduction of commercial oxide nano-powders to iron nano-particles, via exposure to a hydrogen atmosphere. For this reason, a procedure was proposed and tested, as follow:

- A fixed bed of iron oxide nano-powder
- Pure Hydrogen atmosphere for reduction process
- Exposition of the bed to a 2% O_2/N_2 mixture for a period of 3-5 minutes to achieve iron passivation
- Bed's cooling under helium flow

The reduction process was tested under a variable temperature between 600 and 700º C and a range of time between 10 min and 4 hours: just the maximum time of 4 hours allows a complete reduction of Fe_2O_3 into iron.
Finally, some combustion tests were performed: they had been carried out in a close furnace with atmospheric air. An amount of 0.5-1.5 g of Fe and Al was put in and ignition started with a spark; conditions were not real but it's a good initial step to understand the behavior of nano-particles. In particular, these tests pointed out that a reduction of the diameter favored a higher extension of oxidation. Aluminum tests showed that this metal reacts with O_2 but also with N_2 creating AlN: to avoid it, it's necessary to reach a temperature higher than 2517 ºC.

2.1.2 Second semester

During the following months, the attention was focused on the combustion of nano-powders. In particular, some important considerations should be made:

1. Data showed that, depending on boiling and volatilization temperatures of the chosen metal, the combustion can go on in a solid state from the particle surface toward the inner core or in the vapor phase in a thin layer around the particle surface. The second case would make the utilization of metal powders in the engine not feasible [11];
2. In the case of solid state process (nano-scale regime), the comparison between the mass transport and chemical time scales define the regime of combustion mode that can be respectively diffusive or kinetically controlled. The predominance of one with respect to the other defines the combustion start and, in particular, the combustion rate and its duration. These characteristics are fundamental for using metal powder during the engine cycle and depending on different factors: one of the main defining parameters is the primary particle size [11].

A lot of time was spent studying a possible injection system with a CFD simulation. There are three possibilities:

1. IDI: conventional Diesel indirect injection injector, with an intermitten injection; this solution doesn't allow a time control and the use of nano-particles can block injection
2. IDI but without needle: in this case it works good but the continuous flux is not acceptable
3. GDI: Gasoline Direct Injection injector, that permits injection time control with an external electronic device generator.

The last solution seems to be the best one for this project; for this reason it has been designed a pneumatic injection system, as showed in the following image:

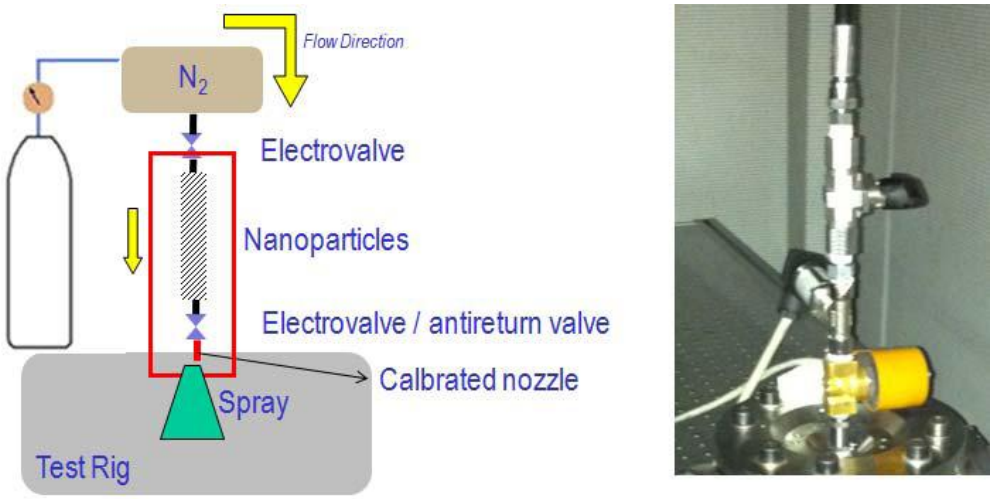

Figure 2: A scheme (left) and an image (right) of injection system [1]

A weighted mass of nano-powder is set in a small reservoir, isolated from the remaining circuit by two valves. Upstream of powder reservoir, a high pressure volume of driver gas (either N_2 or air) is set at the required pressure, so that when the valve is open, the gas flows down and sweeps the powder towards the injection vessel.

A second valve, downstream of powder reservoir, is necessary to avoid that the pressurized hot gas (air) in the vessel flow up and oxidize the metal particulates before injection. Hence, to start injection, both the valves should be open nearly simultaneously. The particles will be injected into the vessel throw a calibrated nozzle. Since both the effective injection duration and the quantity of powder effectively injected will depend on the different volumes and pressures in the circuit, simulation efforts have focused on the determination of these magnitudes for satisfactorily controlled injections.

A series of CFD studies were completed showing the connection between injection time and both injection pressure and nozzle diameter.

In order to characterize the nano-particles combustion's behavior, Istituto Motori started a series of *Shock tube tests*: the aim of these test is to characterize how metallic particles burn in terms of temperature and thermal emission signals. Nano-powders investigated are Iron 25 – 50 – 70 nm, Aluminum 18 – 50 nm and Boron 60 nm, under synthetic air at 10 bar and with a temperature in a range of 700 – 1300 K: in particular, in the following image it is possible to see pressure and temperature conditions used in each kind of test.

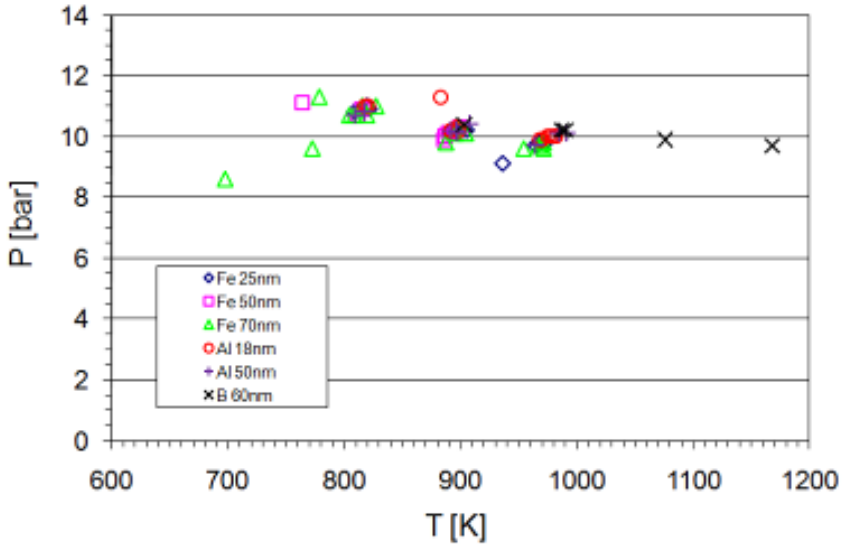

Figure 3: Operating condition for the shock tube tests

These nano-particles are injected with pneumatic system, burnt inside the long tube and finally collected in a TEM grid at approximately the end of the tube; the combustion is investigated with an optical diagnostics, based on two-colour pyrometry and the ratio of thermal emission signals at two wavelengths allows the estimation of particles temperature.

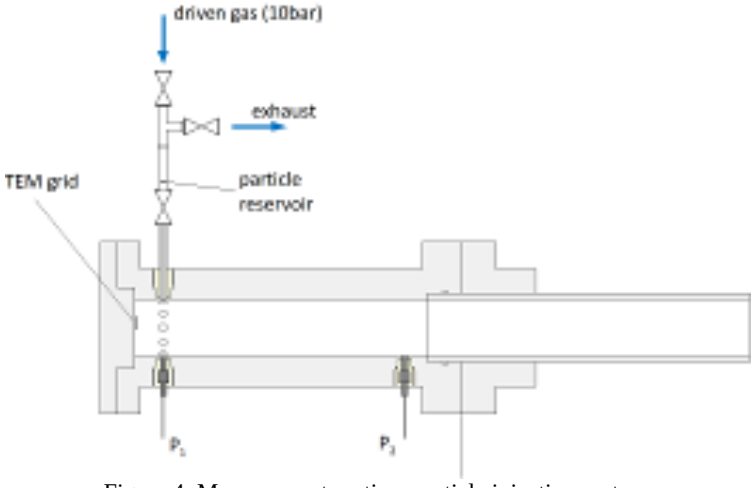

Figure 4: Measurement section particle injection system

The following images, that are an example of the abovementioned results, point out some important information about combustion behavior: figures show the two signals at two different wavelengths and, as explained in the abovementioned lines, the measurement of these signals gives the information about temperature. The right axis reports the temperature scale.

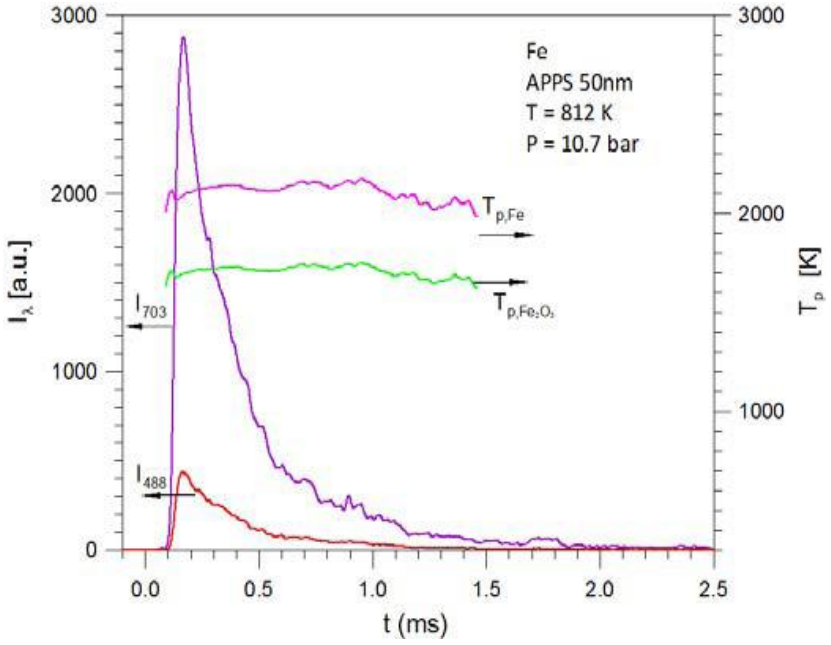

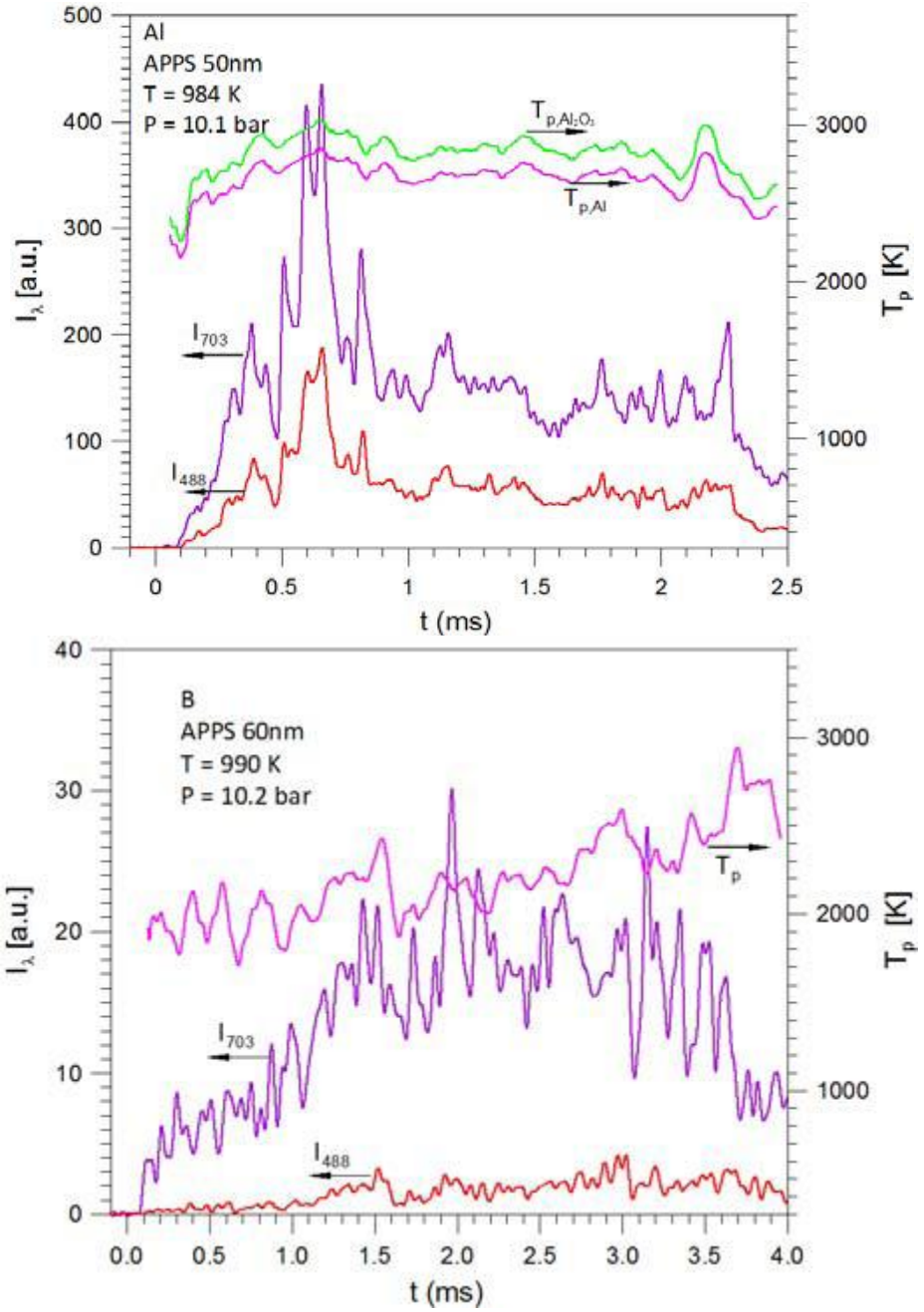

Figure 5: Thermal emission signals and temperature during "burning" nanoparticles

In particular, these results show that Iron burns very quickly in different conditions, as it could be seen for the peak of wavelength signals and the maximum temperature doesn't exceed 2000 K. On the contrary, Aluminum reaction is slower and temperature can reach 2600 K; Boron has a very similar behavior to Aluminum, but the maximum temperature is around 2000 K. The following table summarizes these considerations:

Metal	APPS [nm]	Tmax [K]	Combustion time [ms]
Fe	25	1500-1800	0.5 - 0.7
Fe	50	2000	1
Fe	70	2000	1
Al	18	2000-2200	>2.5
Al	50	2500-2600	>2.5
B	60	2000	> 2.5

Table 1: Shock-tube test matrix with estimated maximum combustion temperatures and combustion durations

At the same time the UPV has started to study the experimental line project, holding the results about shock tube. It's important to take into consideration two fundamental requirements:

1. the combustion chamber has to be provided with wide optical access to allow visualization and application of different optical techniques
2. it must allow heat release analysis to be performed on the basis of the pressure signal in combustion.

The best solution consisted on the installation of an internal coil heater, MHI GA-XP, with a resistance allowing to reach a temperature up to 1300 ºC. Insulation is needed to avoid heat losses through walls and keep the vessel cold, but it has to fulfill different requirements: low density and low thermal conductivity to reach a rapid heating, rigidity and non-porosity in order to measure pressure increase. The best solution seems to be the use of a refractory mortar (Greenlite 45L) as insulation material.

Finally, regarding the preparation of nano-powders, APTL studied how to obtain iron using *calamina* and the regeneration of the metal oxides (this part will be investigated in the following chapter).

2.1.3 Third semester

In these months APTL continues the studies about production of nano-powders: in particular it focuses its attention on ASP technique for Iron production and APS methods for AL and B production. Moreover, it studied the way to reduce Fe_2O_3 into iron nano-particles, using a H_2 atmosphere. At the end of these studies, they got some important conclusions:

1. Production of Fe nano-particles was demonstrated to be feasible through 3 different routes:
   a) Utilization of ASP method, using nitrogen as carrier gas and a 50/50 vol. water/ethanol mixture in which iron nitrate is dissolved within a concentration range of $2 \cdot 10^{-2}$-$5 \cdot 10^{-2}$M.

b) Utilization of ASP method, using air as carrier gas and an aqueous solution of iron nitrate within the same concentration range as shown at the abovementioned a). The iron oxide nano-particles are subsequently exposed to a hydrogen stream in order to obtain a Fe nano-powder of c.a. 85nm (APPS).
c) Utilization of nano-structured (uncalcined) powder obtained by calamina-slag purification method developed by NEO and exposure to a hydrogen stream in order to obtain a Fe nano-powder of c.a. 60nm (APPS).

2. About production of Al nano-particles, main tests with a coarse micron-sized Al powder revealed that Atmospheric Plasma Spraying (APS) technique is able to yield Al-based nano-powders with an APPS of c.a. 20nm.
3. Production of Boron nano-particles was found not to be feasible by neither conventional ASP conditions nor the APS technique employed.

At the same time, in order to know more about combustion of metallic powders, it was carried out a series of tests; with *spark-ignited combustion experiments* it is possible to see that the ignition of micro-powders is not available under under the following conditions: the powders were placed in a scaffold under an air flow and ignited with the aid of a tungsten wire, which was in contact with the powder and connected to two electrodes. This ignition led to the occurrence of a self-sustained oxidation reaction, with its front propagating from the ignition point towards the whole powder mass. These tests pointed out that, despite the negative effect of diameter increase on the oxidation's extension in case of commercial powders, Iron nano-particles 85 nm produced by Neo showed better oxidation characteristics.
In addition to the aforementioned tests, it has been carried out a series of 6 combustion-reduction cycles for the 50nm Fe and the 'inhouse' 85nm Fe nano-powders. After each combustion test, powders were regenerated by exposure to H_2 to retain their metallic form. These tests evidenced that for the first 2 combustion-regeneration cycles, the oxidation characteristics of the powders showed no significant change. From the 3rd cycle on, Fe showed a 'degradation effect'. In particular, after the 2nd cycle the regenerated samples gradually less oxidized during their exposure to 'spark-ignition' conditions.
Secondly, analysis of all regenerated samples showed that after the 2nd cycle their oxidation curves gradually shifted to higher temperatures. In conclusion, it is important to note that the employed 'spark-ignition-like' combustion process significantly affects Fe nano-structuring after 3 repeated combustion-regeneration cycles.

At Istituto Motori, at the same time of shock-tube tests, a real engine was set up in order to prove the combustion of nano-powder under real engine condition. It is a low-cost and commercial Lombardini engine, with the follow properties:

Engine	Single-cylinder Lombardini SP 15 LD 350
Displacement	350 cc
Bore/Stroke/Conrod length	82/66/110 mm
Compression ratio	20.3

Table 2: Lombardini engine characteristics

This engine could give information about temperature and pressure through the installed sensors, and tests have been performed using a simpler powder feeding arrangement, consisting of an on/off valve placed right before the intake valve of the engine. Even though the mass of powder injected in the engine was known, it was impossible to estimate the actual metal quantity inspired and trapped in the cylinder for the combustion; moreover, the injected quantity inside the intake duct had to be much higher than the stoichiometric value for the given intake air flow conditions, in order to ensure proper combustion. Results obtained showed that Iron powder combustion had a behavior comparable to conventional diesel fuels, while the released energy seemed proportional to the injected mass. Calculations of heat release rate (HRR) indicated that combustion started early in the compression stroke and was composed by two distinct phases: an initial phase of very fast combustion with rapid HRR, apparently kinetically controlled, and a later phase of slower combustion. Additional analysis of these results showed that combustion starts at about 550K.
The same tests were carried out with Aluminum and suggested very similar behavior, even if combustion started later than iron and apparently presented only a single phase.
At the same time, regarding tests on real engine, the attention was focused on the project and manufacturing of a suitable continuous powder feeding system for integration with Lombardini engine intake system.

2.1.4 Fourth semester

As concerns shock–tube tests, experiments went on and a finally optical system was realized as it is possible to see in the following image:

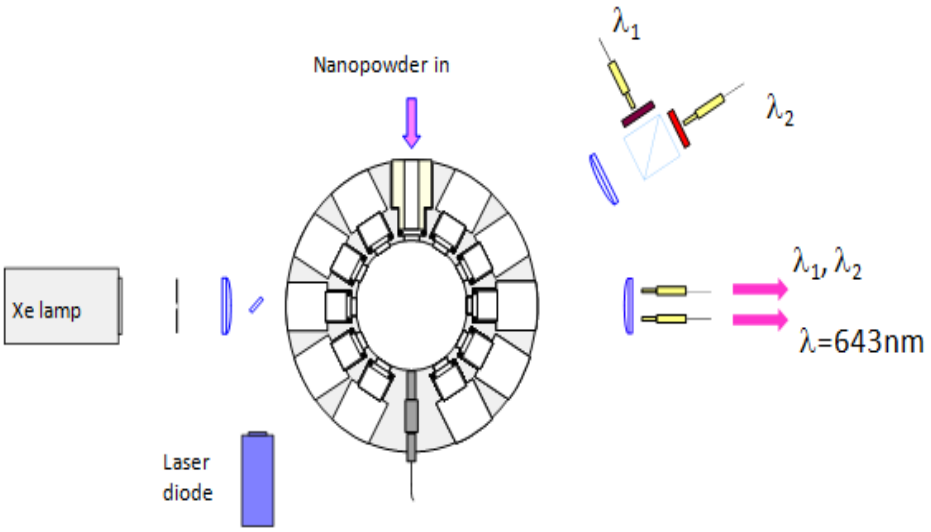

Figure 6: Measurement section: optical diagnostic set up [10]

This arrangement has the aim to consider combustion temperature studying thermal radiation signals emitted by a particle with a diameter d_p. In the following chapter there is an accurate explanation of the law leading to this process.

Extensive tests were carried out on iron nano-powders prepared by APTL (85 nm) and on iron nano-particles obtained from direct reduction with H_2 of purified calamine-slag. In this series of tests, the thermal radiation signals of reacting particles have been measured with the aid of photomultipliers at the wavelength values of λ_1=800nm and λ_2=600nm. These results confirm previous findings, showing a two-stages oxidation process: the reaction starts immediately after the onset of the experimental conditions, as evidenced by a pronounced increase of thermal emission signals.

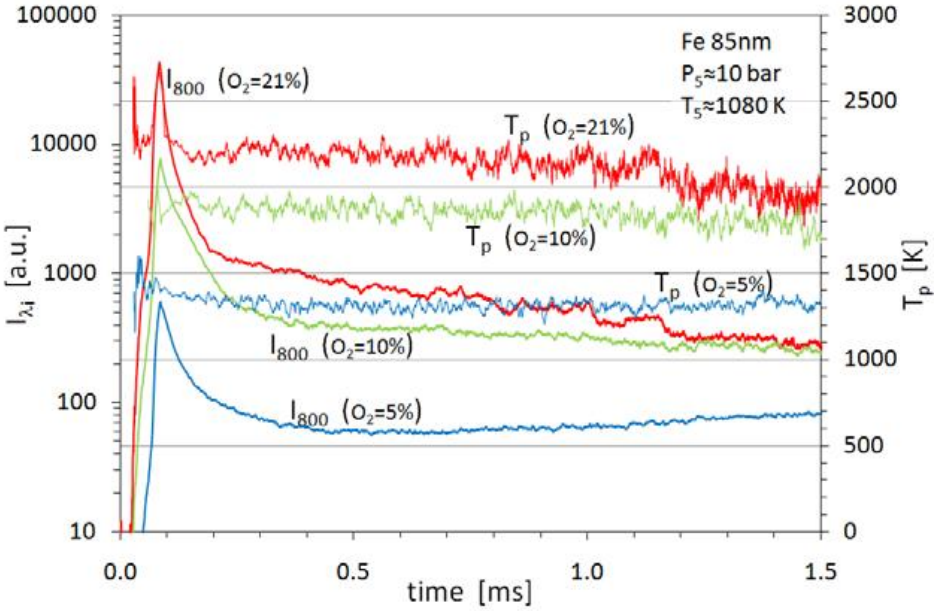

Figure 7: Thermal emission signals at 800 nm and temperatures of Iron nanoparticles (Fe85 nm) for different O_2-N_2 atmospheres at 1080 K and 10 bar [1]

As the reaction goes on, the thermal emission signal rapidly decreases while the particle temperature slowly diminishes. Results clearly show the feasibility to "control" the combustion of iron nano-powders modifying oxygen concentration.

Regarding tests on the real engine, the problem is the inability to estimate the real quantity of powders trupped and burned in the cylinder. Therefore, additional configurations were studied to improve this situation: in particular, two layouts were identified and both of them were based on the employment of a fast solenoid actuation valve, a powder reservoir and a check valve to shut the feeding line when the injection is stopped.

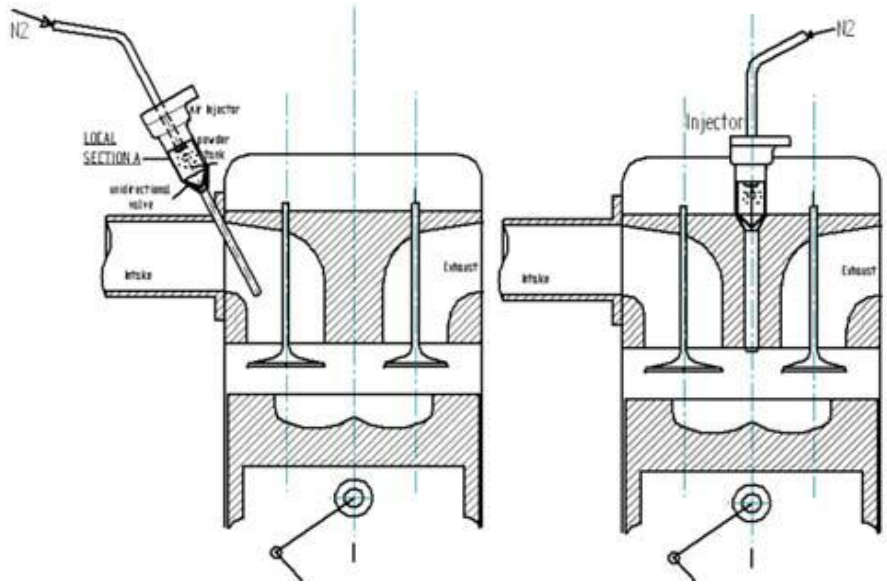

Figure 8: Scheme of the injection configurations for the control of metal powder mass trapped in the cylinder[1]

Although there have been made several attempts they pointed out that it was not possible to perform a synchronized injection in the intake duct or an in-cylinder direct injection, most probably because of the design and operation of the traditional check valve used to isolate the low-pressure delivering feeding line from the cylinder, after the end of injection phase.

The aims of this latest set of tests were to measure the temperature of the particles during combustion and it was found that particle combustion temperatures ranged from 1900 to 2200 K for iron and 2500 to 2700 K for Al. Moreover, as suggested from the thermodynamic analysis of the first series of experiments, aluminum particles exceeded the melting temperature, while iron particles appeared to burn in the solid state.

At the same time, at UPV, the experimental line was terminated and a series of tests were performed in order to define the operation procedure, that will be explained in the appropriate chapter. The first tests showed the influence of oxygen concentration in chamber atmosphere

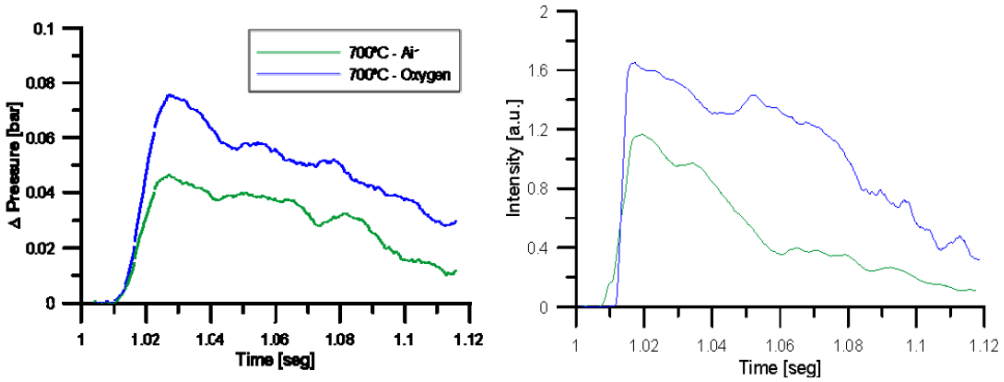

Figure 9: Pressure increase and radiation intensity for 30 mg of Fe85 at 700°C[1]

As can be seen, iron combustion was enhanced to the higher content of oxygen leading to higher pressure increase; due to this fact, the percentage of burned particles apparently increased by increasing the oxygen concentration. Similar trends were also observed in case of aluminum.
Finally, due to the fact that, despite the high number of relevant projects, there are virtually no data available with respect to iron/iron oxide nano-particles health implications, APTL decided to perform some basic, simplified experimental campaigns with the aim of acquiring a general idea about potential health impact of such materials.

In the last year, all the topics described have been developed and new steps undertaken. In particular the activities carried out during my Erasmus period in Valencia will be explained in the following chapters.

Chapter 3

Nano-particles

In this chapter, there is a brief presentation about the nano-particles and their properties. In particular, the attention is focused on the particles that will be used in this project.

3.1 Properties

The first six months of the project were spent in order to choose which metal should be the best fuel. The most suitable metallic fuel should follow some specifications, like:

- energy released during the combustion of this metal should be high enough so that the quantities required are lower or comparable to the respective ones for conventional fuels;
- There should be one or more sources of it that are abundant in nature, meaning that it can be produced in large quantities. Such availability also ensures the reasonable cost of such sources;
- The metal should not be toxic;
- The metal should be easy to ignite, while spontaneous ignition should be avoided;
- The processes involved for the extraction of the metal, its formulation to suitable nano-particles and the subsequent regeneration of the combusted fuel (i.e. metal oxide) should be scalable to an industrial level.

The choice is restricted between three candidate metals: Iron, Boron and Aluminum.

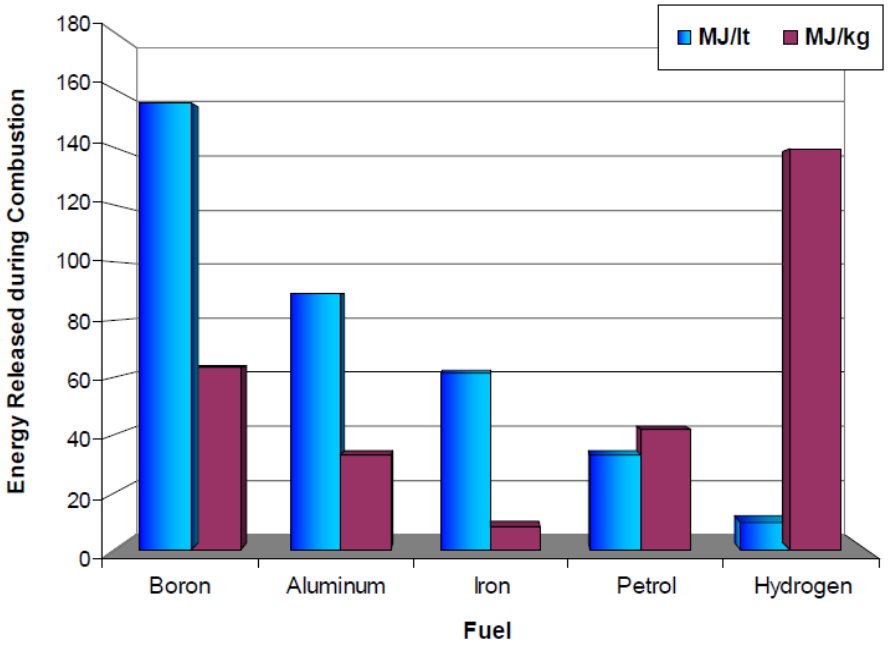

Figure 10: Energy released during the combustion of the 3 metals considered as candidate fuels [1].

As can be seen in the diagram above, showing the energy content of metals, Boron presents the highest volumetric energy density in comparison with other metals and normal fuel. At the same time, Iron is the most naturally available and it is also a low-cost metal, even if its volumetric energy density is lower than Boron and Aluminum. At the end, Aluminum is a compromise between the others two.
Regarding comparison between metals and normal fuel like petrol, even if the energy content of Iron and Aluminum in terms of weight is lower than that of petrol, as regards volumetric energy, the quantity is higher and this is an advantage for engine volume reduction.

Metal	Estimated worldwide reserves [ktons]	Indicative price [$/mton]
Iron	$1.1 \cdot 10^9$	200-300
Aluminum	$6.0 \cdot 10^6$	1600-2000
Boron	$8.8 \cdot 10^5$	N/A

Table 3: Overview of estimated worldwide reserves of the three candidate metallic fuels

For these reasons, finding a compromise between energy, cost and availability, Iron and Aluminum have been chosen as optimal candidates for this project.
The field of investigation involves metal nano-particles with variable diameter, as follow:

- Iron: 25, 50, 85 nm

- Aluminum: 18, 85 nm.

At the end of these tests based on commercial metals, other kind of Iron particles are used:

- Iron 70 produced by NEO
- Iron 70, produced by APTL

The diameter of these particles [17] is a very important parameter in metal fuel, for different reasons:

- If the particle is too fine, the rate of heat production during combustion will be enormous and the engine will be unable to use it properly
- If it is too big, the ignition requires very high temperature and this can damage mechanical components of the engine and/or causes oxide deposition inside the cylinder, inducing engine clogging.

The two metals show different behaviors and each particle dimension has its properties; the importance is that all of them have nano-dimensions.
Furthermore, the different diameter has a peculiar effect on combustion: it is possible to note almost the same behavior for particles having same dimension, even if the operating conditions change.

3.2 Mechanism of combustion

The most important problem, that should be investigated and solved, is the control of metallic fuel combustion process. Some studies [2] conducted using metallic fuels composed of iron nano-particles passivated by an oxide layers, show important results and information about the combustion process. In particular, the attention was focused on the time of combustion and the relationship between this and particle properties.
A group of researchers studied iron nano-particles obtained commercially from Reade Corporation. The structural studies of the iron, before and after combustion, were obtained with TEM, transmission electron microscopy, and XRD, x-ray diffraction. On the contrary, an infrared temperature measurement system was used to register peak combustion temperatures. The tests showed that materials were not spontaneously flammable in air, but were readily ignited when the temperatures exceeded 250 °C. In addition, the authors found the presence of Fe_2O_3 in the combusted particles, and this oxidation was connected with temperatures. The combustion of the clusters went on rapidly, about 0.5 s, and generated a peak temperatures around 1000 K, without observable production of any volatile products.

To understand the combustion of a single iron nano-particle, it is possible to develop the following model of combustion [2], based on kinetic equation for the heat balance:

$$\rho_m Q \frac{d}{dt} V_m = S_m\left[\left(T_b^4 - T_a^4\right)\sigma\varepsilon f + (T_b - T_a)h_c\right] \qquad (1)$$

Where ρ_m is the specific density of iron; Q is the heat of combustion; V_m is the volume of the nanoparticle; S_m is the nanoparticle surface area; T_b is the combustion temperature; T_a is the air temperature; σ is Boltzmann's constant; ε is the emissivity; f is a geometric factor determined by the shape of the cluster (pellet or sphere); and h_c is a convective heat transfer coefficient.

Holding S_m constant and integrating the equation for the combustion time of a single particle, it is possible to obtain the following formula:

$$t = \frac{\rho_m Q r^{1}/_{3}}{\left[\left(T_b^4 - T_a^4\right)\sigma\varepsilon f + (T_b - T_a)h_c\right]} \qquad (2)$$

Where r is the nano-particle radius.
Results obtained from equation (2), lead to the same conclusions concerning the combustion time like considering chemical kinetics, where the kinetic equation for the reaction assumes the form:

$$\rho_m \frac{d}{dt} V_m = S_m K C_{O_2}^{(2/3)} \qquad (3)$$

Where K is the effective rate of reaction and C_{O2} is the mole concentration of oxygen in air. Applying the ideal gas equation to determine C_{O2} and the Arrhenius formula to K and integrating the chemical kinetic equation, it is obtained the combustion time for a single particle:

$$t = \frac{0.825\rho_m r (RT_a)^{0.66} e^{\left(E_a/RT_b\right)}}{P_a^{0.66} T_b A^n} \qquad (4)$$

Making a comparison between (2) and (4), the following important conclusions can be made:

- Direct dependence on the radius of a nano-particle
- Higher combustion temperatures and air pressure allow shorter combustion times
- Higher air temperatures cause longer *t*

However, considering a temperature around 1000 K and using equation (2), a combustion time on the order of 10^{-3} is obtained: this short time means that would be unsuitable for most applications, but the possibility to form the nano-particles into clusters allows a way to control combustion.
The process of clusters is not so easy but we have to make some considerations:

- The effective surface for oxidation of a clusters is much higher than for a solid body of the same size and shape, so it is expected that the oxidation rate may be several orders of magnitude higher
- The oxidation rate of the particles that are inside the clusters depends on the rate of air flow inside
- The heat released during combustion goes on from inside to the surface of the clusters and after to the environmental by radiative and convective heat transfer.

The formation of the oxide layer implies that oxidation process will be governed by the diffusion of the reactants through the oxide layer and will not involve gas phase oxidation as that of a micron sized particle. However, if the gas temperature is sufficiently high, then metal evaporation will lead to vapor phase combustion. Therefore, as reported by *Rai et al.*[3] oxidation can thus proceed in two distinct regimes: at temperatures below the melting point of the metal, oxidation goes on thanks to the diffusion of O_2 through the oxide shell, and it is the slow oxidation regime observed in conventional thermal techniques with longer residence time. If the oxidation temperature is above the melting point of the metal, it is the fast oxidation regime, and in this regime the oxidation will proceed through the melting of the metal, the rupture and thinning of oxide shell and diffusion of both metal and O_2. The following figure shows the case-scheme for an aluminum particle.

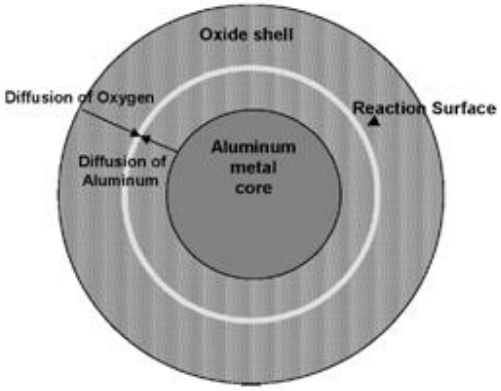

Figure 11: Schematic of an oxide-coated aluminum particle showing the metal core, oxide shell and the dynamic reaction surface [3]

So, regarding the possible use of metal nano-particles as fuel in an ICE cycle, the first key to be analyzed is the oxidation process of the metal nano-powders in relation to nature, structure and ambient conditions.
A possible thermodynamic engine cycle burning metal fuels has to be evaluated compared to the following circumstances:

1. The combustion has to proceed in solid state (melting point or vaporization has to be avoided);
2. The major part of heat combustion has to be transferred to the ambient gas with pressure increase;
3. The ignition process has to be controlled in some way; in other words nano-particle ignition has to be sensible to the control of the thermodynamic cylinder conditions (compression ignition) or to the local temperature conditions (spark ignition).

Unfortunately, the great number of nano-particle combustion data reported in literature are difficultly exportable to the engine case: the main answers have to be found out directly with engine tests and in particular, have to be verified for ICE application:
• What happens in an high pressure and closed ambient as the cylinder of an ICE;
• Ignition has to be carefully characterized as function of metal particle properties and ambient condition.
Taking into account the possible occurring combustion regimes of metal nano-particles, with respect to metal and oxide characteristics and aerosol transport regimes, the following observations can be drawn:
In the nano-scale regime and $Kn>>1$, the transport regime falls in the free molecular range, for which the gas-phase combustion regime is controlled from ambient temperature.

Although aggregates of nano-particles may appear as large particles, their combustion properties differ from micron-particles and are closer to the single primary nano-particles. As reported by Rai et al. [3] for Al case, in the free molecular range regime, nano-particles cannot sustain a particle-boundary diffusion flame in the gas-phase, but they can burn in vapor phase only if the metal vaporization temperature is reached. Moreover, the heat transfer inside the particle and from nano-particles to gas is so fast that they can be considered isothermal.

The engine cylinder peak temperature is lower than boiling and vaporization temperatures of both metal and oxide (2791K and 3133K for Al and Fe, and 4000K and 3400K for Al_2O_3 and FeO, at ambient pressure). Then, before opposing confirmations, it is thinkable that combustion occurs in heterogeneous condensed-phase combustion regime (solid or liquid), at least for Fe, while for Al case the hypothesis of solid/liquid combustion seems quite risky.
Ignition occurs in the temperature range of 550K-650K (for iron) and 600-680K (for aluminum), in line with results of Beach [2] for Fe (≈500K): regarding the ignition mechanism, the exothermic growth of oxide layer seems the most appropriate. Following the description given by Trunov *et al*.[9], the rate of the oxidation layer can be described with an Arrhenius law:

$$\frac{dh}{dt} = K \frac{C_{oxidizer}^{m}}{h^{n}} exp\left(-\frac{E}{RT}\right) \qquad (5)$$

where *h* is the thickness of the oxidation film, *t* is time, *C* is concentration, *R* is the universal gas constant and *E* and *K* are activation energy and pre-exponent, respectively; the exponent *m* and *n* represent the effect of the oxidizer pressure and oxide thickness on the oxidation law.
Actually, the Cabrera-Mott mechanism should be considered as the basic process of the diffusion of ions Al^{+} (or Fe^{+}) and O^{-} within the thin oxide shell layer that gives the kinetic behavior of autoignition process. The other two autoignition criteria described in literature are based on the thermomechanical rupture of the oxide shell by means of melting metal core, or, on the direct melting of the oxide; but for these two mechanisms, it is required a temperature higher than the Al melting point (933K) or the Al_2O_3 liquefaction (4000K).
As it has just been explained, after ignition, the combustion time of metal nano-particles occurs within some milliseconds: in this case, the combustion rate is not controlled by the diffusion of the agglomerates in the surround gas, but it is limited by the oxidation rate of the single particles.
As oxidation proceeds, looking at the heterogeneous combustion of the single primary particle, the oxide shell grows and the oxidation rate is more and more

limited by the oxygen and metal ion exchange through the oxide shell between the core and the external surface respectively.

Opposite to the kinetically-controlled oxidation process assumed for the first short period after ignition, during the second phase of combustion process, the experimental data seems in line with the model described by *Park et al[3].:* the diffusion of ions through the oxide shell can be written as:

$$w_o = -D\frac{\partial c}{\partial r} + cv_{ox} \qquad (6)$$

Where w_o is the diffusion of oxygen, D is the diffusion coefficient, v_{ox} is the velocity of oxygen rising from this pressure gradient, and c is the concentration of oxygen in the oxide shell, then, cv_{ox} is the convective flux of oxygen due to the pressure gradient. The coefficient D can be written as:

$$D = K_B T \times \frac{v_{ox}}{(-\Delta P V_0)} \qquad (7)$$

D is function of the particle temperature (T), the pressure gradient (ΔP) and oxygen solubility in the oxide shell (V_o). Particularly for small particles, the pressure gradient is quite significant [3], and may have a significant impact on the oxidation process.
In the aluminum case [12], the combustion heat is very high and the melting point (933K) is quite low: in this case, the rupture of the oxide shell by the liquid metal core can occur, exposing the metal core to the external oxygen and maintaining the oxidation rate at very high values. Therefore, it is thinkable that for Al engine combustion, the change from initial exothermic growth of oxide shell to the melt dispersion mechanism, with very high heat release, is very short and indistinguishable in heat release pattern. Moreover, in engine environment, the large part of the combustion occurs during engine compression stroke when gas temperature is substantially increasing. The combination of particle self heat and the cylinder gas compression could induce particle overheating above the Al_2O_3 melting point (2357K). In this phase, the heterogeneous oxidation of nano-particles is very rapid leading to the complete oxidation of the metal particles [13].

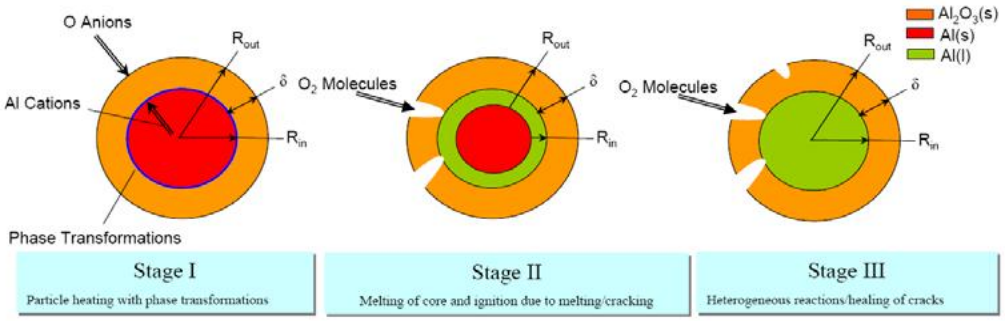

Figure 12: Scheme of the process occurring during fast heating of an aluminum nano-particle covered by a strong oxide shell and representing a melt-dispersion mechanism[4]

More details on the models describing the Al nano-particle combustion process can be found in literature [12-15-16].

In the case of Fe, even if few information on Fe nano-particles combustion have been found in literature, the same autoignition process and kinetic combustion phase of Al could be assumed, at least at a preliminarily approach, as valid. However, as reported before, after the first kinetic oxidation phase, a second ‘‘smooth’’ heat release is generally present: the time scale and pattern of this second phase seems to be in line with a heterogeneous combustion in solid phase. In fact, the measured particle temperatures are close to (but not exceeding) the melting point of both iron and iron oxide (1803 and 1838 K respectively), indicating the possibility of an oxidation process in solid phase. After the combustion rate peak, the increased oxide shell thickness and the reduced metal core surface lead to the final stage of combustion [14].

3.3 Shock tube tests

The shock tube-tests pointed out the combustion temperature of nano-particles with optical technique; in particular, as it has just explained before, at the end of the tube there are two windows for an optical access that allow to use two-colors pyrometry technique:

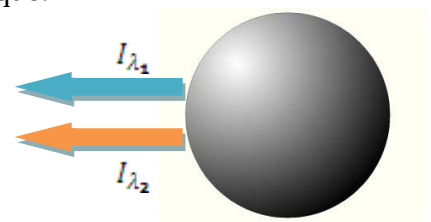

Figure 13: Scheme of signals emitted by a particle

The thermal radiation signal emitted by a particle of diameter d_p obeys the Planck's law:

$$I_{\lambda_i} \propto \frac{2hc^2}{\lambda_i^5}\left[exp\left(\frac{hc}{\lambda_i k_B T}\right)-1\right]^{-1}\pi d_P^2 \varepsilon_{\lambda_i} \qquad (8)$$

Where ε_{λ_i} is the spectral emissivity of the particle, *c* is the speed of light, *h* is the Planck's constant and k_B is the Bolzmann's constant.

According to the Kirchhoff's law, the spectral emissivity equals the absorption coefficient of the particles. In the Rayleigh regime, for particles much smaller than the radiation wavelength, the following relation holds:

$$\varepsilon_{\lambda_i} = Q_{abs} = \frac{C_{abs}}{\pi d_P^2/4} \qquad (9)$$

Where Q_{abs} is the absorption coefficient, and C_{abs} is the "absorption cross section". It is also possible to write C_{abs} in this way:

$$C_{abs} = \frac{\pi^2 E(m)}{\lambda_i} d_P^3 \qquad (10)$$

Where $E(m) = -Im\{(m^2-1)/(m^2+2)\}$ is a function of "complex refractive index" $m=n-ik$.
From the above relations, mentioned by Istituto Motori, the particle temperature can be obtained, as follow:

$$T_P = \frac{hc}{k_B}\frac{\frac{1}{\lambda_2}-\frac{1}{\lambda_1}}{ln\left[\left(\frac{\lambda_1}{\lambda_2}\right)^5 \frac{I_{\lambda_1}\varepsilon_{\lambda_2}}{I_{\lambda_2}\varepsilon_{\lambda_1}}\right]} \qquad (11)$$

Assuming that the ratio of absorption and extinction efficiencies is almost constant at the selected wavelengths, the following relation holds:

$$\frac{\varepsilon_{\lambda_2}}{\varepsilon_{\lambda_1}} = \frac{Q_{abs,\lambda_2}}{Q_{abs,\lambda_1}} \cong \frac{Q_{ext,\lambda_2}}{Q_{ext,\lambda_1}} = \frac{K_{ext,\lambda_2}}{K_{ext,\lambda_1}} \qquad (12)$$

Thus, the particles temperature can be deduced from measured data only.

$$T_P = \frac{hc}{k_B} \frac{\frac{1}{\lambda_2} - \frac{1}{\lambda_1}}{ln\left[\left(\frac{\lambda_1}{\lambda_2}\right)^5 \frac{I_{\lambda_1} K_{ext,\lambda_2}}{I_{\lambda_2} K_{ext,\lambda_1}}\right]} \qquad (13)$$

Where the Extinction Coefficient $K_{ext} = -\frac{1}{L} ln\left(\frac{I}{I_0}\right)$, derived from *Lambert Beer's law*.

The main uncertainties in determining the particles temperature arise from the lack of knowledge of nano-particles optical properties, both in the initial state and mainly during the oxidative process.

All the tests pointed out that the particles temperature rapidly attains its maximum value and afterwards it slowly decreases; an overall reaction time slightly above 1 ms was estimated.

Finally, to verify the behavior of the particles with Oxygen, combustion tests were also carried out with lower oxygen concentration (0.05% of O_2), thus simulating the exhaust gas recirculation of internal combustion engine: the particles reach their maximum temperature later, and its value is below 1900K, which is lower than the respective case of combustion in synthetic air (0.21% of O_2).

3.4 Production and regeneration

One of the key point of this project is the tayloring of metal nano-particles and the regeneration of burned fuel: during the months, it has been demonstrated that Synthesis of aluminum-based nano-particles via a plasma-spray aided method (APS) is feasible, on the contrary for the case of boron, APS synthesis of B-based nano-particles is not praticable. Synthesis of Fe nano-particles either via ASP or by direct reduction of the purified powder with the aid of H_2 has been achieved; also, the preparation of suitable Fe-precursors from calamina-slag, with the aid of a process that has been developed by NEO and further studied by AEIF and APTL, was demonstrated.

Regarding the preparation of suitable Fe-precursors, calamina-slag is considered the best choice, but due to the fact that it contains several impurities, the first step is to set up an efficient purification process. NEO developed an important process, characterized by these main following steps: milling to improve slag dissolution, dissolution in HCl at 65ºC and after addition of HNO_3, in order to oxidize Fe species to Fe(III); the Fe(III) has to be extracted into organic solvent and then into water. At the end, after the addition of a gel precipitation, the

product has to be filtered, washed with water and dried, and the final purified product is obtained.
The use of this process pointed out that milling improves significantly slag dissolution by HCl: in particular, a milling time of 6 hours is sufficient to slag dissolution in 5-10 minutes, instead the dissolution period lasts about 90 minutes for unmilled samples.
The product obtained from purification process can be dissolved in nitric acid and employed in APTL's Aerosol Spray Pyrolysis units to produce iron-based nano-particles.
In addition to the above synthesis method, efforts to synthesize suitable iron nano-particles via reduction of an iron oxide nano-powder with an Average Primary Particle Size (APPS) of approx. 40nm were made. Another possibility taken into consideration for the production of iron nano-partricles was to directly reduce the purified calamina-slag samples produced according to purification process developed by NEO.

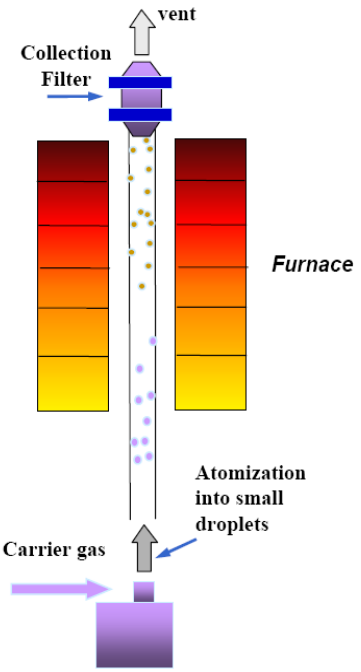

Figure 14: Schematic description of APTL's lab-scale ASP-facility

In terms of plasma-aided nano-particles synthesis technique, micron-sized Al, B and Fe powders (20- 45μm, 6-8μm and 6-9μm respectively) were utilized as raw materials for the investigation of the method feasibility. The technique used is based on the Atmospheric Plasma Spraying (APS) approach, in which the raw-powder is aerosolized in Ar, then injected into a hot plasma-zone and is evaporated. After leaving the plasma-zone, the particles are cooled and forced to

condense. If the cooling downstream of the hot-plasma zone is rapid enough, the powders are obtained in the form of spherical nano-particles.

Another important aim of this project is the possibility to regenerate iron nano-particles from iron combusted powders: a detailed parametric study for the reduction of a Fe_2O_3 nano-powder to metallic Fe nano-particles via exposure to H_2 at moderate temperatures was performed; the goal was to determine suitable conditions for achieving regeneration of combusted Fe nano-particles (i.e. iron oxide). These conditions are also applicable to the case of both ASP prepared and 'calamina slag-derived' iron oxide nano-powders that can subsequently be reduced to iron nano-particles.
The iron oxides utilized in the parametric studies had a diameter of 40 nm and the reduction temperature was chosen around 400°C in order to minimize sintering effects during reduction that could cause the loss of reduced products nano-structuring. The tests showed that an exposure time of 4 hours and a Gas Hourly Space Velocity (GHSV) of 5 gr of $H_2 \cdot (\text{gr oxide nanoparticles} \cdot h)^{-1}$ are required to obtain a complete reduction into metallic iron; they also evidenced that the effects on nano-structuring were not significant since the final product was a Fe nano-powder with a diameter of 85 nm.
In order to avoid spontaneous ignition phenomena, for the passivation of the iron nano-powders prepared by reduction with H_2, two different methods were considered and employed:
a. Cooling of the reduced sample under an inert flow (He or N_2) to a temperature of 150-200°C and subsequently exposure to a low O_2-content stream for a period of 2-3 minutes;
b. Cooling of the reduced sample to room temperature under an inert flow: the sample is left settled at ambient conditions for a period of c.a. 12 hours.
It was found that the second method was the most efficient and repeatable for the passivation.
Another possibility for the production of iron nano-powder was to directly reduce the calamina-slag purified with the NEO process, just explained before; in this case, tests showed that the powder was more resilient to the reduction process and in order to obtain a full reduction was required and exposure of 4 hours and a GHSV of 7.6 gr of $H_2 \cdot (\text{gr oxide nanoparticles} \cdot h)^{-1}$.

Chapter 4

Experimental part

From this chapter onwards, the things reported are referred to the activities performed in UPV during my stage. In this section in particular the idea is to explain the experimental line and show the procedure for combustion tests. Furthermore, regarding the second part of this work, a brief introduction about pollutant emissions investigation and the study of regenerated nano-particles, is presented.

4.1 Experimental line

The experimental line is principally composed by a cylinder combustion chamber with two windows, with a 54 mm diameter, to have the possibility of seeing inside. This vessel has two entrances, both connected to the air bomb: one is necessary to insert the air directly in the chamber, and the other one is connected to the injection system. The chamber is also furnished by one exit, connected to a filter and by one electrovalve. The temperature is controlled via an internal electrical heater, heating the air up to 1173K in a few minutes; to avoid heat loses through the walls and to keep the vessel cold, insulation is required. The selected insulation was made of machined refractory brick with low density and low thermal conductivity allowing rapid gas heating: so the vessel has an internal insulating wall of 20 mm.

Main characteristics:
High temperature: 600 – 800ºC
High Pressure: 60 Bar
Electrical resistance heater
Internally insulated

Table 4: Characteristics of combustion chamber

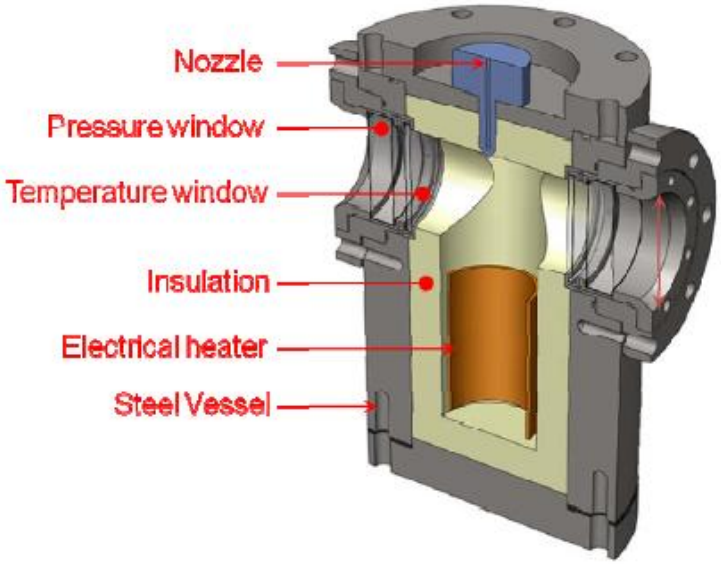

Figure 15: Scheme of the combustion chamber

There are also some sensors:

- One sensor to measure the pressure in the injection system
- One piezo-resistive sensor to measure the average Pressure in the chamber
- One piezo-electric sensor to measure the Instantaneous Pressure
- Two thermocouples to measure, respectively, the temperature near the injector and the temperature in the center of the heater, where the combustion takes place.

Figure 16: Combustion test system

The aim of these tests is to make measurements about combustion pressure and luminosity, and in order to do this, it is necessary to connect the vessel to different instruments.
For pressure, the presence of an oscilloscope YOKO and an amplifier is sufficient; for the luminosity there are two options:

- A photodiode connected to oscilloscope

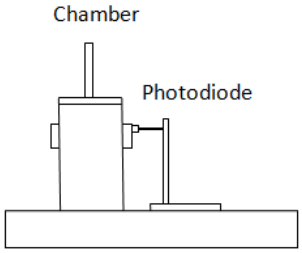

Figure 17: Scheme for testing with photodiode

- A camera Photron directly connected to a pc.

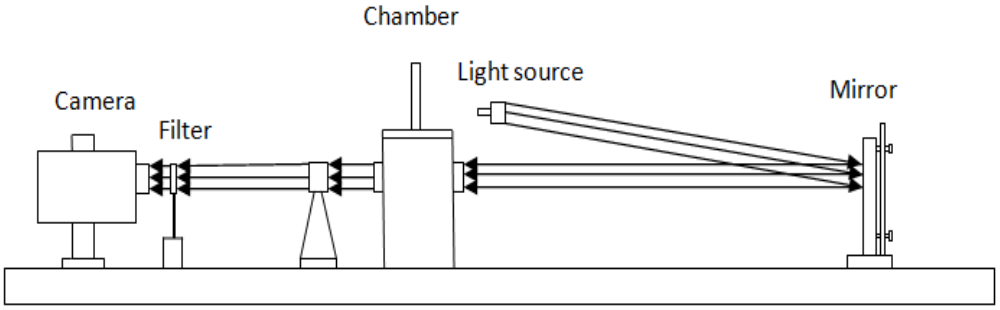

Figure 18: Scheme for testing with high speed camera

In order to perform isolated aerosol injections with pre-defined quantities at the desired test conditions, the pneumatic injection system, designed on the basis of CFD studies carried out in the previous months, is used. In the follow image there is a schematic representation of the aerosol injection system: it consists of a high pressure volume, a solenoid valve, the particle reservoir, a check valve and the injector nozzle, machined in the top cover of the vessel.

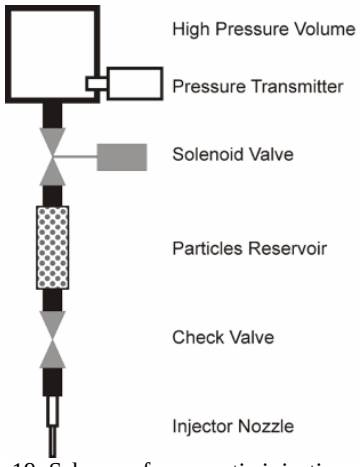

Figure 19: Scheme of pneumatic injection system

The injection system is connected with the air bomb and this permits to fill the air just before to perform combustion, with a value of 60 bar.

In the follow image, a resumed scheme of the test rig used for the tests is presented :

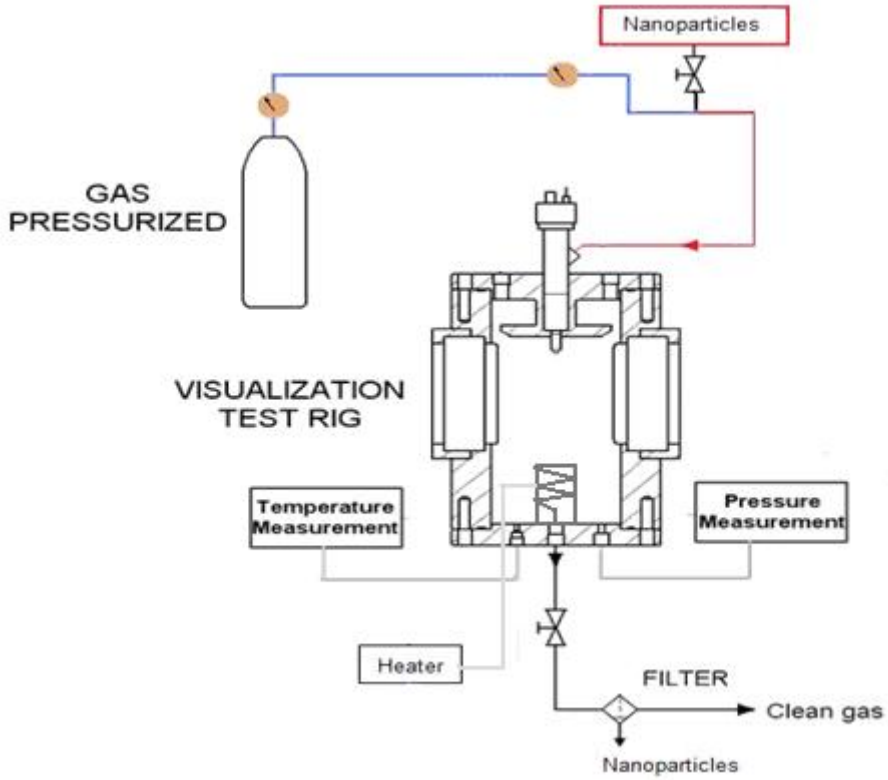

Figure 20: Schematic of constant volume combustion test rig

4.2 Procedure

Regarding the first part of the project, the experimental procedure should be divided in two parts:

- Calibration of video-optic system
- Combustion test

In fact, in the first part, the aim is to evaluate nano-particles combustion, both in terms of pressure increment and luminous intensity: for pressure is sufficient the use of a sensor, on the contrary, for luminosity is necessary a video-optic system or a photodiode.

Calibration of the video-optic system: It is necessary to know the relationship between pixel and millimeters because the camera works with pixels. In order to

realize this, when the camera is well-focused, a paper with concentric rings is put on one of the windows and a video of three or four frames is made.

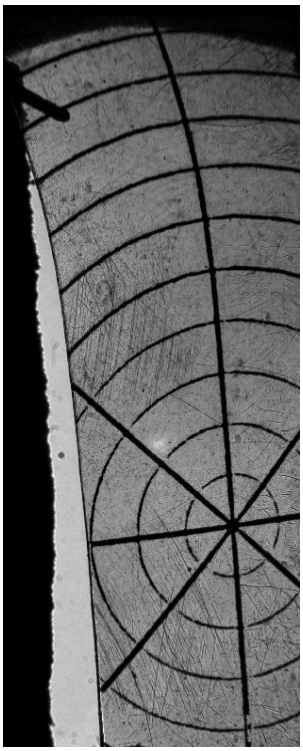

Figure 21: A frame of combustion chamber for camera's calibration

Knowing the distance between two rings in millimeters and measuring the distance in pixel with the program *ImageJ*, it is possible to obtain the correspondence.

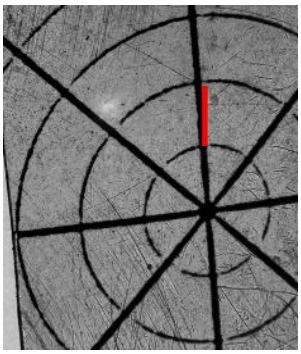

Figure 22: A detail of calibration grid

$$\begin{cases} d_{real} = 2.5\ mm \\ d_{measured} = 48\ px \end{cases} \Longrightarrow \quad d = 19.2\ {}^{px}/_{mm} \qquad \textbf{(14)}$$

The main aspect is that the configuration of the camera must be the same for the following tests.

Combustion test: the procedure is the same both for photodiode and camera, like follows:

1. Fill the closed vessel with fresh air until obtains 8 bar
2. Increase the air temperature to 200ºC and keep it constant during 10 min to ensure the temperature homogenization.
3. Adjust the pressure at final pressure by a filter valve
4. Heat the ambient air up to the target temperature (700 °C)
5. Unscrew the injection system and put the nano-particles inside
6. Screw everything again and put the electrovalve
7. Switch off the heater and push the trigger button
8. Empty the closed vessel and wait until the temperature in the chamber goes down

In case of using an optical system with a camera, the procedure is exactly the same even if, before screwing the trigger, it is necessary to start recording the video. On the contrary, if you use the photodiode, the signal of luminosity is directly read by oscilloscope and saved on pc.

The tests are conducted under different operating conditions:

- 10 and 15 Bar, as starting pressure
- 700 and 750°C

Each experiment is repeated twice, one with photodiode and one with the camera in order to verify that the luminous intensity is the same.

4.3 Acquisition of data and video

Two programs are used to save data and videos:

- Program Yoko DL716 Beta
- Photron FASTCAM Viewer

Program Yoko DL716 Beta: this program saves the data coming from oscilloscope, but, before starting, it is necessary to set the configuration; in particular the channels, where signals enter directly from the sensors, have to be fixed.

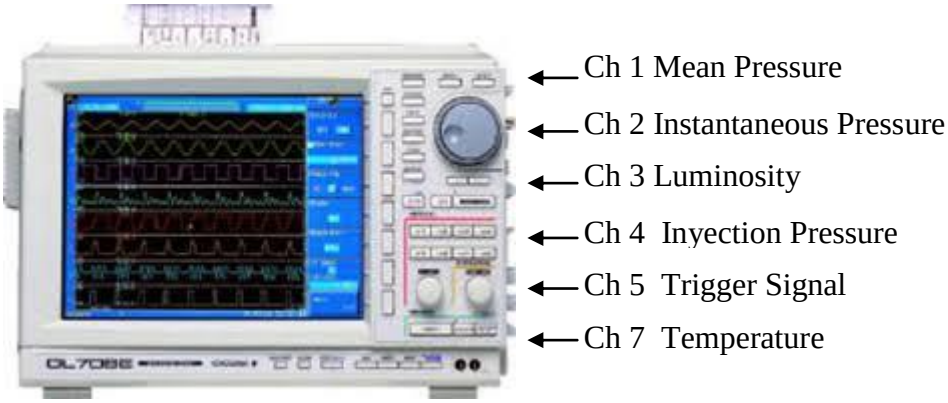

Figure 23: A scheme of oscilloscope

For each channel, there are some parameters that should be chosen and should be the same for all the tests, like offset, Moltiplicative coefficients and Number points for cycle.
The following images show an example of the real signals saved and transferred to pc by the oscilloscope:

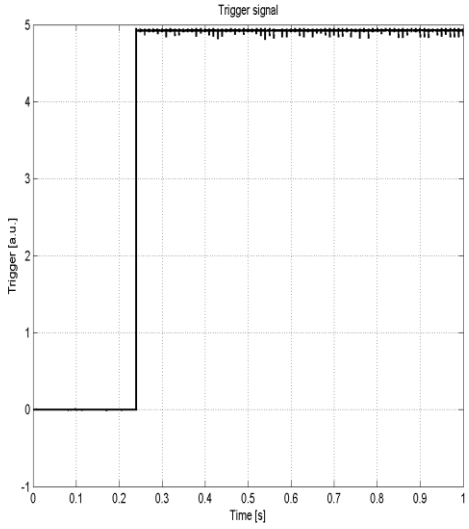

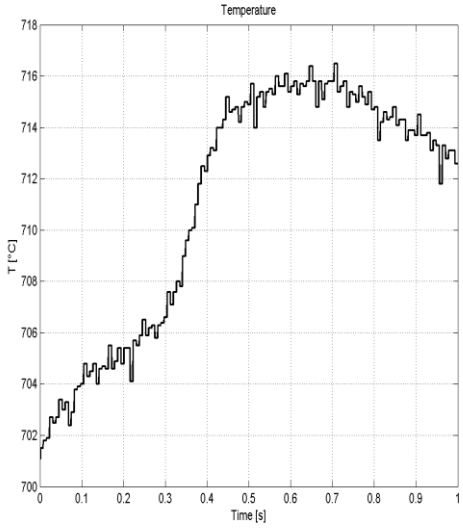

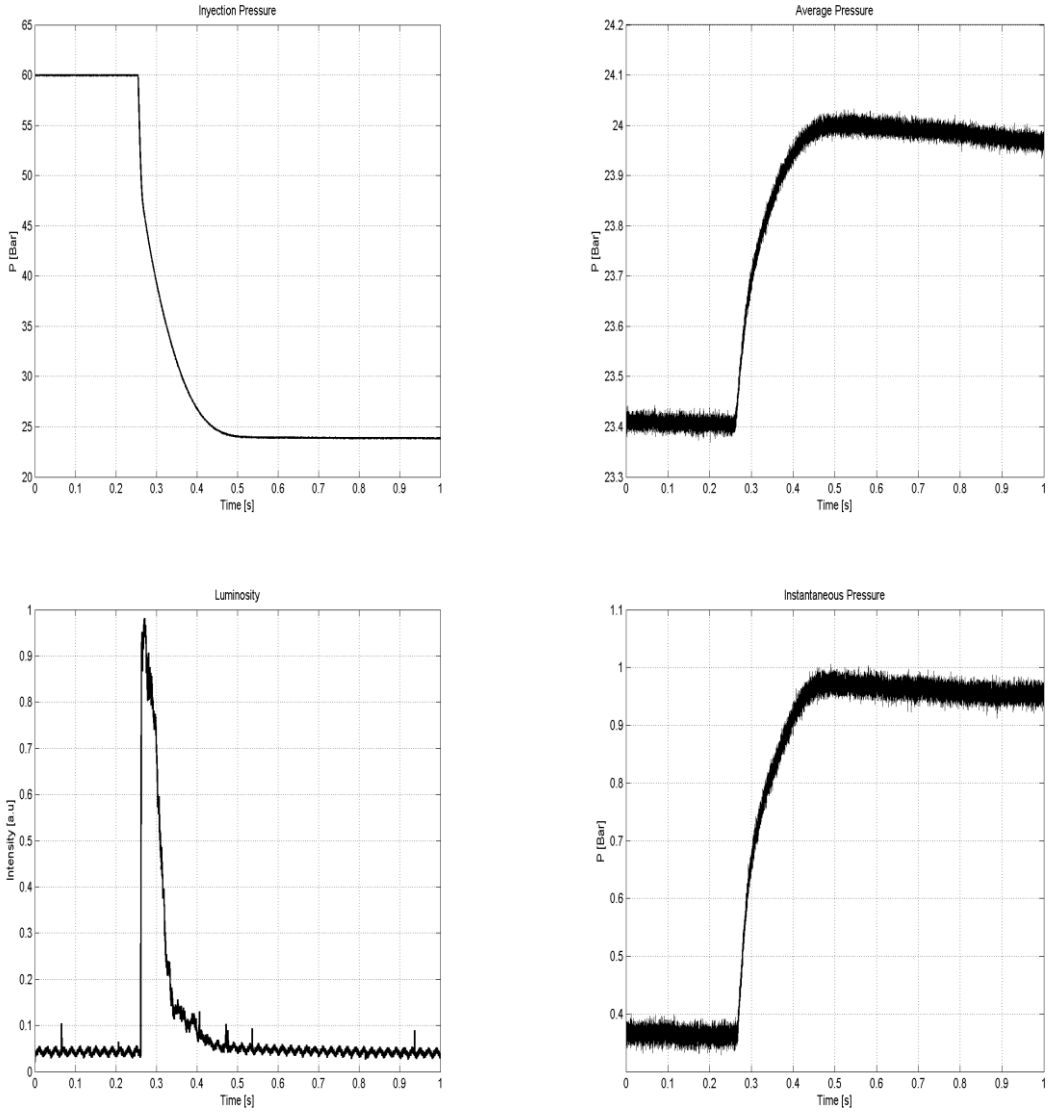

Figure 24: Signals registered by the oscilloscope

As can be seen in the trigger image, the test takes 1 second and the oscilloscope records the behavior of parameters investigated, saving always 0.24 s before the start of combustion .

Photron: The camera saves videos in digital form and, for this reason, is indispensable to set it. The configuration of the camera consists in the choice of some parameters, that must be the same for all the tests. In particular, It is necessary to set:

- Exposition time: 1/228000 sec

- Frame-rate: 21000 fps
- Resolution: 960 x 320

This program allows to save video of combustion in different formats: in particular, the most important for this work is the AVI format, which shows the complete video, and the PNG format, which saves the video as a sequence of images.

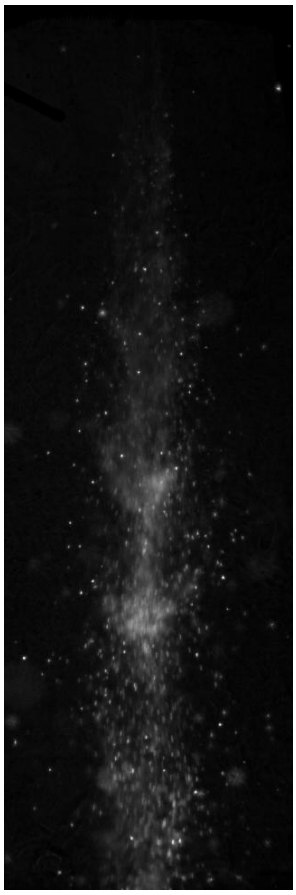

Figure 25: A frame of iron combustion test

4.4 Software for analysis

After the acquisition of combustion videos and data, the work follows up with their post-process. For both of them, the unique program used is Matlab.

As regards pressure and luminosity data from photodiode, the post-process consists in the elaboration of the values with matlab using an *Average Moving*

Filter that can eliminate the fluctuations without losing important information, as shown in the following image:

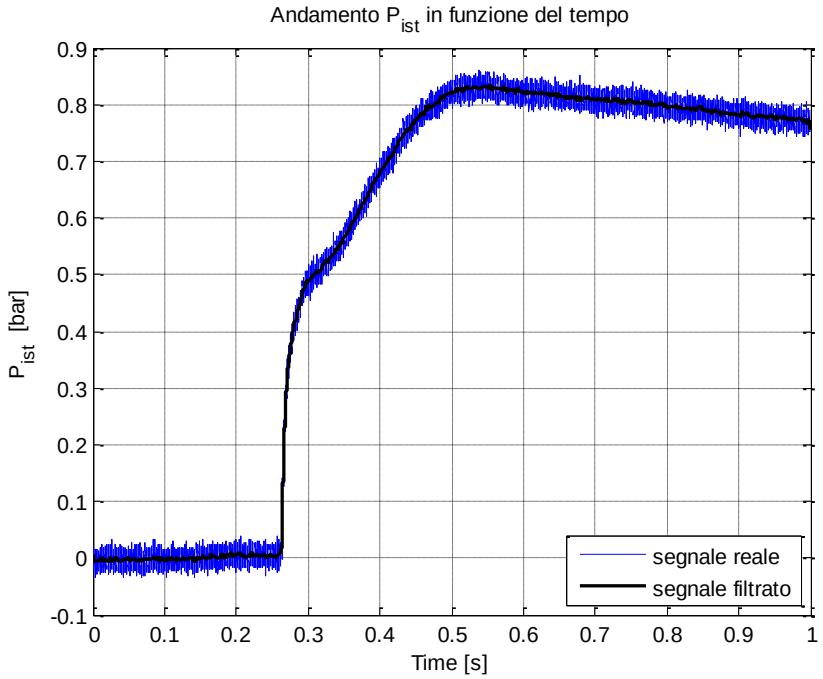

Figure 26: Real instantaneous pressure signal (blue line) and filtered signal (black line)

This procedure is repeated for all data since the final aim is to make comparisons between the different kinds of particles.

Regarding the video, only videos in PNG format are post-processed. Some scripts are written in order to analyzed the images and obtain some information about how and when combustion takes place in the chamber. This part will be shown in more detail in one of the following chapters. In particular, each image is analyzed line by line underlining to the hot region, where there is a gradient temperature; by this way, it is possible to identify the background (dark) and the combustion (light) and reduce the image to a vector $V_{t,}$, which represents the accumulation of intensity for all the lines. The union of the all vectors produces a color map containing combustion qualitative analysis. This part will be fully detailed in chapter 7.

4.5 NO_x emissions

After the investigation about combustion behavior, it is interesting having an idea about the quantity of emissions that this kind of combustion produces. In order to know it, a series of tests are repeated with Iron 70 manufactured by NEO, making a modification in the experimental line.
A transparent bag is connected to the filter in the exit line; the procedure of the test is always the same but, at the end of the test, instead of discharging the exhausted gas outside, they are collected in this bag.
After that, it is possible to analyze the gas, using an appropriate test rig, *Motor Exhausted Gas Analyzer* produced by Horiba, that provides emission concentration: in particular, results are focused on the presence of NO, NO_2 and N_2O.

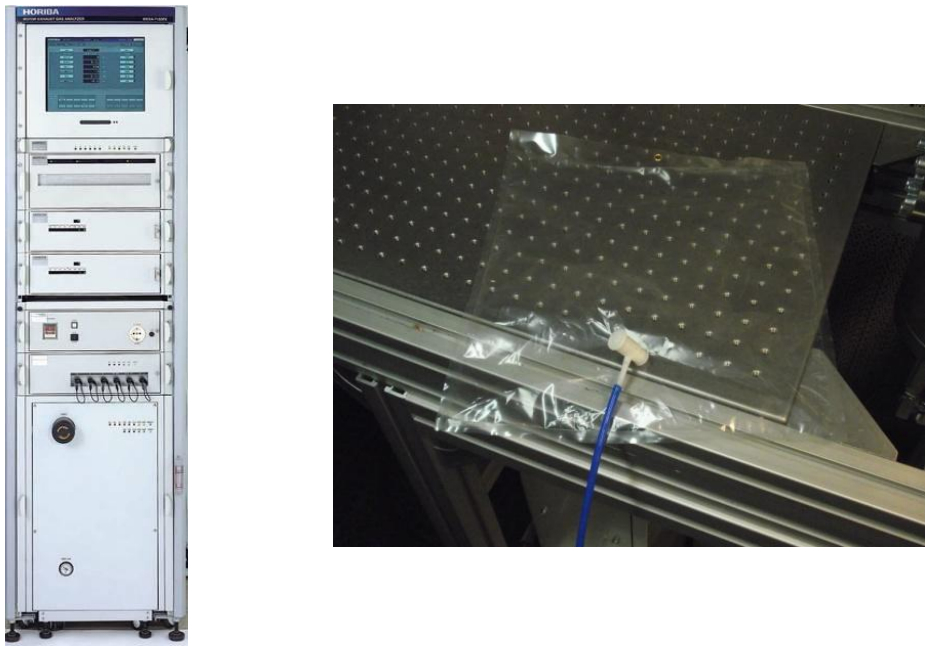

Figure 27: Image of Motor Exhausted gas Analyzer (left) and a photo of bag for collecting exhausted gas (right)

The test consists in connecting the bag with exhausted gas to the Gas Analyzer and then to empty it; the monitor shows the trend of gas in ppm. It is possible to calculate the total volume of the exhausted gas, considering the flow rate and the time needed to empty the bag.

The result of one test, filtered with Matlab, is shown in the following image, that points out NO_x; the time indicated in the x-axis is referred to the time that Horiba takes to empty the bag.

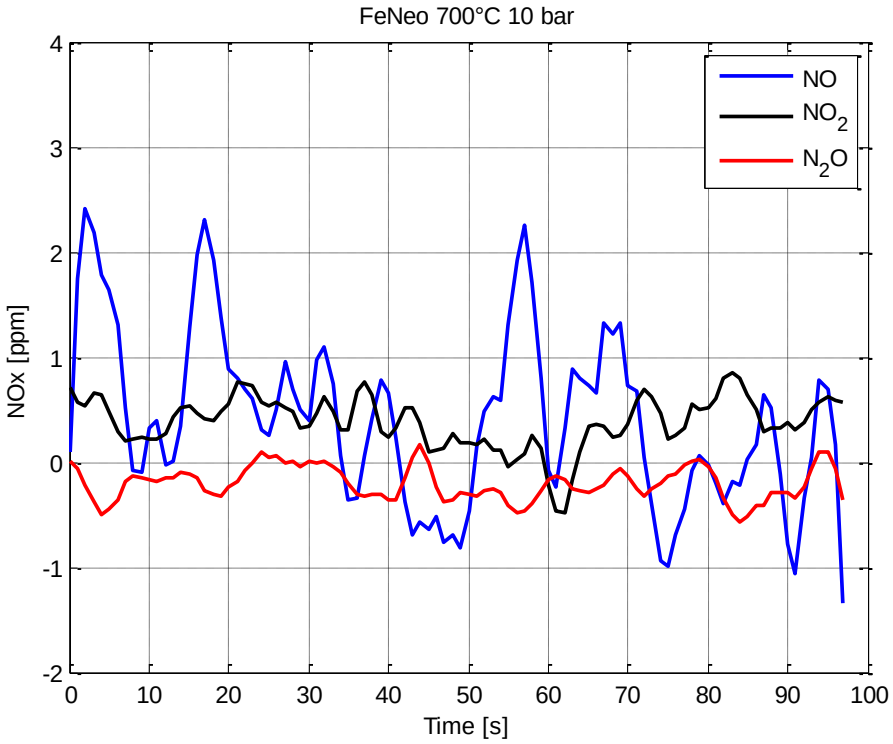

Figure 28: An example of NOx signals

The presence of negative values is associated to an error in the Horiba's calibration, making it difficult to calculate values so small.
At the end, a test without combustion is performed: the aim is to verify if the heater, reaching high temperature, reacts with the air inside the vessel and creates pollution.

4.6 Regenerated nano powders

The last experimental part of this project, is focused on the study of regenerated nano-particles. As it has just been explained in Chapter 3, a lot of efforts were

done in the last three years in order to obtain a method that gives the possibility to reuse the combusted nano-particles.
Consequently, with the available test rig, iron and aluminum regenerated powders are tested in order to verify their characteristics: the same combustion tests are carried out with an amount of 30 mg, using the same operating conditions reported before.
The attention is focused on the value of Instantaneous Pressure and the main goal is to calculate the pressure increment, generated with their combustion.
An example of these results, referring to one-time regenerated nano-particle, is shown in the following image:

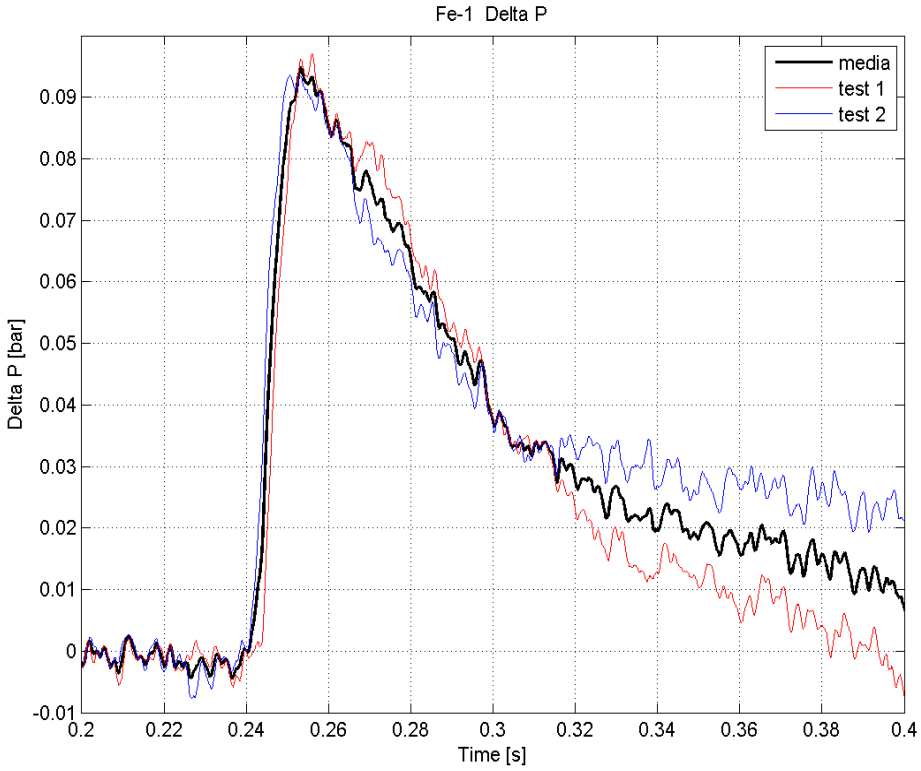

Figure 29: An example of ΔP produced by nano-particles one-time regenerated

For each kind of regenerated particle, some tests are conducted in order to calculate the average value, as can be seen in the picture above; the aim is to compare all average values in a single image. This argument will be explained in chapter 8.

Chapter 5

Analysis and data processing

In this chapter it is possible to find the results about the behavior of pressure and luminous intensity; after the first series of tests a problem with the injected valve occurred and, for this reason, it was replaced. The new one is different: for this reason, all the tests required were repeated; hereafter it is possible to find the new results.

5.1 The first series of tests

With regard to the first series of tests, the attention was focused in particular on the behavior of pressure and luminous intensity; the data were taken with the pressure sensors and the photodiode. In the following paragraphs, results about pressure and luminosity and the comparison between different nano-particles will be reported.

5.1.1 Pressure

Each test provides important information about pressure during combustion.
First of all, a lot of tests were performed without combustion; the aim of this procedure is to compare at the end the ΔP between combustion and no-combustion, in order to measure the quantity of energy that powders can release.
The following images show the instantaneous pressure for tests without combustion, under different conditions:

- 10 bar and 700 °C
- 15 bar and 700 °C

In both cases, were performed some tests and the results showed very similar behavior.

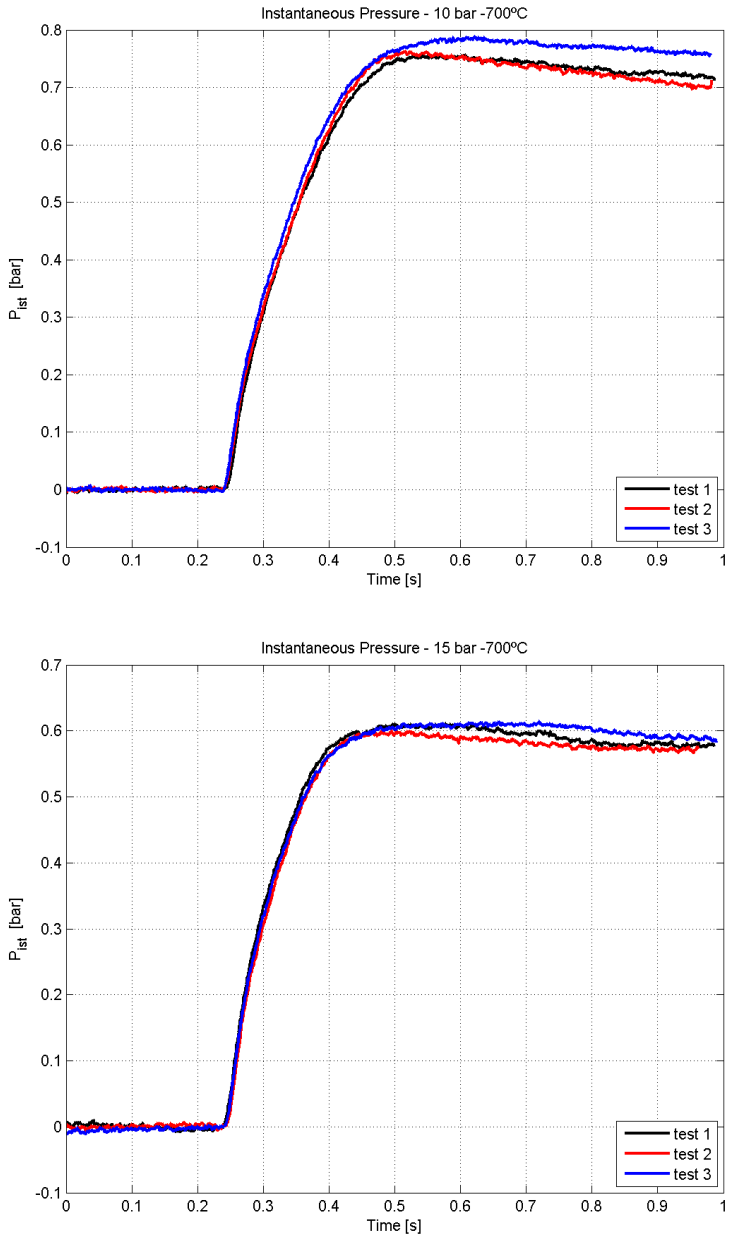

Figure 30: a) Instantaneous Pressure for tests without combustion at 700°C and pressure of 10 bar; b) Instantaneous Pressure for tests without combustion at 700°C and pressure of 15 bar

For each picture, average values were calculated and the next figure reports the comparison between the two different operating conditions:

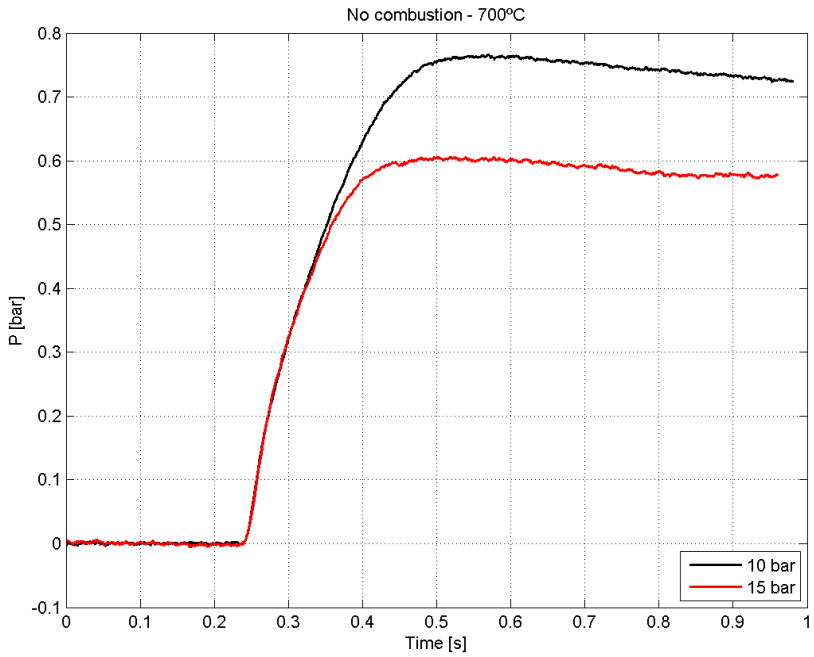

Figure 31: A comparison between instantaneous pressure for tests without combustion for initial pressure of 10 and 15 bar

Obviously, the data are filtered, as it was explained in the previous chapter.
The pressure increment for an initial pressure of 10 bar results higher than the same at 15 bar: the reason regards operating conditions. In fact, the injection pressure is constant at 60 bar and also the injection duration is constant: consequently, ΔP released in case of 10 bar as initial pressure is higher than the same at 15 bar.

After the tests without combustion, a series of combustion experiments with different nano-particles were made: both Iron and Aluminum were investigated at the same operating conditions of the previous tests because the aim is to calculate the pressure increment released during nano-particle combustion.
Below you will find an example of Iron at 10 bar and another at 15 bar: all the test show a very similar behavior.

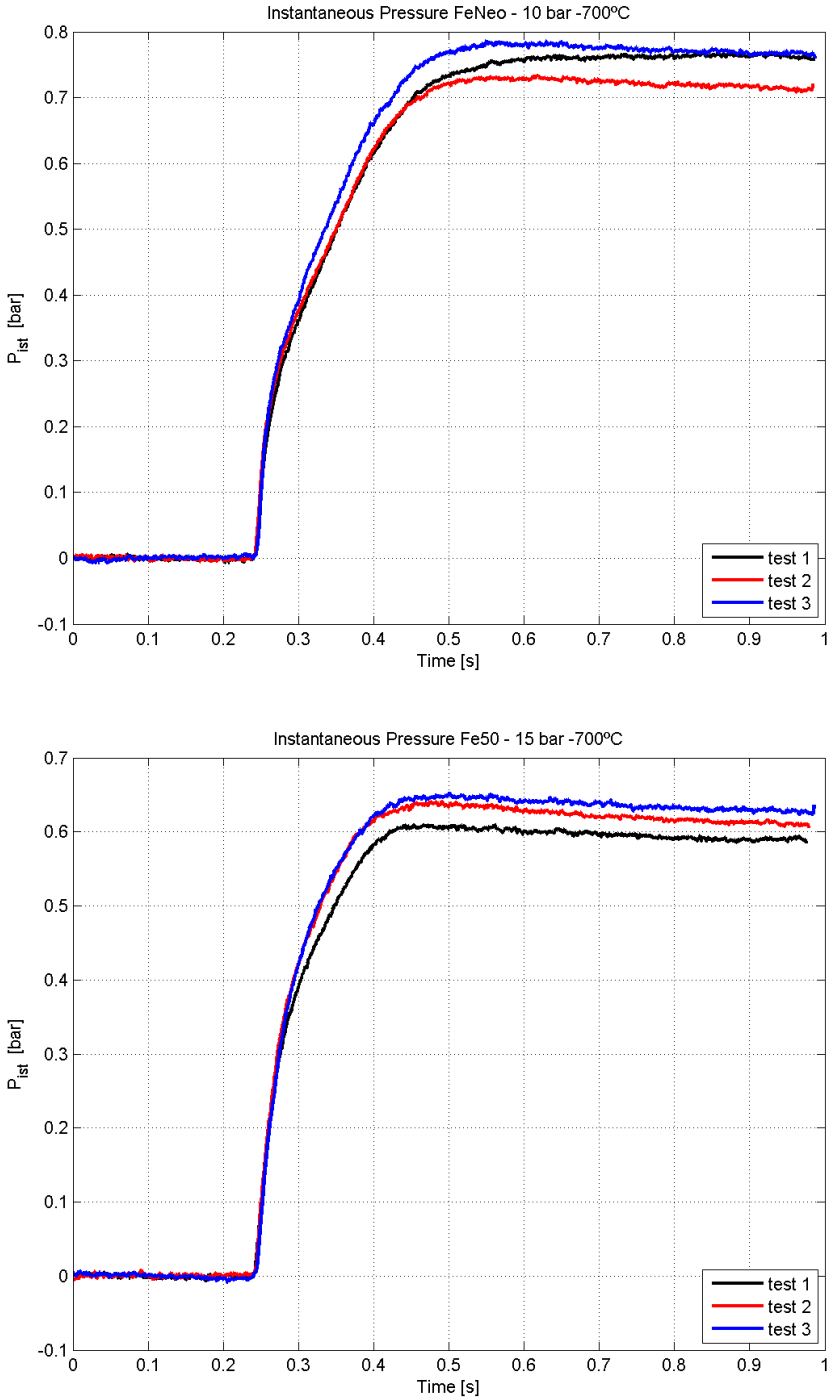

Figure 32: a) An example of Instantaneous pressure for tests with the combustion of Fe70 Neo at 10 bar; b) An example of Instantaneous pressure for tests with the combustion of Fe50 at 15 bar.

5.2 Comparison

5.2.1 Combustion and No combustion

Now, knowing the behavior of the Instantaneous Pressure, It is possible to measure the mean value for each category of particles in order to compare combustion and no combustion tests.
In particular, at the end of the tests, it has been decided to make comparison only for tests at 700 °C operating temperature.

- Test at 10 bar

Regarding the instantaneous Pressure of Aluminum, both Al18 and Al85 reach a value higher than the test carried out without combustion and the pressure increment related to Al 85nm is higher than Al 18nm with a peak around 0.3 bar. The strange trend of the aluminum in general, should be associated at the difficult to burn it.
The following images show the results just explained:

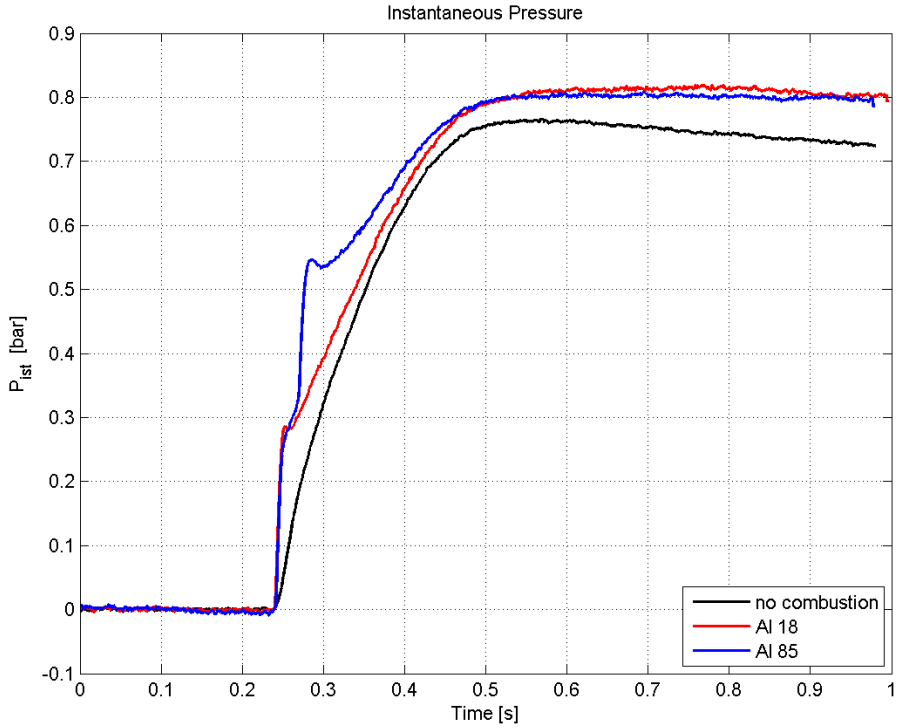

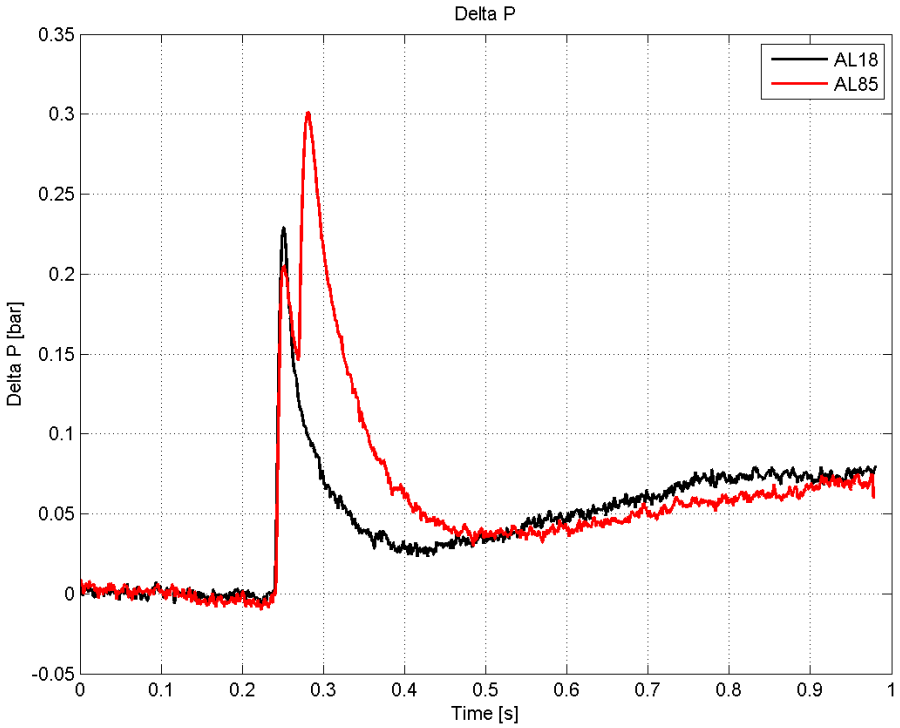

Figure 33: a) Comparison for Instantaneous pressure between tests without combustion and tests with Aluminum at 10 bar and 700°C; b) ΔP generated by the combustion of Aluminum

As concerns Iron, nano-powders with different diameter show quite the same performances, with very comparable values. All the test produce a pressure increment: in particular, Iron 70 nm points out the major ΔP, followed by Iron 50 nm, the best one between commercial powders, as evidenced in the images below:

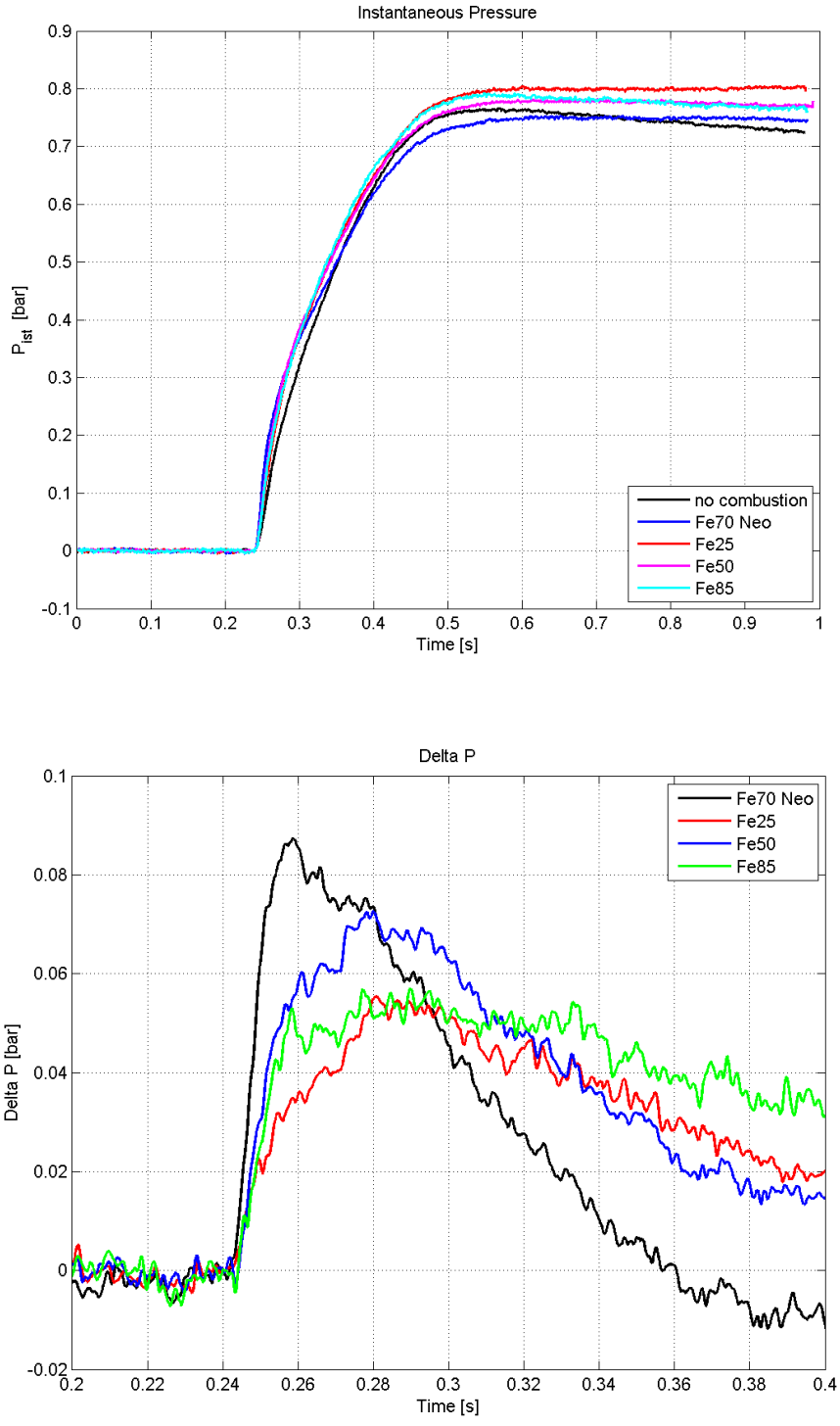

Figure 34: a) Comparison for Instantaneous pressure between tests without combustion and tests with Iron at 10 bar and 700°C; b) ΔP generated by the combustion of Iron

- 15 bar

At 15 bar, the Al85 reach a value higher than Al18 even if the behavior is always the same; the increment of Instantaneous pressure for Al85 is evident and the ΔP is around 0.23 bar. On the contrary, Al18 shows a behavior very similar to the test without combustion, so in that case, ΔP should not be calculated.
However, the test on Aluminum are not so reliable, so it is necessary to carry them out again in order to obtain consistent results.

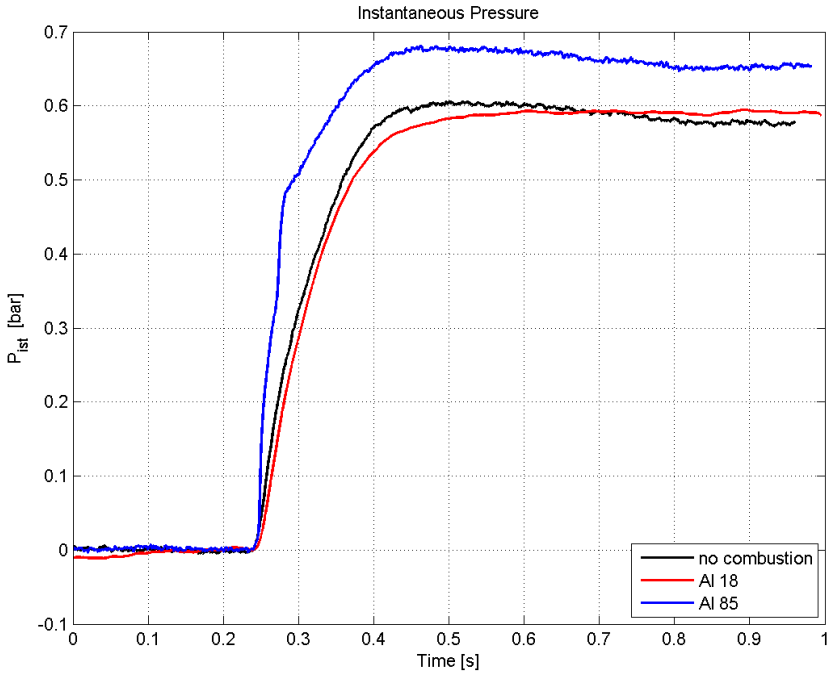

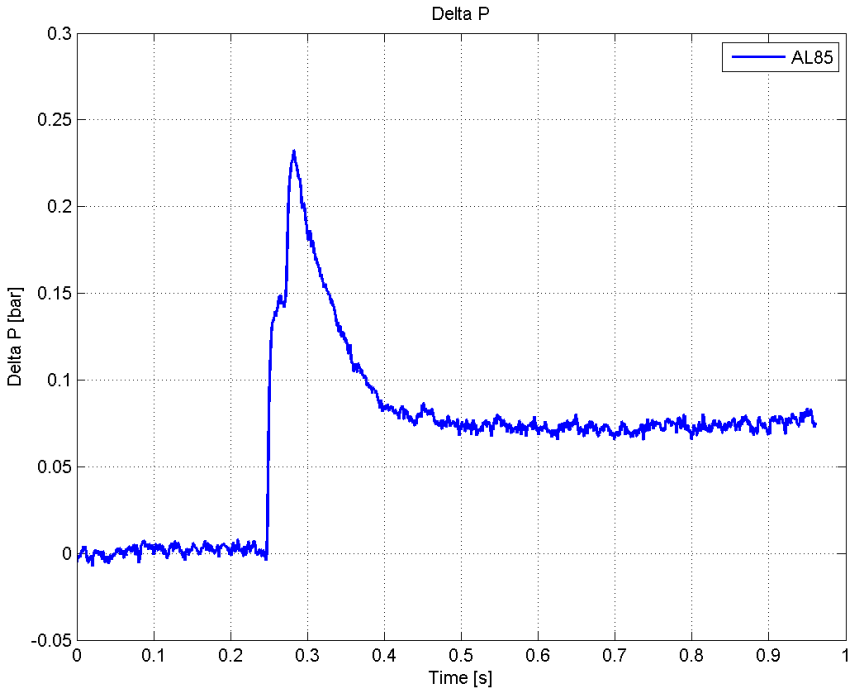

Figure 35: a) Comparison for Instantaneous pressure between tests without combustion and tests with Aluminum at 15 bar and 700°C; b) ΔP generated by the combustion of Aluminum

As has been explained before, the pressure increment for Al 18nm could not be calculated; so the image above reports only the increment for Al 85nm.

In the case of Iron, all kinds of nano-particles present a very similar behavior: the highest ΔP is reached by Iron 70nm produced from NEO with a peak of 0.12 bar. On the contrary, among the commercial ones, Iron with an APPS of 50 nm reaches a ΔP around 0.1 bar. The trend of Iron 85nm appears singular compared with the results for 10 bar: probably some errors had affected the measurements.

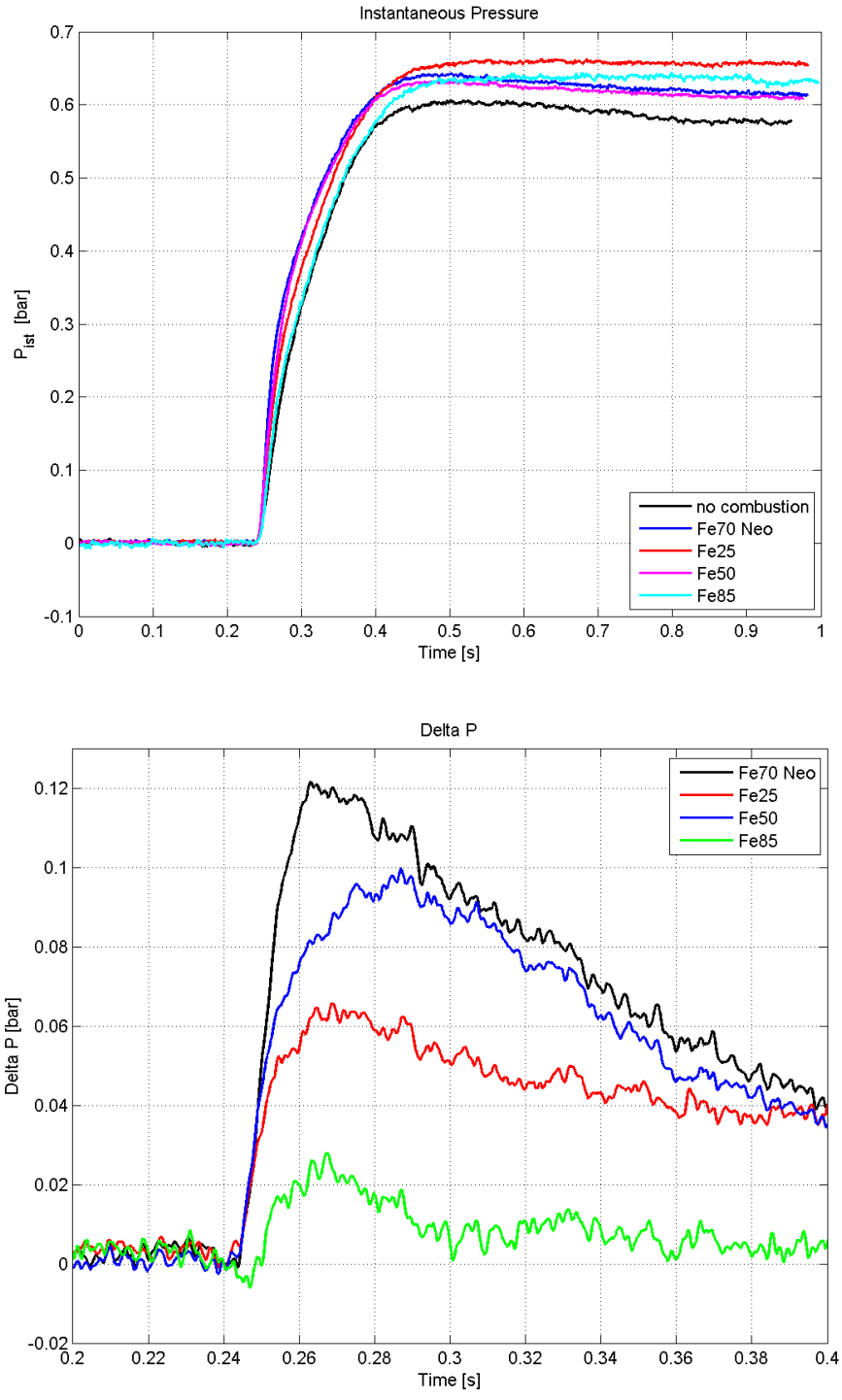

Figure 36: a) Comparison for Instantaneous pressure between tests without combustion and tests with Iron at 15 bar and 700°C; b) ΔP generated by the combustion of Iron

5.3 Luminous intensity

Thanks to the photodiode, It is possible to measure the intensity of combustion: in particular combustion corresponds to the peak of luminous intensity, as It can be seen in the following image.
The investigation is made both for Aluminum and Iron, for every kind of nano-particles: hereafter it is possible to find the results for the different types and operating conditions.

- Aluminum at 10 and 15 bar

In the case of 10 bar, the luminous intensity is higher for Al85 than Al 18nm, and It reaches a value around 1.15, in accordance with the trend of pressure.
At 15 bar, only the luminosity of Al85 is registered: this is the evidence that something was wrong with the combustion of nano-particles with APPS of 18 nm.

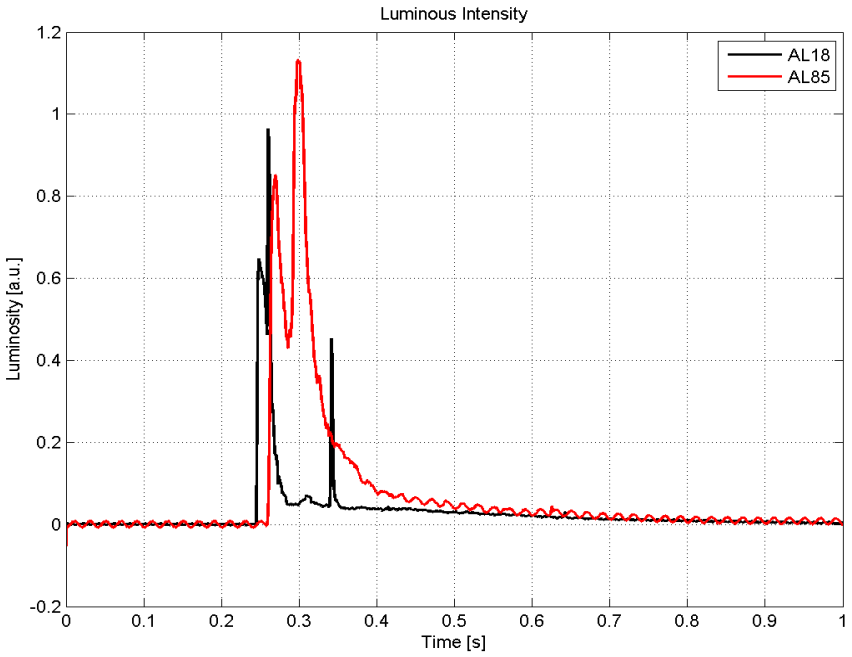

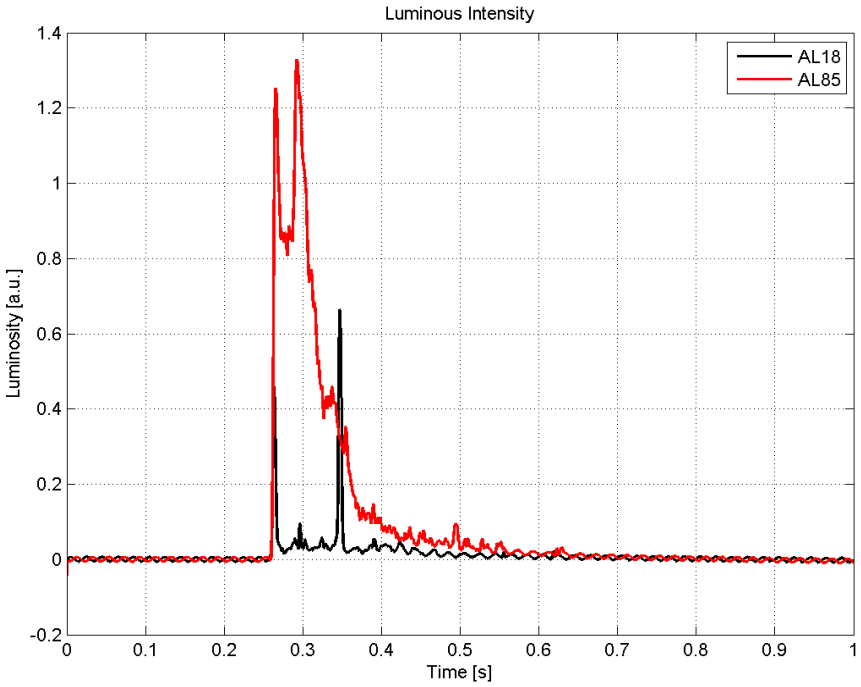

Figure 37: a) Luminous intensity generated by the combustion of Aluminum at 10 bar; b)) Luminous intensity generated by the combustion of Aluminum at 15 bar

- Iron at 10 and 15 bar

In case of 10 bar, the luminous intensity appears lower than Aluminum, even if the trend between the different nano-particles is in accordance with the pressure. On the contrary, for 15 bar of pressure, the peak of luminosity is lower than the correspondent at 10 bar and it is reached by Fe70 Neo: however, the other particles are not so in accordance with pressure trends.

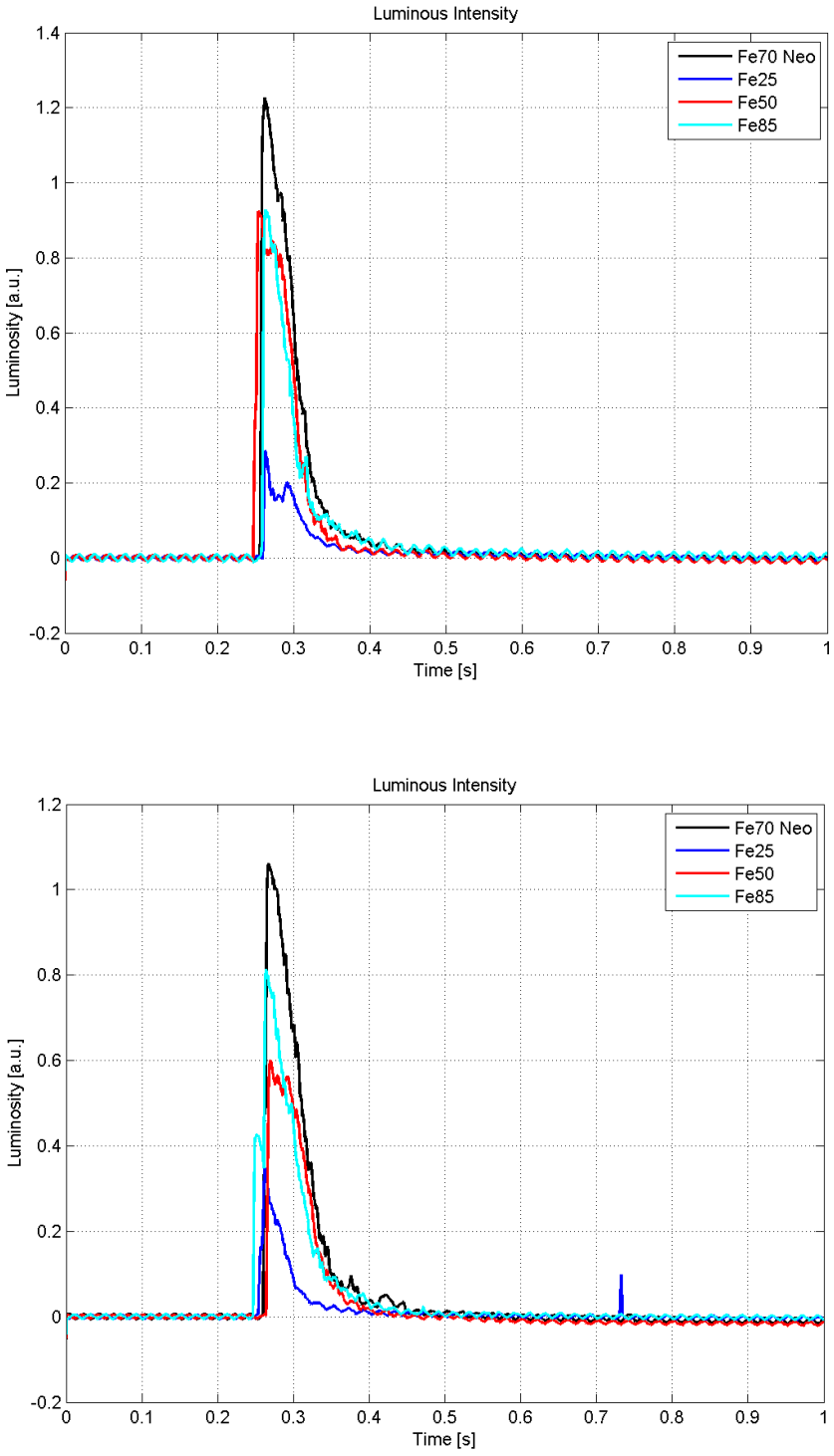

Figure 38: a) Luminous intensity generated by the combustion of Iron at 10 bar; b) Luminous intensity generated by the combustion of Iron at 15 bar

In conclusion, the information about luminous intensity obtained with the photodiode are not so reliable, probably as a consequence of particle dimensions, being very small. For this reason, the following analysis are carried out with the camera.

5.5 The second series of tests

After a few months, the injection valve broke down: for this reason it was substituted but, the new one had a bigger volume, so all the tests should have to be remade.
First of all, it is important to carry out tests without combustion again, because they are necessary in order to calculate the pressure increment. In this part of the chapter, it is possible to find only the results regarding pressure.

In the image below, it can be seen the pressure trend during a test without combustion compared with the same for the old valve at 10 bar: the difference is evident.

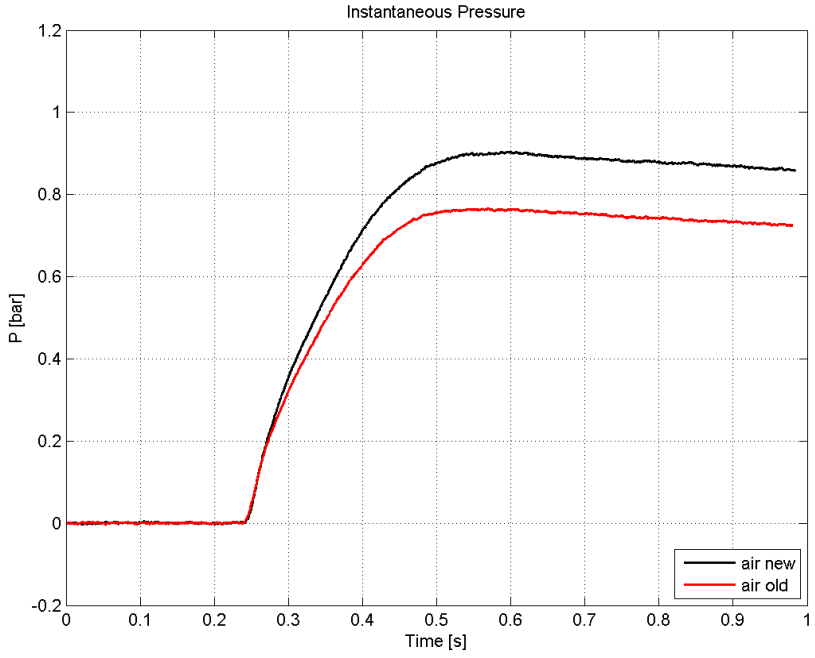

Figure 39: Comparison of instantaneous pressure between signals obtained at 10 bar and 700°C with old and new valve

For this reason, all the tests should be carried out and the pressure increment recalculated.
The attention was focused in particular on Iron tests, since the use of aluminum seems to be very complicated for its properties and attitude to create clusters for the humidity.
In this second phase, a new kind of nano-particle was investigated: its diameter is around 70 nm but it was produced by APTL with a different process from the other one produced from NEO.
For each type of nano-particle, a lot of test were done in order to point out an average trend comparable to the others, and the ΔP was calculated, as it is pointed out in the image below. The nano-particles with a diameter of 70 nm show the greatest amount of energy: for this reason their peak is the highest; however, the one produced by NEO releases more energy than that produced by APTL with a different process. Among commercial nano-particles, Fe50 always shows the best combustion attitude.
Comparing these results with those previously obtained with the old valve, they reach higher values than the older but the diameter trend is the same. In the image below it is reported only the ΔP that was calculated evaluating the pressure difference between combustion and no-combustion tests.

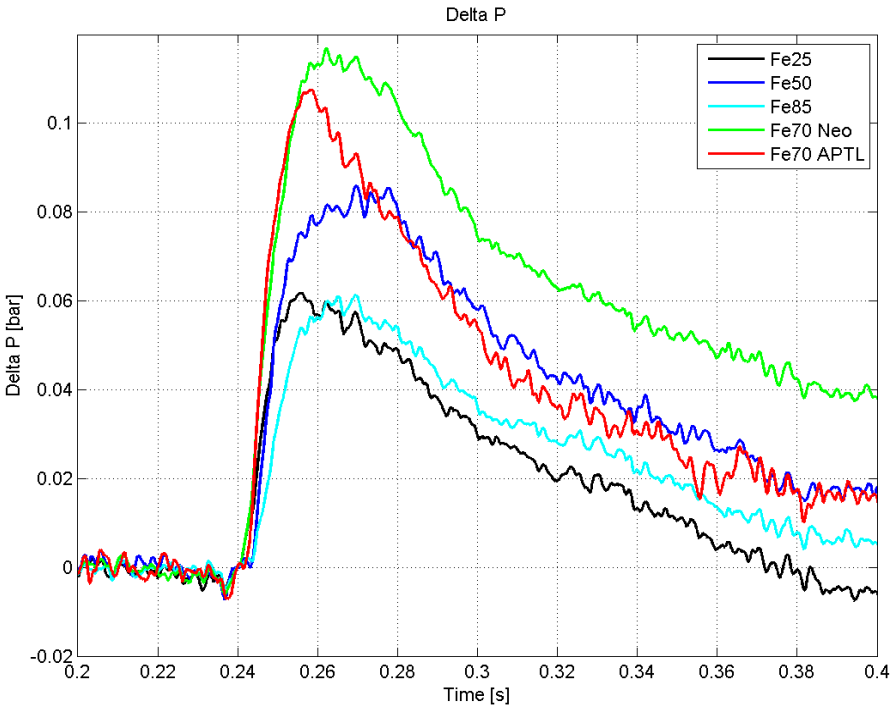

Figure 40: ΔP generated by the combustion of Iron at 700°C and 10 bar

5.6 Comparison between different amount

At the end of these consideration, it is interesting to point out another result that it has been obtained. In particular, as Fe 70 produced by NEO performs the best attitudes for combustion, some tests with different amount of nano-particles were carried out (these test are also investigated for the emission analysis that will be explained in the following chapter).
The quantities investigated are: 30mg , 50mg and 70mg; the procedure is always the same and the attention is focused on the pressure increment.
The results are interesting because show that an amount of 30 and 50 mg produces the same increment, on the contrary the use of more nano-particles evidently increases the pressure, compared to the test without combustion. The following image points out these considerations:

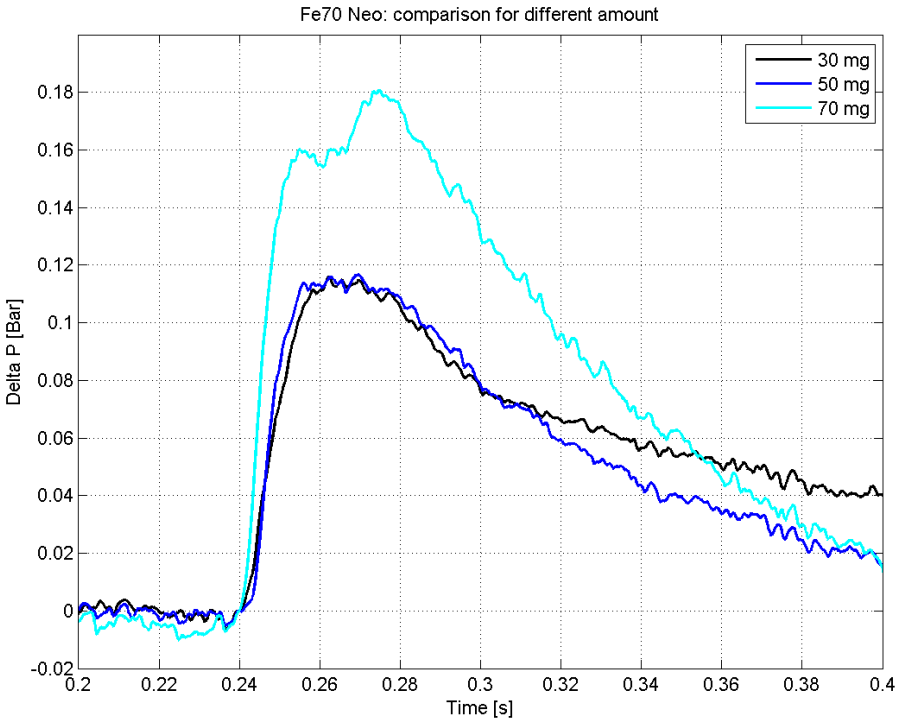

Figure 41: ΔP generated by the combustion of Iron in different amount at 700°C and 10 bar

As it is evident from the image, the pressure increment for an amount of 70mg is clearly higher than the other two quantities ant the peak reaches a value around 0.18 bar. The strange behavior recorded for 30 and 50 mg, probably is related to material impurities.

Chapter 6

Measurement of pollutant emissions

In this chapter will be presented the analysis of NO_x emissions: in particular, following a brief explanation about their formation and the procedure to measure them, the results are reported.

6.1 NO_x formation

As It has just been explained in the previous chapter, the attention is focused on emission measurements: in particular, the results are concentrated on NO production, because the presence of NO_2 and N_2O is so small that the Horiba produces a negative concentration and this could not be taken into consideration.

In general, Nitrogen N can combine with Oxigen and form a group of pollutants called "Nitrogen Oxides", very dangerous for the environment and for human health. In the clean air, the most abundant oxides are NO and NO_2 and their presence is incremented by humans activities: normally they are indicated with the name NO_x as a sum of them.
The engines are one of the most important cause of NO production: in fact, in an engine, a complete and stoichiometric combustion with air should not generate pollutants; however, the small combustion time and the non homogeneous mixture, the rapid variation of temperature and the presence of other compounds in fuel and air, could not allow to obtain an optimal combustion without developing any product harmful for the environment.
The NO_x emissions are the most controlled contaminants in the engine also with particles and they are composed, principally, by NO and NO_2. During the

combustion process, it is possible to identify three different mechanisms for NO formation:

- Thermal
- Prompt
- From fuel

Different studies were conducted about these mechanisms coming to the conclusion that, for internal combustion engine, the most important is the first one: the thermal formation is known as "Zeldovich Mechanism" [5], based on the fact that the mechanism starts with the formation of Oxygen mono-atomic at high temperatures; in particular, the first reaction is:

$$O_2 \rightarrow 2O$$

Secondly, the Nitrogen is easy oxidized, as:

$$O + N_2 \rightarrow NO + N$$
$$N + O_2 \rightarrow NO + O$$
$$N + OH \rightarrow NO + H$$

Lavoie [6], also proposed other three reactions taking into consideration the formation of NO via N_2O, as follow:

$$H + N_2O \rightarrow N_2 + OH$$
$$O + N_2O \rightarrow N_2 + O_2$$
$$O + N_2 \rightarrow NO + NO$$

From these equations and considering the velocity of reaction in both directions, it is possible to calculate the evolution of the NO, N and N_2O concentrations.
Lavoie proposed an equation for the calculation of NO concentration evolution, as follow:

$$\frac{1}{V}\frac{d[NO]V}{dt} = 2(1-\alpha^2)\left[\frac{R_1}{1+\frac{\alpha R_1}{(R_2+R_3)}} + \frac{R_6}{1+\frac{R_6}{(R_4+R_5)}}\right] \quad \textbf{(15)}$$

Where $\alpha = {[NO]}/{[NO]_e}$ is the quotient between actual concentration of NO and the one obtained in equilibrium with the same conditions of temperature and Pressure, and the index 1-6 referred to the reaction velocity *R* of the last six equations; the formation rate is zero when α=0.
If we don't consider the influence of N_2O in the formation of NO, and taking into account that [NO] at the beginning of combustion is minor than $[NO]_e$, the formation rate can be expressed with the following equation:

$$\frac{d[NO]}{dt} = 6.10^{16}\, exp\left(\frac{-69090}{T}\right) T^{0.5}[O_2]_e^{0.5}[N_2]_e \qquad \textbf{(16)}$$

Where T is the temperature in Kelvin and $[O_2]$ and $[N_2]$ represent the molar fractions calculated in equilibrium conditions, as showed with 'e' index.
It is possible to observe the strong relationship between the formation of NO and the temperature that influences more than the concentration of N_2 and O_2. For this reason, it is evidenced that the temperature characterizing the combustion process is one of the most important factor in the NO_x formation: one of the criteria for its reduction is the use of a lower combustion temperature.

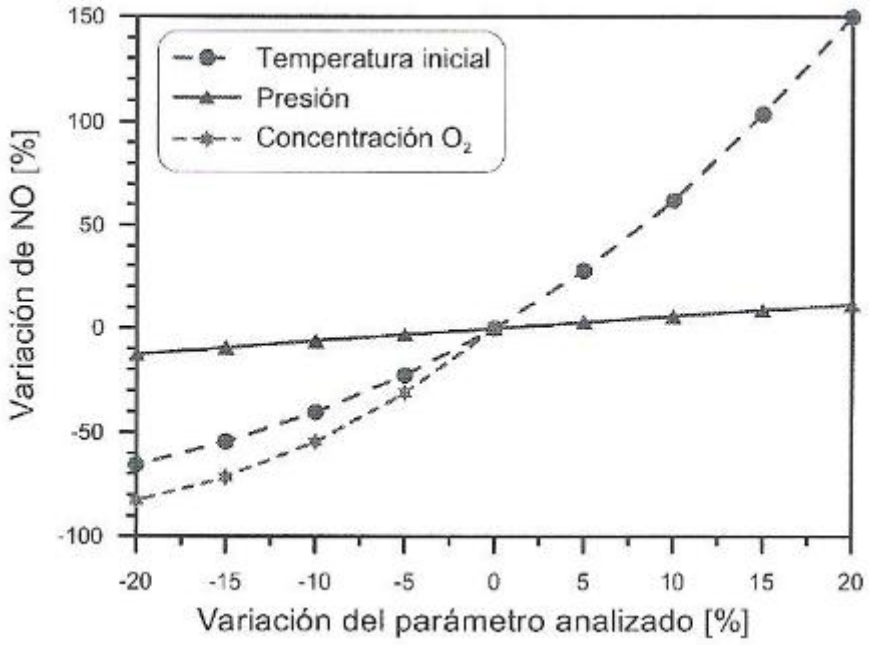

Figure 42: Percentage variation of NO concentration as a function of the percentage variation of Temperature, Pressure and $[O_2]$[5]

The presence of Nitrogen Oxides in the atmosphere causes problems in three different aspects:

- Interaction with Ozone
- Acid rain phenomena
- Harm to human health

For these reasons the study of engine emissions is a very important part in the creation of a new engine-fuel.

6.2 Procedure and results

In order to calculate emissions, some combustion tests have been carried out in the same operating conditions of the normal tests explained above; the difference is that, after the test, the exhausted gas collected into the filter, is put into a suitable bag, with a maximum volume of 5 liters. Following, this bag is analyzed by Horiba.

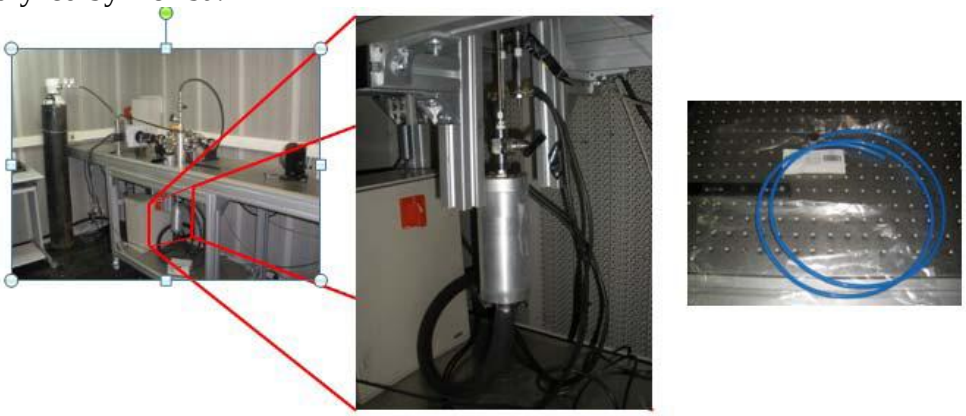

Figure 43: Image of filter system and the bag for exhausted gas

Different tests with different amount of nano-powders and temperature have been carried out, as summarized in the table below; the last column reports the average values of NO concentration, that are pointed out in the following images.

Nano-Powders	Injected mass [mg]	Temperature [°C]	Valid repetitions	NO average [ppm]
Air	0	700	1	0,7462
Fe 70 Neo	30	700	3	0,9610
Fe 70 Neo	50	700	4	1,1659
Fe 70 Neo	70	700	3	1,3979
Fe 70 Neo	50	750	2	1,9720
Al 18	30	750	2	2,1636

Table 5: Data regarding results of emission tests

The following images show the results about formation of NO during combustion. Each image points out NO measurements of the different tests and the line represents the avarage value.

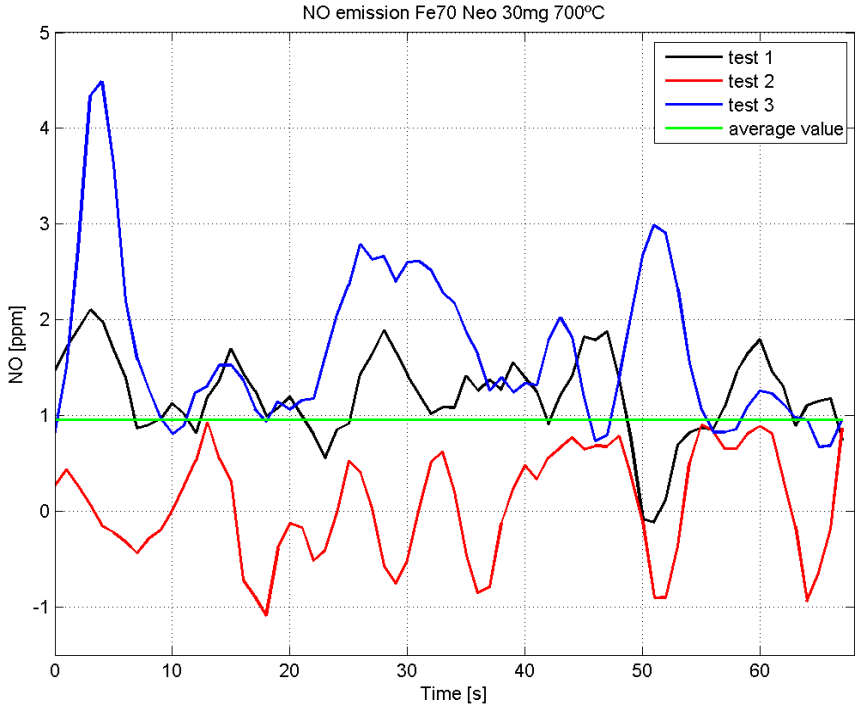

Figure 44: Results of NO emission for 30 mg of Fe70Neo at 700°C

In the case of 30 mg, the average value is around 1 ppm or little more if test 2 is eliminated.

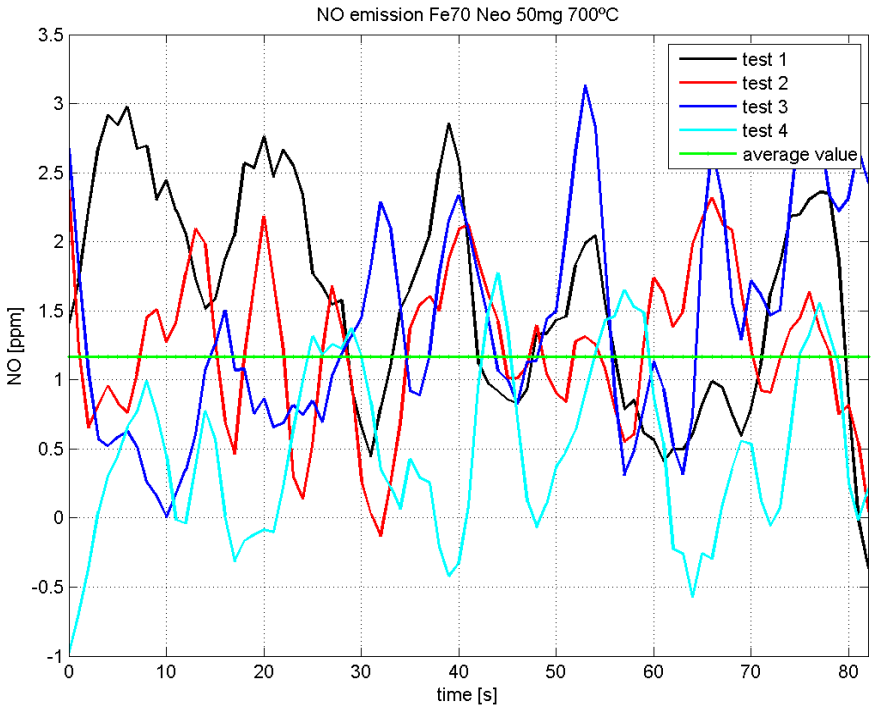

Figure 45: Results of NO emission for 50 mg of Fe70Neo at 700°C

In this case (50 mg), the average value is more than 1 ppm, around 1.2 ppm; if tests 4 is eliminated, the mean value has increased near to 1.4 ppm.

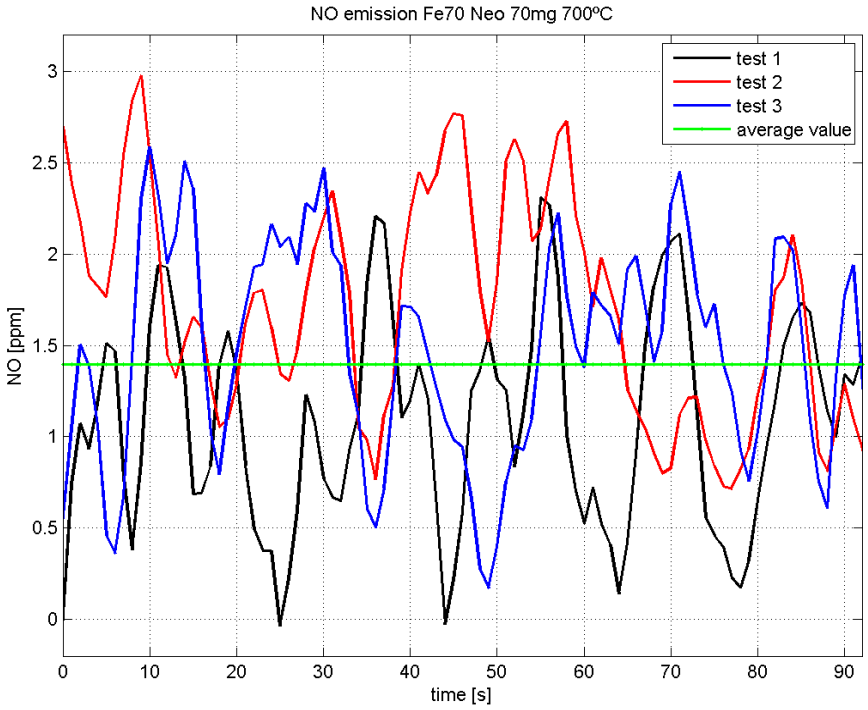

Figure 46: Results of NO emission for 70 mg of Fe70Neo at 700°C

The average value is higher than others tests with a minor quantity of nano-powder and it is around 1.4 ppm.
In order to have a complete idea of NO formations, same tests with 50 mg are have been performed reaching 750°C before the combustion.

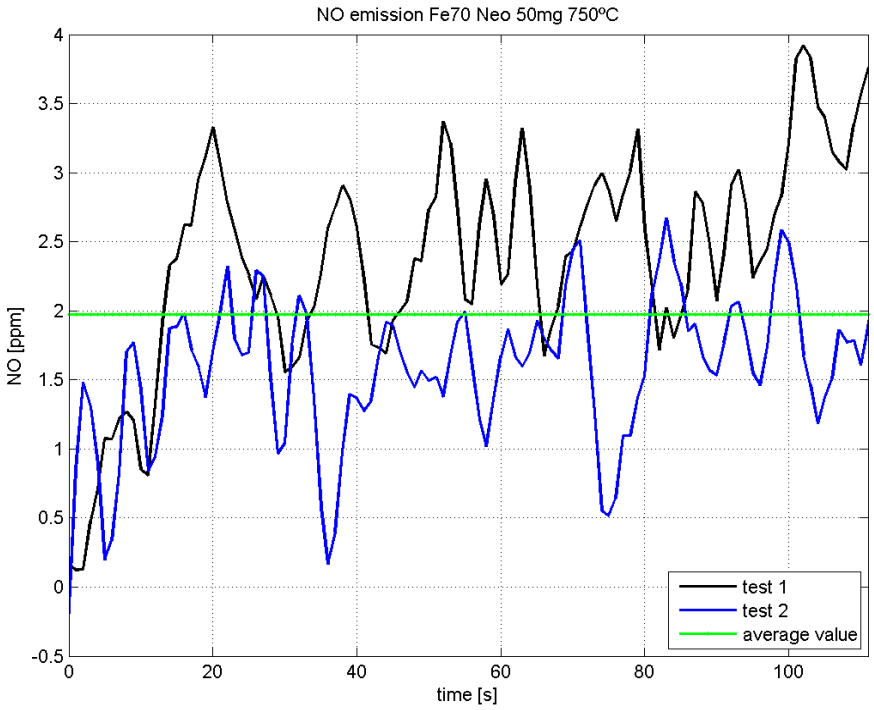

Figure 47: Results of NO emission for 50 mg of Fe70Neo at 750°C

As can be seen, the average value is higher (around 2 ppm) than the same amount of particles at 700ºC. This result is in accordance with the aforesaid theory, in which the temperature resulted the most important factor in the NO formation.

Finally, some tests were conducted to see the NO formation during combustion of Aluminum 18 nm; in this case, the operating temperature was 750ºC.

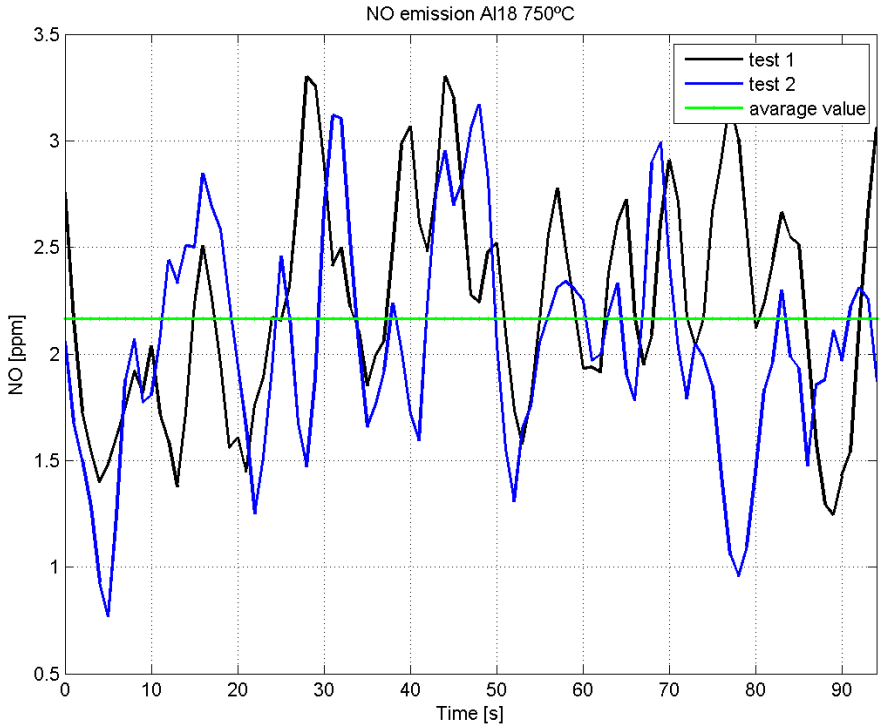

Figure 48: Results of NO emission for 30 mg of Al18 at 750°C

Due to the higher peak combustion temperatures, the average value of NO emissions is higher than iron, and it is around 2.2 ppm.
The following image is a result resume and points out the average values of different tests:

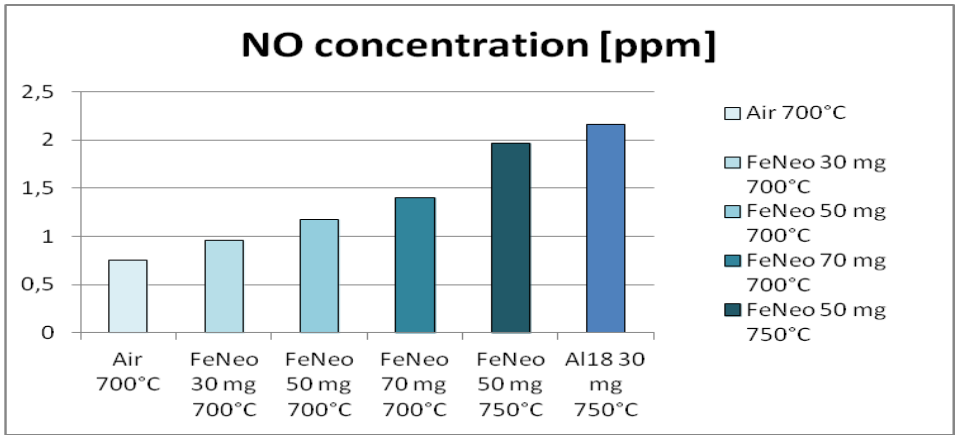

Figure 49: Comparison between the average values of NO concentration

The above image shows a test made without injected nano-particles, just to check if the air, heated at about 700ºC, reacts with the N2 present in the air; the test consists in analyzing the bag containing the air; the results showed an average value of 0.7 ppm, the smallest one.

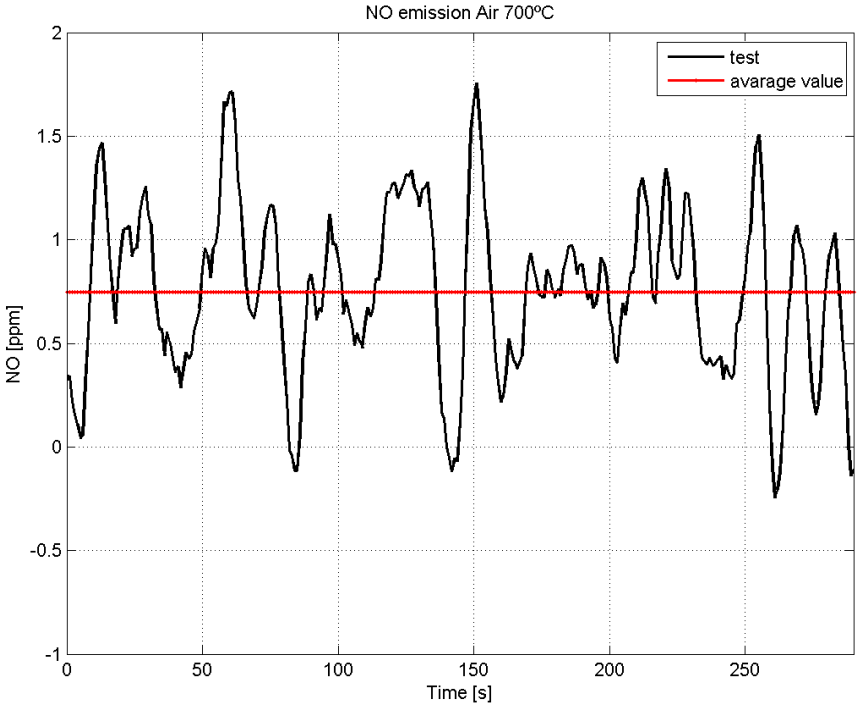

Figure 50: Results of NO emission for air at 700°C

Chapter 7

Post process of optical data

The second part of the analysis is about optical data. In this chapter, it is possible to find a brief explanation about optical techniques and the procedure for data post process saved with the camera and their subsequent results.

7.1 About optical techniques

A very important step in the flow visualization studies is the use of the Optical Technique; these techniques allow to develop experimental fluid mechanics and understand the complex phenomena that normally occurs. The visual observations alone can give only a qualitative information, like the ones obtained in this work.

In the early ‘60, the introduction of the laser, made possible the development of new optical techniques for non-intrusive measurements, based on the interaction between light and particles.

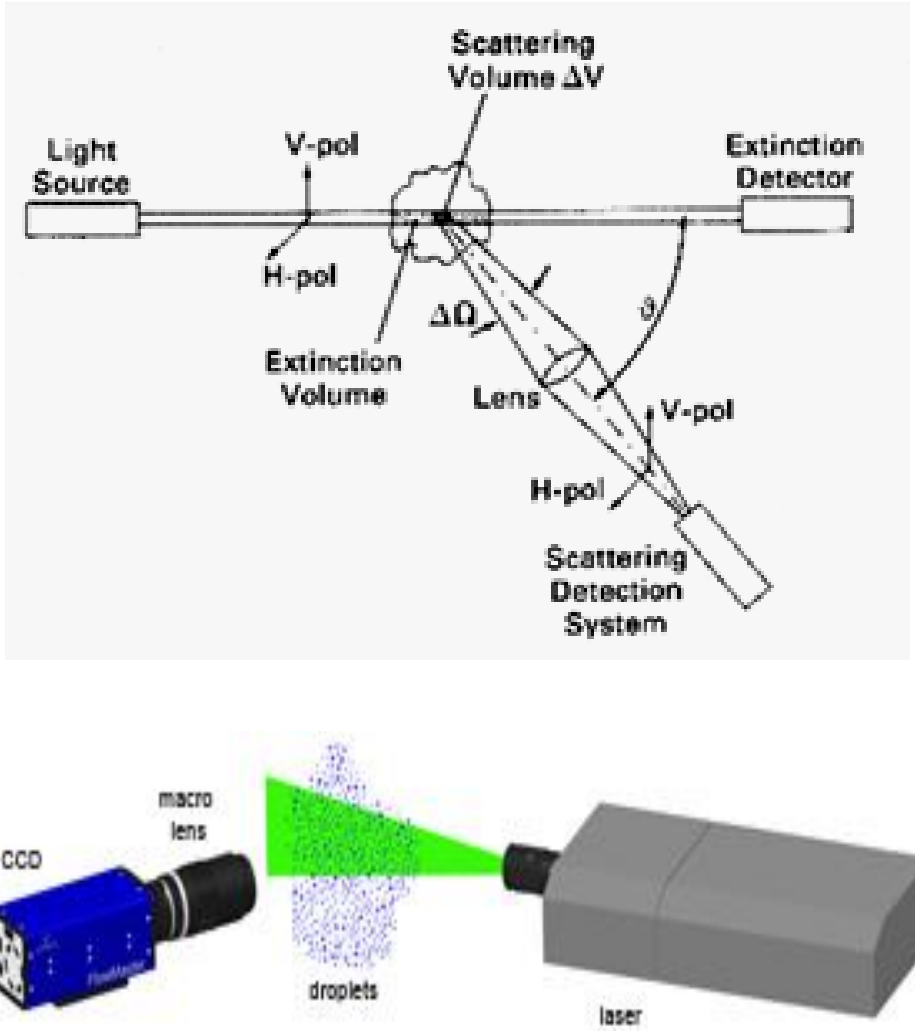

Figure 51: Scheme and components for optical analysis

One of the main basic concept of optical technique is the *Scattering*: it is determined by interaction of light with particles and its description was given by the Lorenz-Mye Theory, which is valid only for spherical particles. Whereas the diameter of these particles is larger than the light wavelength, the scatter intensity is approximately proportional to the diameter square.

There are different optical techniques but, in this case, a path integrated visualization method, called *Schlieren Technique*, is used as it's fundamental to focus the combustion region instead of single particles. For this reason, the camera is placed in front of the light. This technique is a method based on the changes in the fluid index of refraction [7-8]

$$n = \frac{c_0}{c} \qquad (17)$$

Where c_0 is the light celerity in vacuum, and c, the light celerity in the medium in question. This technique comes from a more simple one, the Shadowgraph, in which changes of light intensity on the screen are approximately proportional to the $\left(\frac{\partial^2 n}{\partial y^2}\right)$: It can be used to image flames or sprays, where the variation of temperature or density causes differences in the refraction index. In the Schlieren technique, the unique difference is the presence of a disturbance in the optical path that causes a deviation of light rays that are deflected of an angle α. This method is normally applied in optical visualizations in thermodynamics to visualize flows with no constant density gradients; it gives a qualitative but more clear idea about flows.
In the Schlieren technique, a collimated beam is purposely formed to go across the region of interest: when the rays face optical in-homogeneities, they refract proportionally to the gradients of refractive index they are going through, as explains in the follow equation:

$$\varepsilon_y = \frac{L}{n_o}\frac{\partial n}{\partial y} \qquad (18)$$

with ε is the refractive angle, L the path length, n_0 the surrounding refractive index, and $\vec{x}$ the ray direction in an orthonormal basis $(\vec{x},\vec{y})$.
The refractive index is specific of the element and of its density as given by Gladstone-Dale relationship: its constant *k* is determined by the phase, the component molecular content and organization and also changes with the ray wavelength.

$$n = k \cdot \rho + 1 \qquad (19)$$

When the rays pass through the particle laden gas, the interaction is different if they match nano-particles or the hot air; the follow image shows a schematic representation of the light deflection in case of a vaporizing liquid fuel. The ray deflection and their projection on a screen is a function of the density gradients: in the dense vapor region, the refractive index is higher and enhances greatly ray deflection, while in the mixing region of hot and cold air the refractive index decreases asymptotically down to ambient gas

values, reducing the refraction angle accordingly.

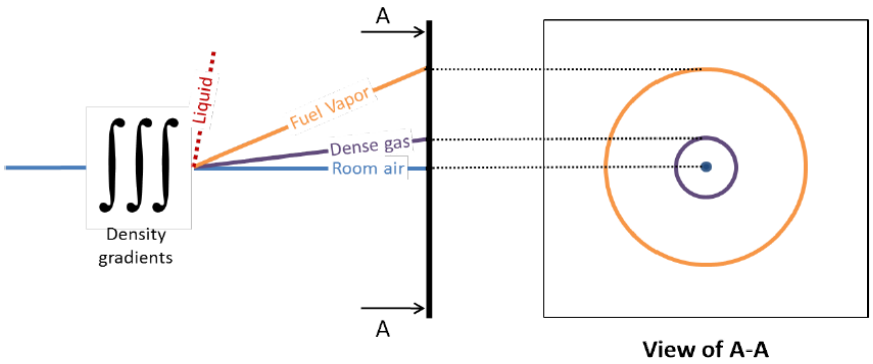

Figure 52: Schematic representation of the ray deflection caused by gradients of refractive index existing in a diesel spray [8]

In presence of burning solid particles, the hot gases surrounding the particles behave as the vapor phase in Fig.52 and deflect the incident rays. The particles may scatter or absorb the light and also produce spontaneous thermal emission which adds to the schlieren image and provide a combined information about the particle luminosity and their spatial distribution and the extension of the flame region. When this pattern of deflected rays and particle luminosity is collected by a lens and re-focused, their organization is maintained. Hence, all the rays with the same angle of refraction are focused on the same radius, and this offers the opportunity to select and filter rays as a function of their deflection.
When a camera lens system is used to collect the image, it collects both the schlieren image and the focused images of the particles. In fact, the imaging system, although focused, was actually sensitive to the schlieren effect, since the the most deflected rays were probably missing the collection system, composed by a collection lens and a camera lens. This makes of our setup an "uncontrolled" focused Schlieren setup. Therefore, as for numerous other optical techniques, the collection angle also plays a preeminent role and should be defined to make the image processing more reliable. To conclude, a Schlieren setup for spray visualization should focus on the spray, while maximizing the collection angle in order to control as much as possible the filtering in the plane of Fourier, the plane where the image where collected. Filtering in the plane of Fourier should be performed and accurately quantified: for this study, a filter of 30% was used in order to have clear images with combustion (light) and the background (dark).

Proper lighting is one of the most important aspect of flow visualization: a white light source is the best choice and it is the one used in this work. Also mirrors and arrangements configuration are very important to obtain clear and accurate

images; the first problem is to create parallel rays that can cross the vessel. The configuration is showed in the image below:

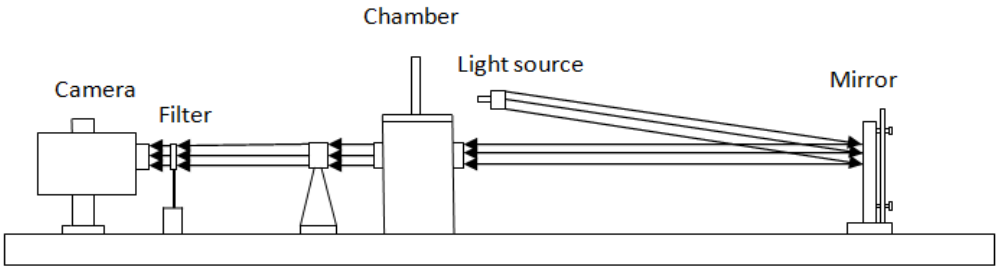

Figure 53: Scheme for testing with high speed camera

Figure 54: Real arrangement for testing with high speed camera

7.2 Procedure

As concerns the explanation quoted in chapter 4, the optical investigation is obtained with the use of a Photron: the camera records the combustion video in high definition. The optical technique allows to investigate in details what happens in the vessel and how the combustion takes place, showing also the different powder luminosity.
There is the possibility to save the whole video and also a video as a sequence of images, one for each frame: the second option is necessary to obtain an analysis of the total combustion in an unique image.
Each image is analyzed line by line to obtain information regarding the hot region, where there is a gradient temperature; by this way it is possible to identify the background (dark) and the combustion (light) and reduce the image to a vector $V_{t,,}$ which represents intensity accumulation for all the lines.

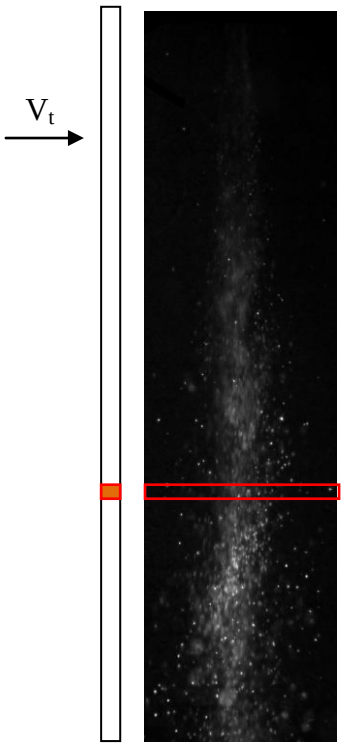

Figure 55: A real frame of combustion test

The sequence of all the vectors, one for each frame, gives the information about combustion in progress, concentrated in an unique image. The different colors point out combustion characteristics: in particular the red color is representative of the complete combustion of nano-particles, on the contrary the blue represents the background.

7.3 Results

The zero refers to the injector so the images should be read from zero to the top, corresponding to the bottom of the vessel, and from the left to the right for the behavior in progress. This analysis was realized for Iron at 700°C and under both 10 and 15 bar of pressure; on the contrary, Aluminum was investigated only at 10 bar but with a temperature of 750°C, because the higher temperature helps its combustion. Photron was set for working always with the following parameters:

- Frame speed: 21000 fps
- Exposition time: 1/228000 sec
- Resolution: 960 x 320

The colored maps reported in this chapter are the result of a single video.

7.3.1 Iron 25 nm

The two images below, both relating to Iron 25 nm at 700 ºC, show that the combustion is very quickly and concentrated at the top of the vessel; the combustion also presents a weak intensity in accordance with luminosity results listed in the previous chapter, which pointed out that Iron 25 nm releases the minor quantity of energy and luminosity, both for 10 and 15 bar as initial pressure.

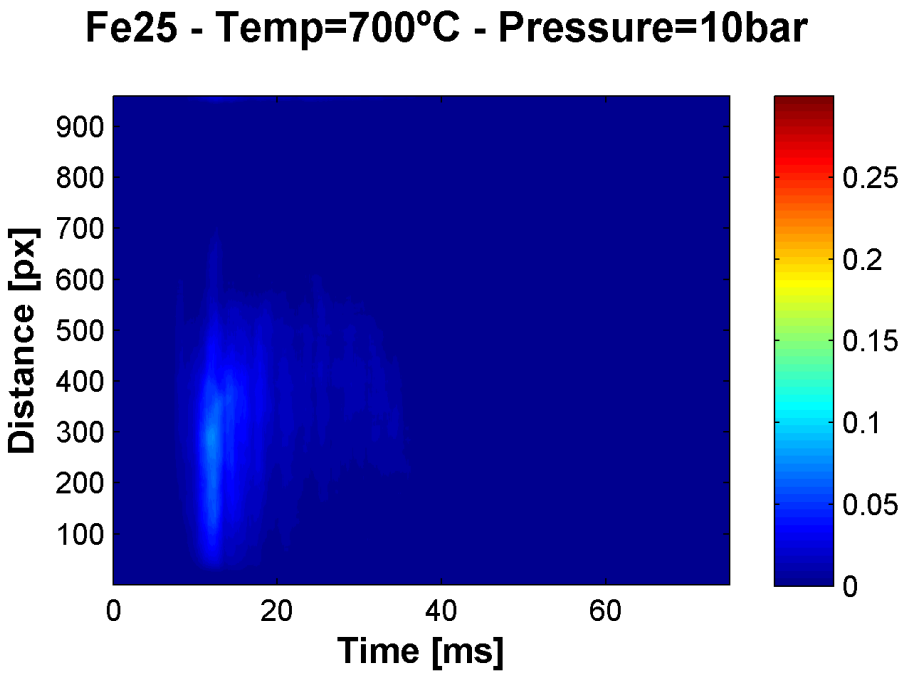

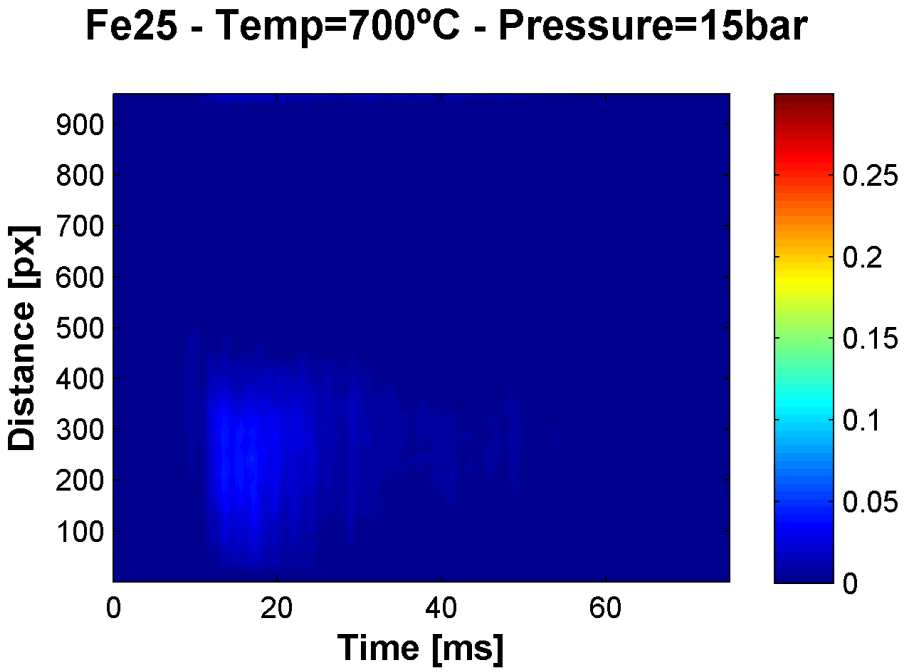

Figure 56:a) Image of Fe25 combustion process at 700ºC and 10bar; b) Fe25 at 700°C and 15 bar

7.3.2 Iron 50 nm

In these cases, the combustion shows more intensity than Iron 25, in accordance with the higher intensity registered by the photodiode; under 15 bar, the combustion appears in two steps in progress.

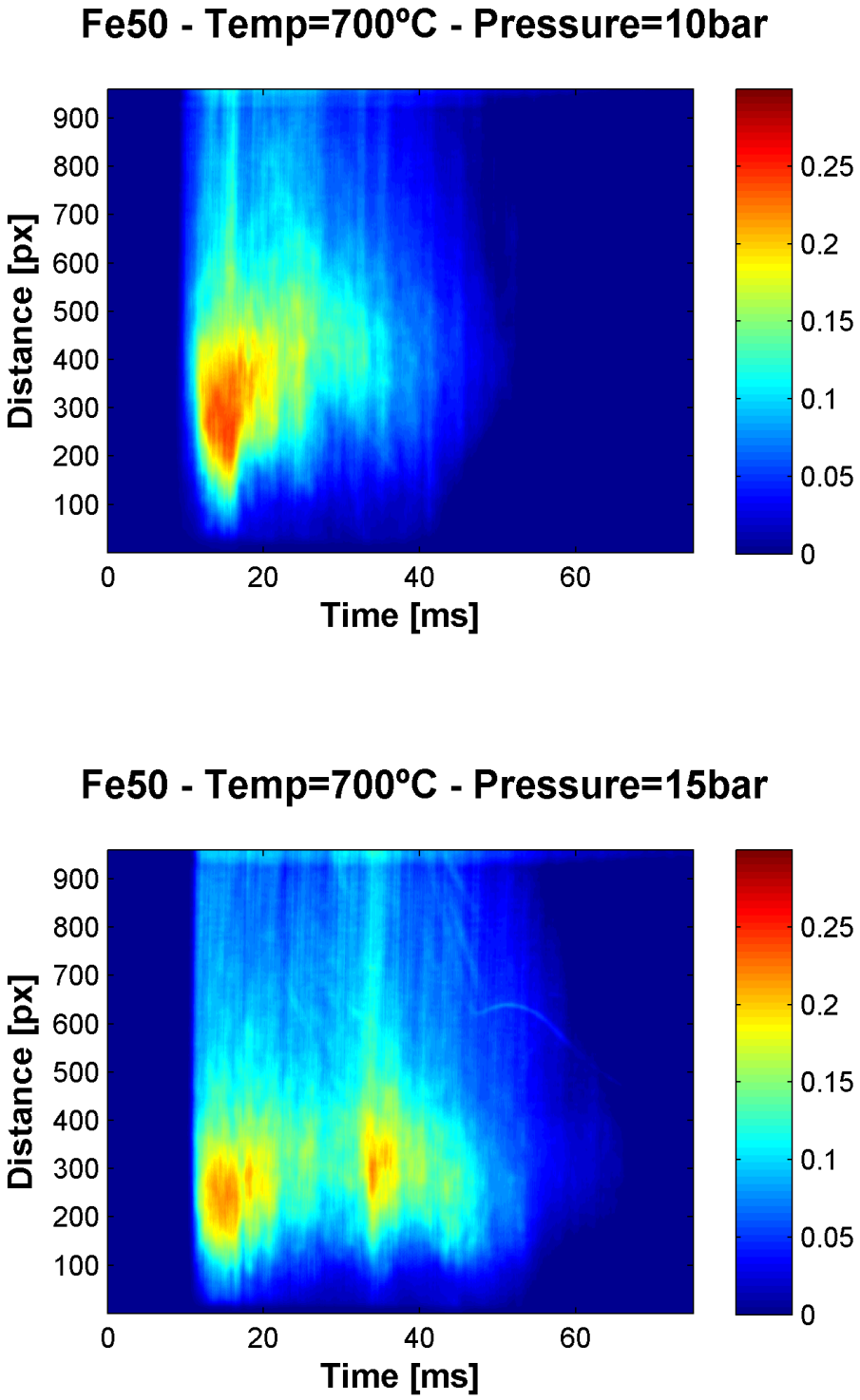

Figure 57: a) Image of Fe50 combustion process at 700ºC and 10bar; b) Fe50 at 700°C and 15 bar

7.3.3 Iron 85 nm

In the case of Iron 85 nm, the combustion seemed to be the most intense one, as it is possible to see by the presence of the red color. It occurred also in each part of the vessel, from the injector to the bottom of the chamber, and it is concentrated in a small time period.

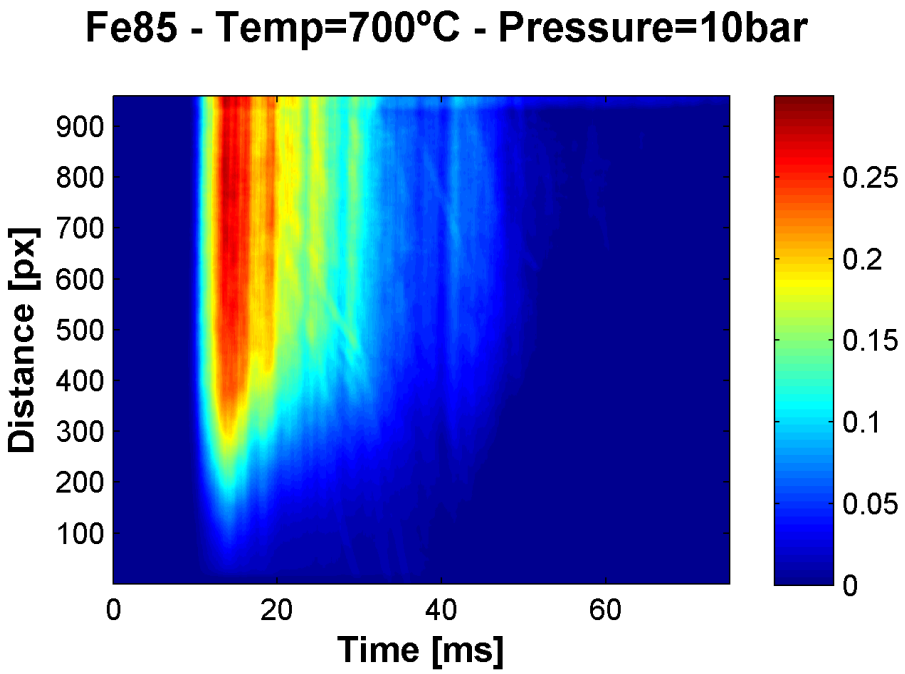

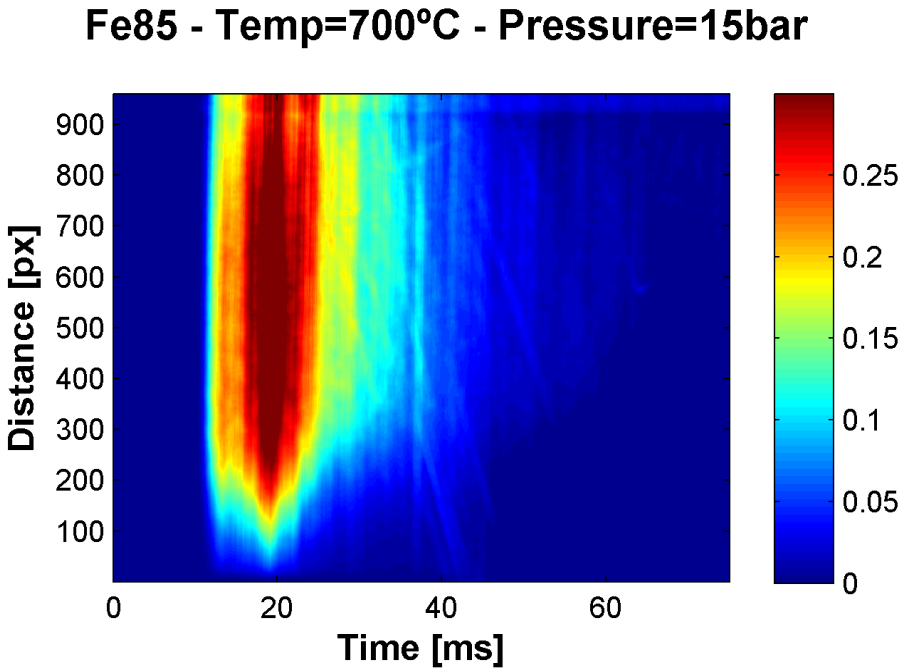

Figure 58: a) Image of Fe85 combustion process at 700ºC and 10bar; b) Fe85 at 700°C and 15 bar

7.3.4 Iron 70 nm produced by Neo

The results point out the most lasting combustion during time compared with other nano-powders; at 10 bar the combustion looks well diffused in the cylinder, instead at 15 it is more concentrated around the injector.

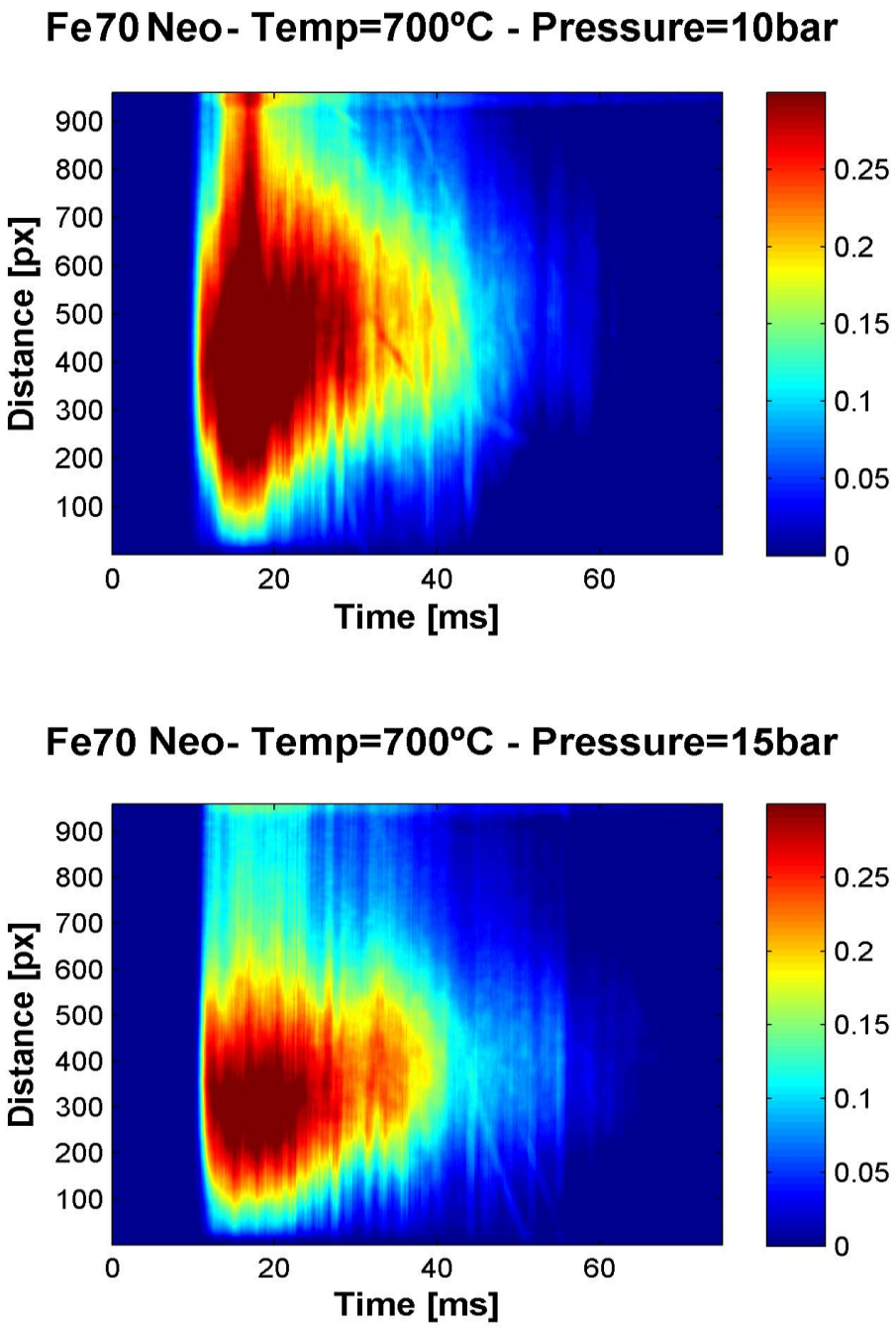

Figure 59: a) Image of Fe70 Neo combustion process at 700ºC and 10bar; b) Fe70 Neo at 700°C and 15 bar

7.3.5 Aluminum

In the case of Aluminum, the combustion looks very intense, as evidenced by the red color, and more concentrated at the bottom of the chamber, in particular for Al18; Al85, in accordance with the results about luminous intensity listed in chapter 5, produces a major luminosity and its combustion goes on for more time than Al18.

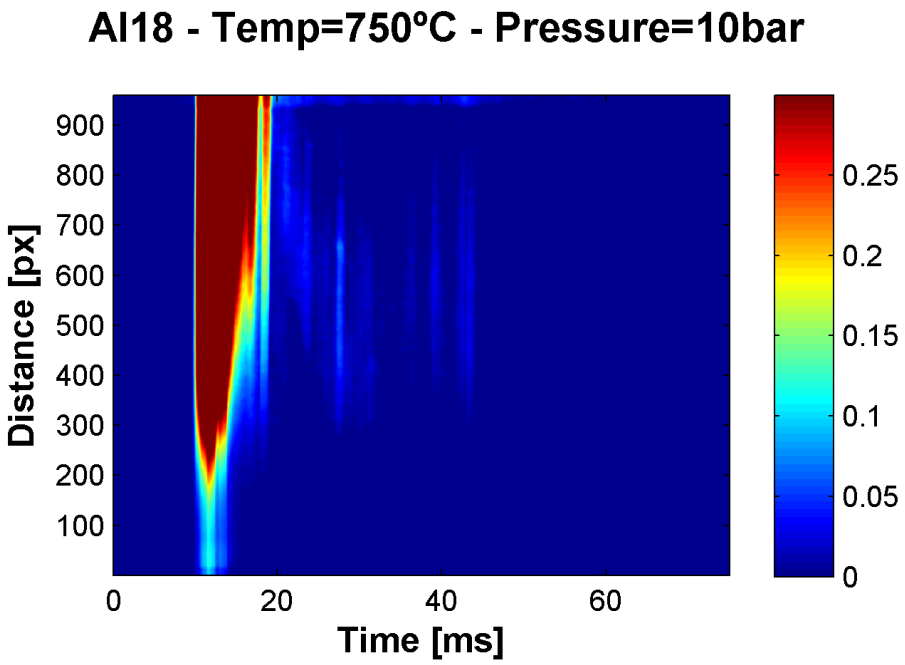

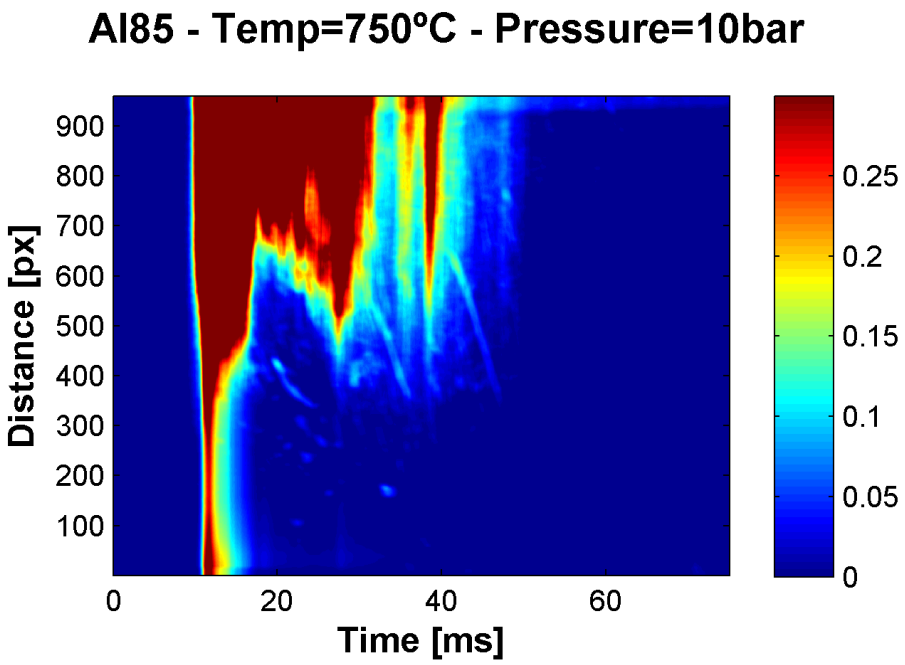

Figure 60: a) Image of Al18 combustion process at 750ºC and 10bar; b) (up) Image of Al85 combustion process at 750°C and 10 bar

7.3 Comparison

The images above gives a clear idea of the differences during combustion connected to dimensions and type of nano-particles. However, only observing the single frame registered by the camera, it is possible to notice them.
In the following images a comparison at 22 ms after particle injection is reported; pictures refer to test at 10 bar and 700°C for Iron and at 15 bar and 750°C for aluminum.

Iron:

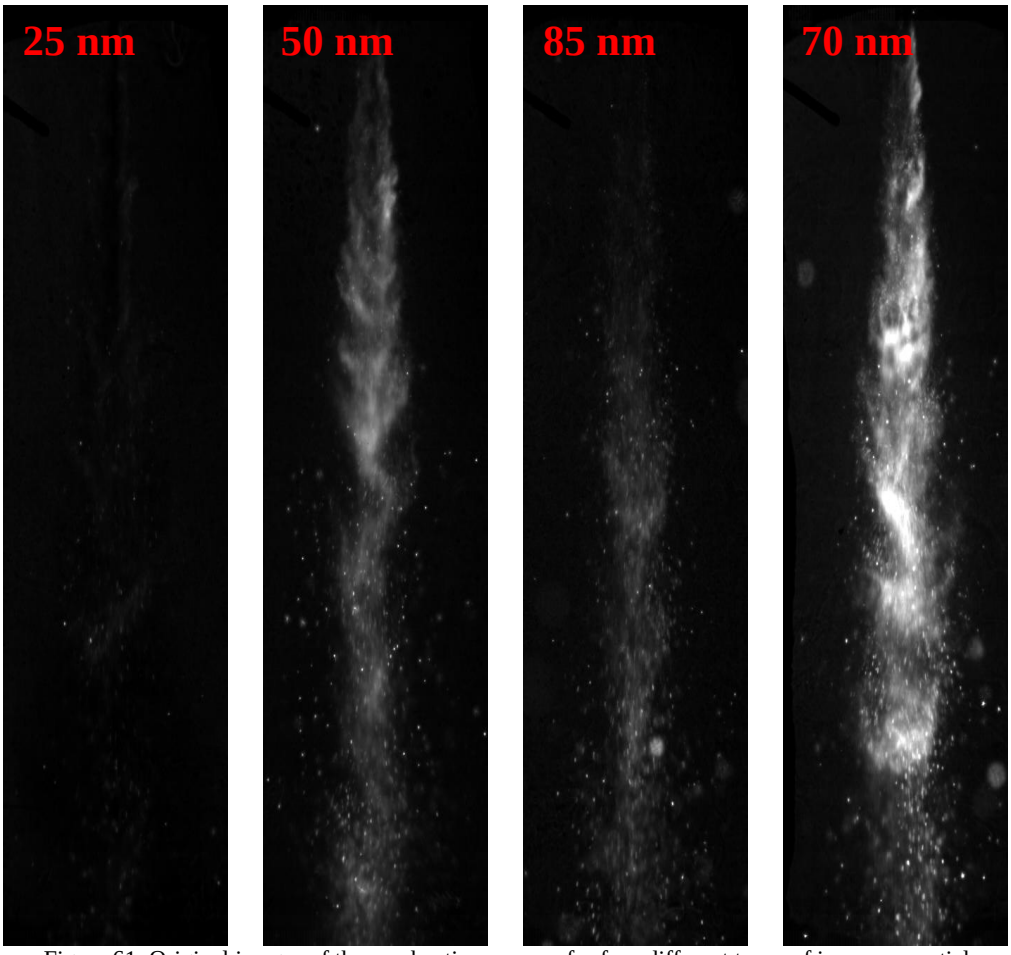

Figure 61: Original images of the combustion process for four different types of iron nanoparticles

Aluminum:

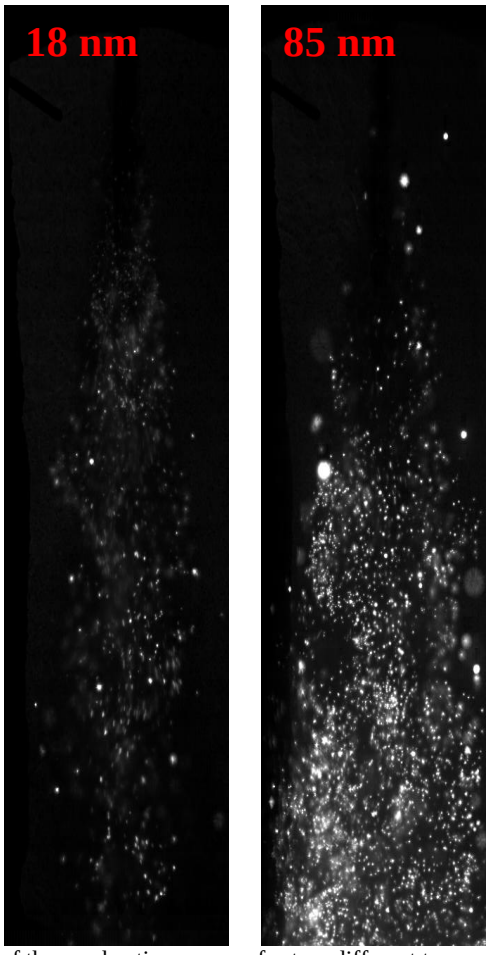

Figure 62: Original images of the combustion process for two different types of Aluminum nano-particles

As it has just been explained above, these pictures represent what the camera has registered during test combustion. As can be seen in these photos, the luminosity is also linked to thermal emission of burning particles, mainly for particles having bigger diameter.

Chapter 8

Regeneration

This chapter is focused on the performances for regenerated nano-particles. Actually, one of Cometnano project aim, is the validation of the possible re-use of nano-powders: the scope of this investigation consists in confirming this possibility, measuring the pressure increment generated during combustion.

8.1 Regenerated nano-particles

As it has just been explained in chapter 3, one of the most important characteristic in the use of nano-powders, is the possibility to regenerate oxides created after combustion, in order to use them again, without producing waste material.

It is possible to find hereafter an explanation of the tests conducted in order to obtain some information and propose a complete Fe nano-particles production/oxidation/regeneration scheme; a similar scheme is provided for the case of Al, but in this particular case, it is the intrinsic thermodynamic limitation to define such a scheme, rather than the effect of combustion to its nano-structuring. The experiments herein quoted involve the conduction of repeated 'spark-aided' combustion/'regeneration-by-H_2' tests during which oxidation characteristics of regenerated iron are reported with the aid of TGA under air, while TEM/EDS analysis shows the effects of this cyclic process on the nano-structuring of the metallic nano-powder.
The sample considered is Fe50 commercial nano-powder and the total number of combustion/regeneration cycles implemented is six; the conditions of the procedure are the same reported above.

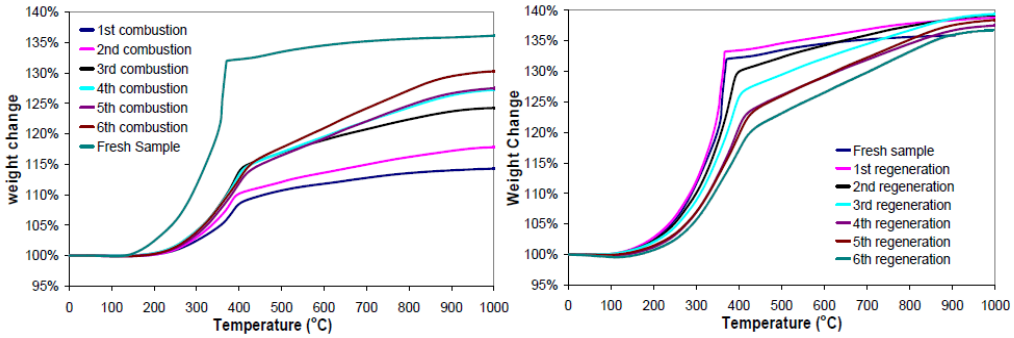

Figure 63: TGA under air analysis of combusted (left diagram) and regenerated with H_2 (right diagram) Fe50 nano-particles after each (combustion or regeneration) cycle [1]

A series of TGA analyses under air of oxidized and regenerated Fe50 nano-powder after each cycle are performed and the results are depicted in the image: the main observation is the fact that there is a clear degradation of the Fe50 oxidation characteristics as the number of cycles increases. In the case of combusted samples, it is evident that from 3rd combustion, the weight increase of oxidized samples is significantly higher in comparison to the samples after 1st and 2nd combustion. Regarding the regenerated particles, the Fe50 sample after its 1st regeneration with H_2 is essentially identical to the 'fresh' sample, in terms of its oxidation characteristics and non-negligible deviations are observed in the case of respective Fe50 sample after its 2nd regeneration.

About the nano-structuring, pointed out that there aren't evident differences between the fresh and the 1-time-regenerated Fe50 powder, as it is confirmed in the comparative TEM images below: the estimated APPS of the 1-time-regenerated Fe50 nano-powder is approximately 75nm, as compared to the respective 50nm value of the 'fresh' powder.

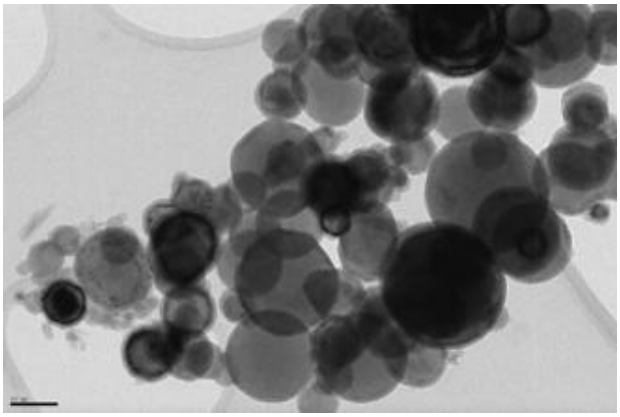

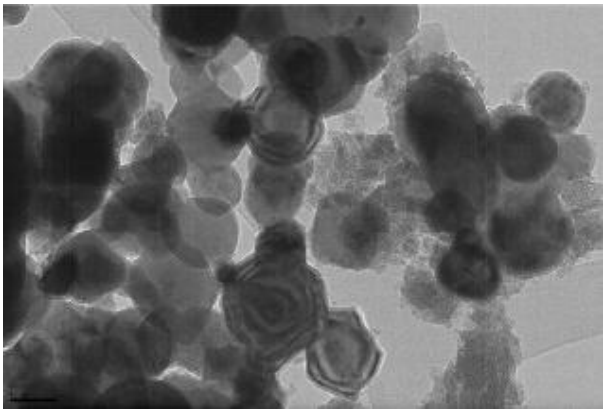

Figure 64: a) TEM images of Fe50 fresh powder; b) One-time regenerated Fe50

During these three years of this European project, there have been made many efforts on the possibility to reuse nano-particles: regarding Iron, a procedure should be found to transform Fe_2O_3 into Fe nano-particle, suitable for a new combustion and the same was performed for aluminum.

8.1.1 Iron

There are two possibilities for the preparation of Fe nano-particles with the aid of ASP:

1. Direct synthesis of carbon-coated Fe nano-particles by an iron-dispersible precursor dissolved in water/ethanol (1/1 molar ratio) with N_2 as carrier gas. These particles are, in most cases, surrounded by a 2-3 nm oxide layer and a 1-3 nm carbon one.
2. Synthesis of iron oxide nano-particles by an iron-dispersible precursor dissolved in water with air as carrier gas under suitable conditions. The oxidized nano-particles are subsequently reduced with H_2 at 400ºC for an exposure time of about 4 hours and at a Gas Hourly Space Velocity (GHSV) value of 5.0 gr $H_2 \cdot$(gr oxide nano-particles$\cdot$h)$^{-1}$. In this case, passivation can be performed by either exposure of the resulted metallic nano-powder to a low O_2 content gas or by leaving the powder for 12-14 hours under ambient conditions.

The choice of the most suitable procedure has been based on two criteria: the environmental impact of both methods and the combustion of regenerated nano-particles, and the quantitative experimental results obtained during the engine-like combustion tests. As a conclusion of these investigations, a suitable scheme for iron regeneration was pointed out and it can be resumed in the image below:

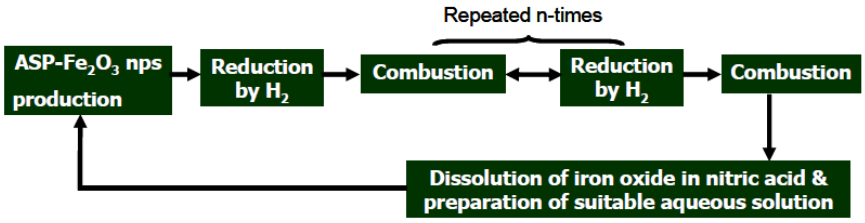

Figure 65: Proposed concept for the Fe nano-fuel, based on the relevant project results so far

8.1.2 Aluminum

The attention and the efforts were also focused on the Aluminum regeneration: in this case, the thermodynamic limitations allow only a method able to create/regenerate Al nano-particles, called Atmospheric Plasma Spraying (APS), due to its intrinsic capability of reaching temperatures in excess of Al sublimation point (about 2520ºC), which is a prerequisite for the preparation of Al nano-particles. The raw material was a micron-sized Al powder (20-45μm); they were sprayed at ambient atmosphere and the produced particles were hot-collected on a supported quartz filter: at the end of the process, it can be seen that the powders were clearly nano-structured with an APPS at about 20 nm.
A scheme of the production-regeneration cycle can be resumed in the following image:

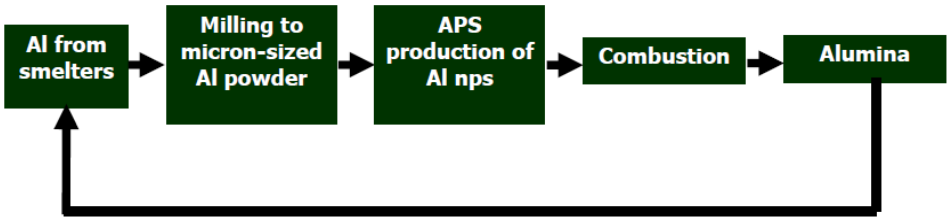

Figure 66: Proposed production/combustion Al scheme (APS: Atmospheric Plasma Spraying method)

8.2 Procedure

Test procedure with regenerated nano-particles is always the same, as showed for the nano-powders combustion. In particular, the operating conditions employed are the following:

- Amount: 30 mg
- Temperature: 700ºC
- Initial Pressure: 10 bar

All the tests were performed under the same values of pressure, in order to obtain reliable results:

- Average pressure: 16 bar
- Injection pressure: 60 bar

Regarding Iron, the available nano-particles were regenerated six times from burnt particles: for each kind, two or three tests were conducted and the average value was calculated; instead for Aluminum, nano-particles available are only regenerated from no combusted ones.

8.3 Iron

8.3.1 Instantaneous and Increment Pressure

The attention was focused on the Instantaneous Pressure: the measurements of different tests were compared and the average value was calculated. The following images show the behavior of P_{ins} and the relative pressure increment, referring to the difference of tests without combustion.

- 1st Regeneration:

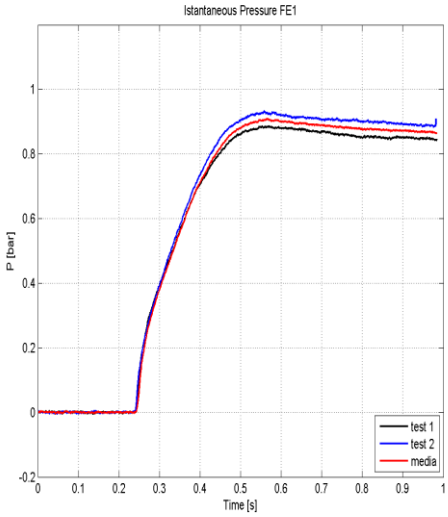

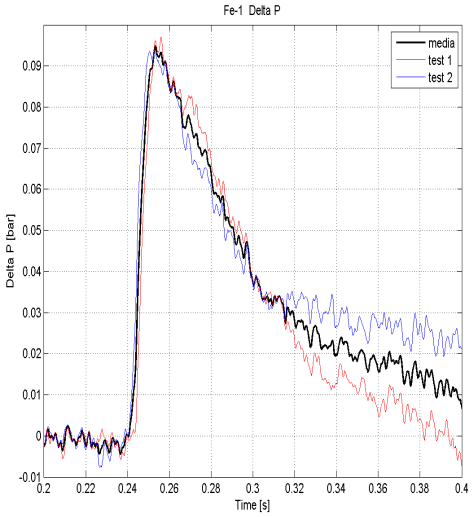

- 2nd Regeneration:

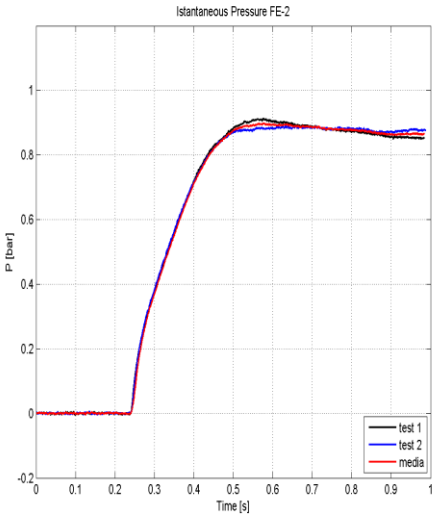

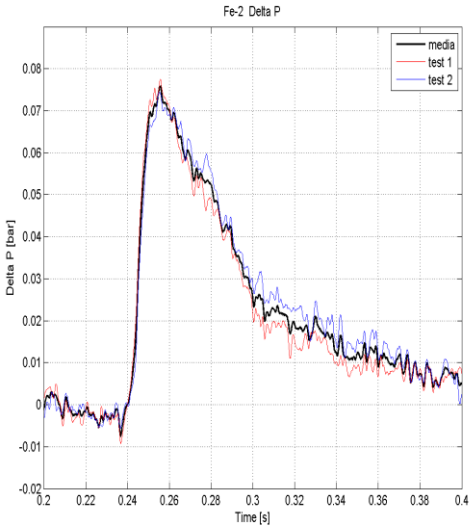

- 3rd Regeneration:

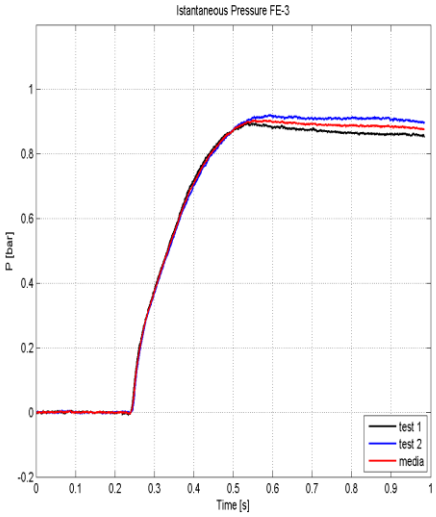

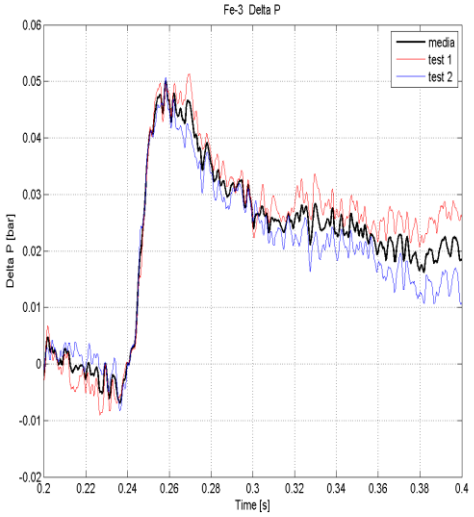

- 4th Regeneration:

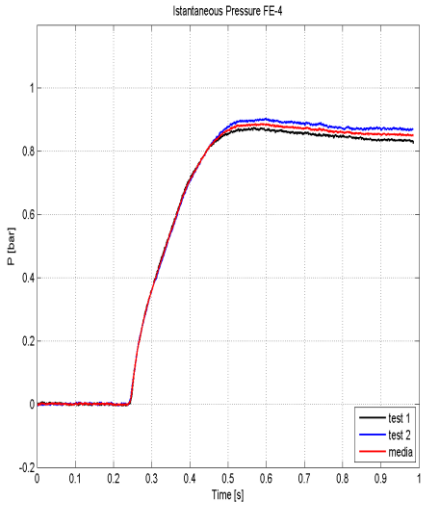

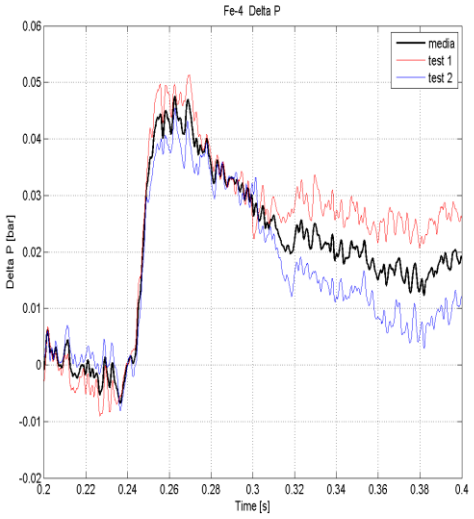

- 5th Regeneration:

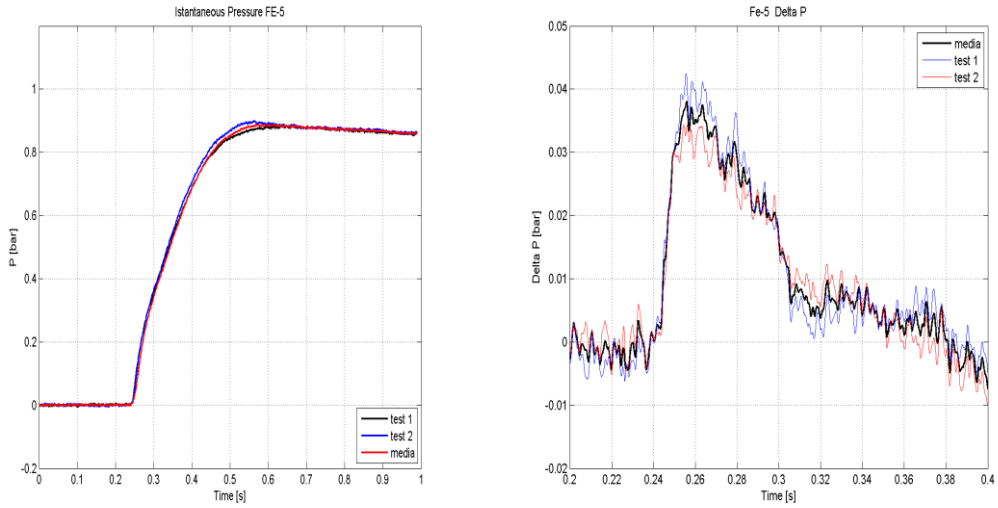

- 6th Regeneration:

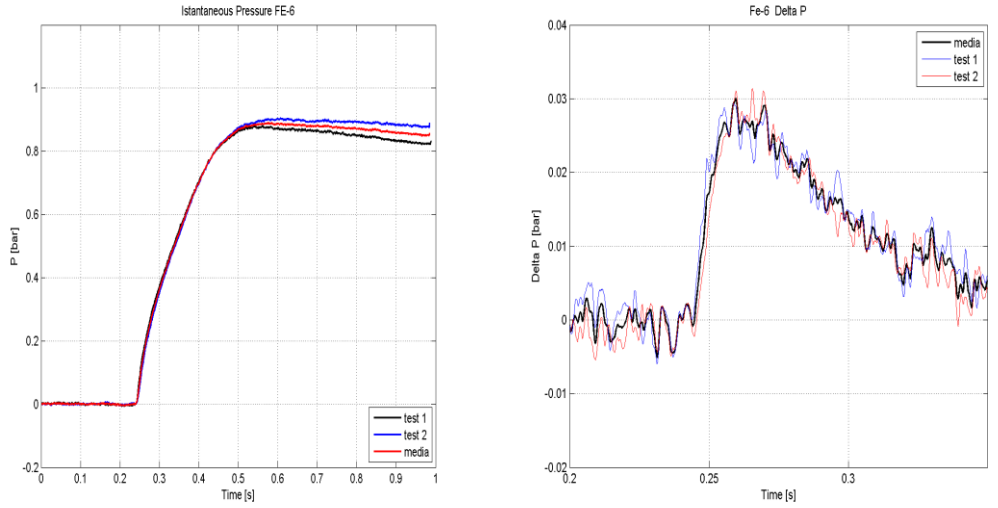

Figure 67: Instantaneous pressure for each cycle of combustion-regeneration (left); ΔP generated by the combustion of regenerated particles (right)

8.3.2 Comparison

After the calculation of average values for each regenerated nano-particle, the aim is to compare the results in order to verify the attitude of the samples. In the

following image, it is possible to see the behavior of all the particles in a unique image:

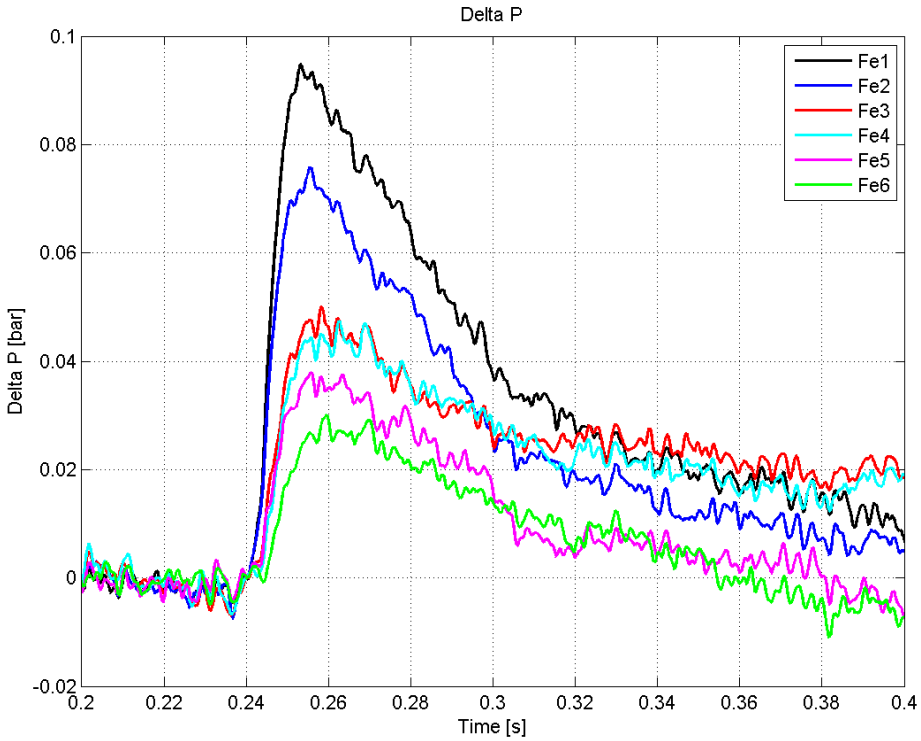

Figure 68: Comparison between ΔP produced by the regenerated particles

The image points out that, in accordance with the theory, the first and the second regeneration are useful, but, from the third on, the nanostructure is probably so modified that the energy content decreases sensibly. We can find another reason for this trend: each time that the regeneration process takes place, a part of burnt nano-particles can't be regenerated, so their performances evidently decrease.

The following important comparison, able to give useful information, is between the regenerated particles and the original ones. The following images point out the pressure increments released to the regenerated particles in comparison with all kinds of nano-particles studied in this work.

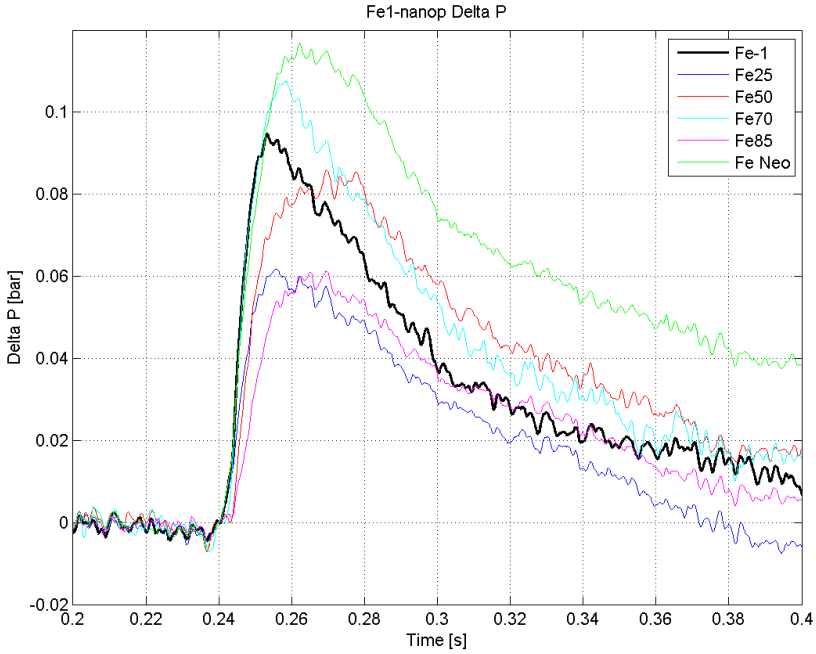

Figure 69: Comparison between ΔP generated by the combustion of 1-time regenerated particles and the different types of fresh iron-powders

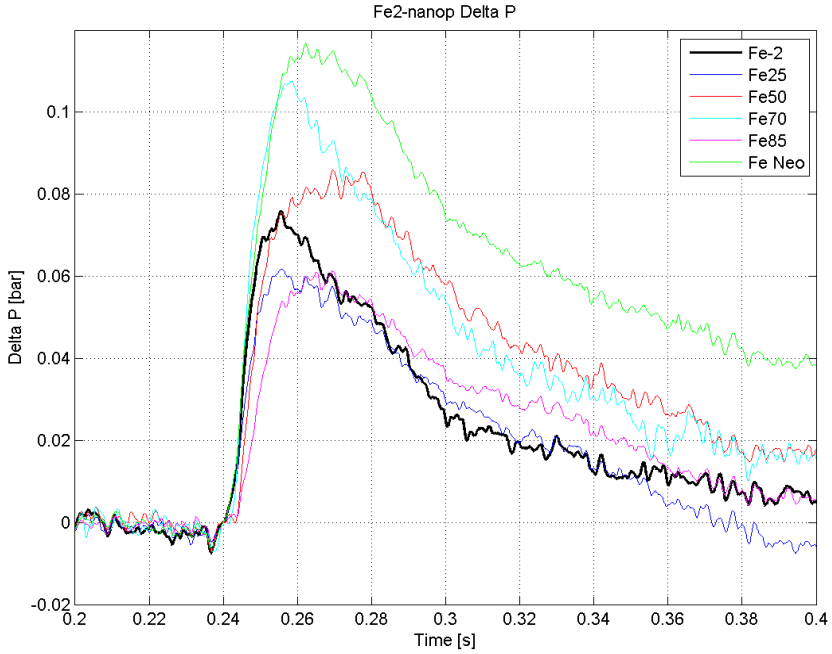

Figure 70: Comparison between ΔP generated by the combustion of 2-time regenerated particles and the different types of fresh iron-powders

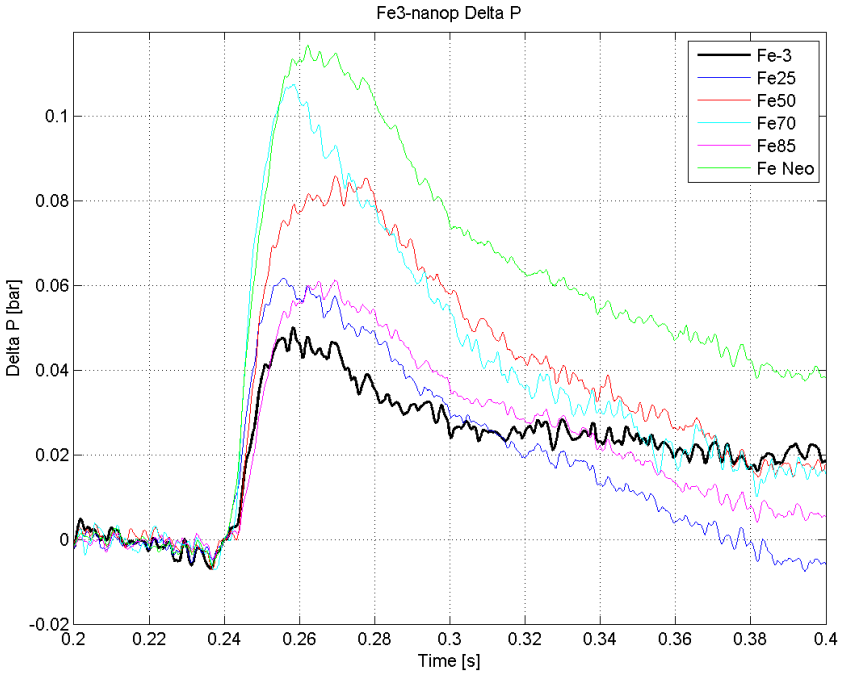

Figure 71: Comparison between ΔP generated by the combustion of 3-time regenerated particles and the different types of fresh iron-powders

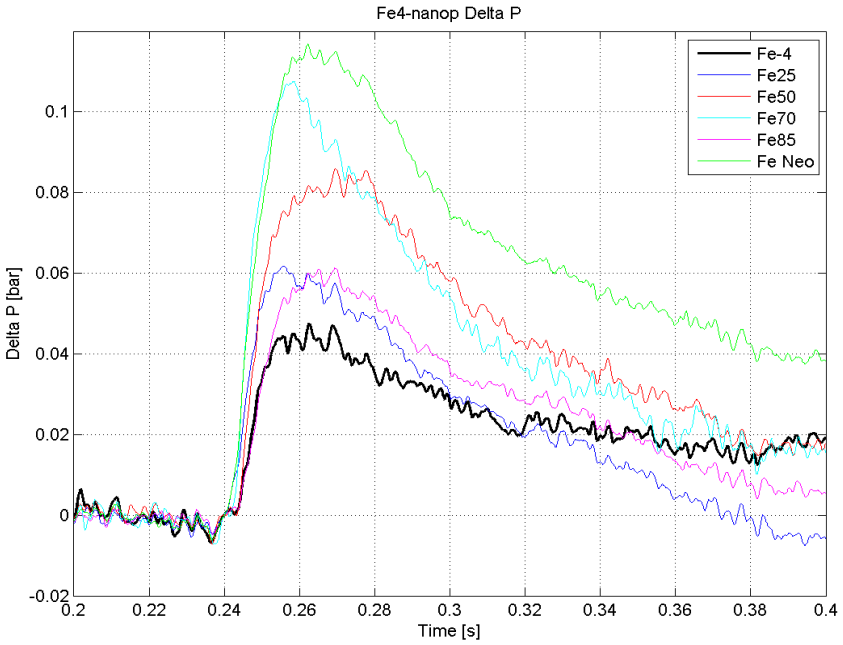

Figure 72: Comparison between ΔP generated by the combustion of 4-time regenerated particles and the different types of fresh iron-powders

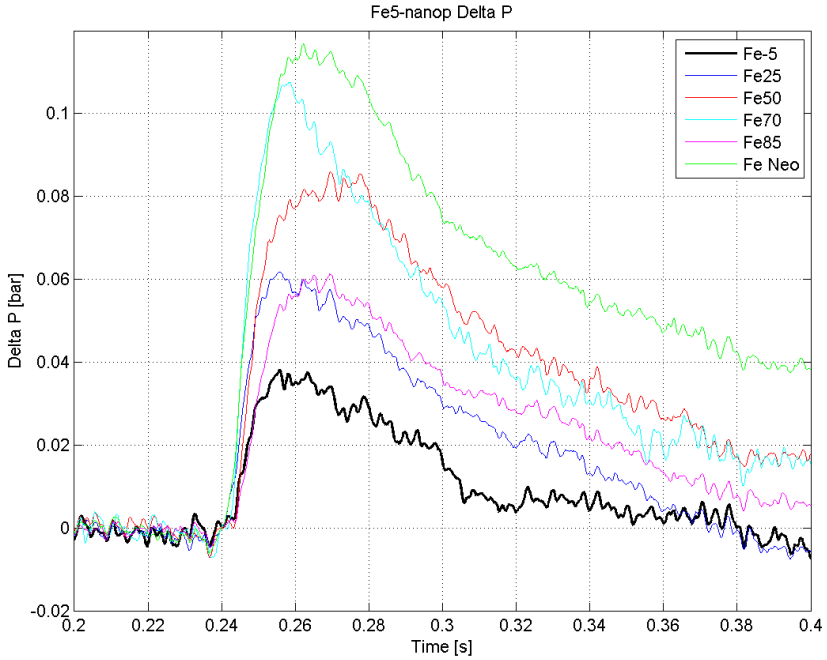

Figure 73: Comparison between ΔP generated by the combustion of 5-time regenerated particles and the different types of fresh iron-powders

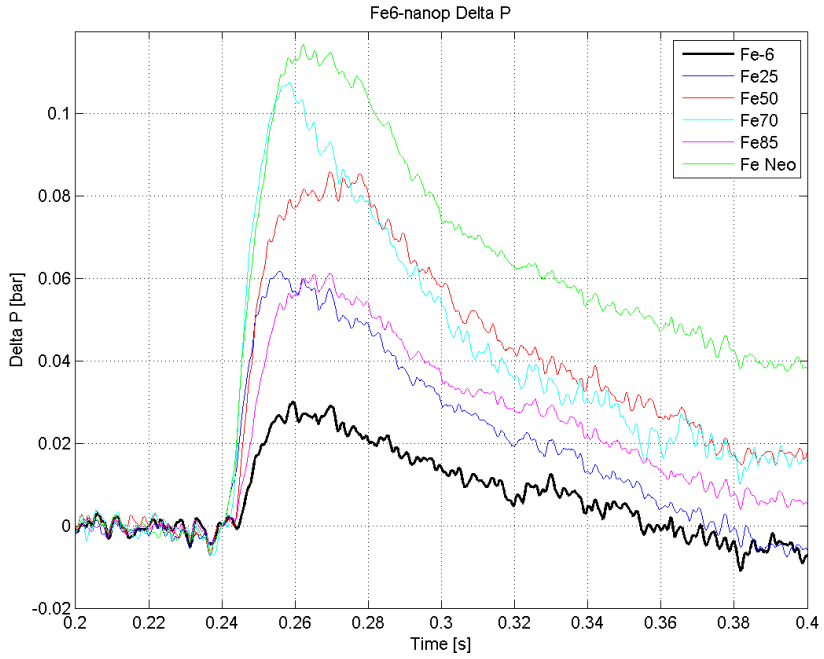

Figure 74: Comparison between ΔP generated by the combustion of 6-time regenerated particles and the different types of fresh iron-powders

This comparison confirms that only nano-particles once or two-times regenerated can be used in place of original ones, because after the second regeneration, the energy released is so little that the required amount particles necessary to produce the same energy of the original ones should be enormous.

Another possible comparison is between all regenerated nano-particles (from one to six-times regeneration cycles) and each kind of original ones, that are marked in black color in the images. In fact, the diameter of regenerated nano-particles is unknown; the following images point out when the use of regenerated particles is better compared to those having the original diameter.

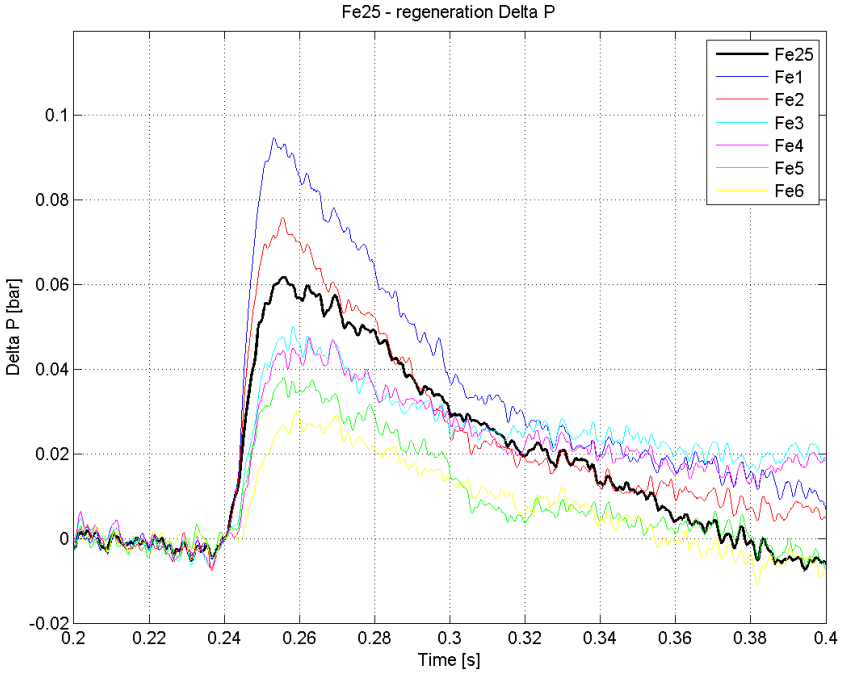

Figure 75: Comparison between ΔP generated by the combustion of Fe25 and regenerated particles

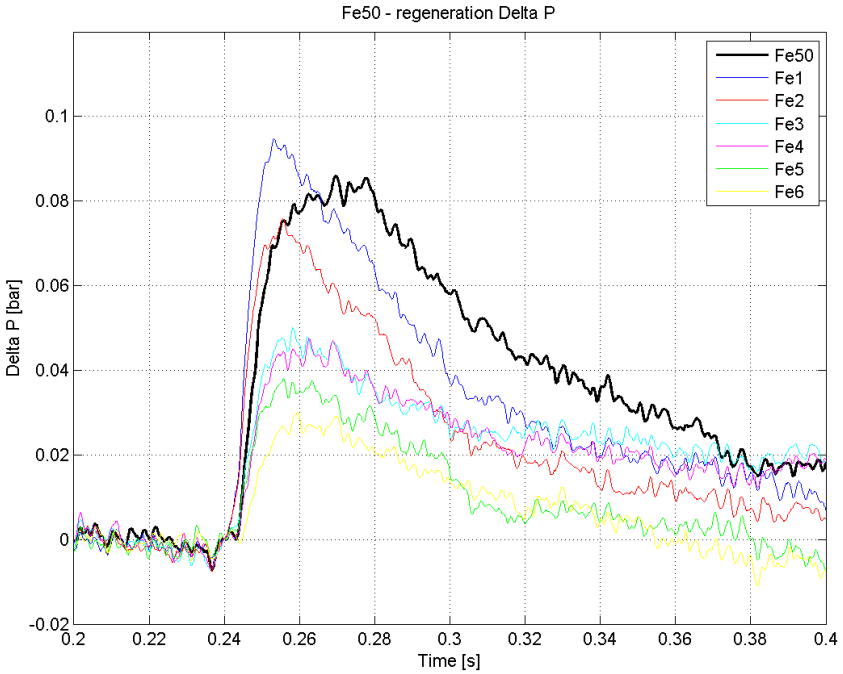

Figure 76: Figure 74: Comparison between ΔP generated by the combustion of Fe50 and regenerated particles

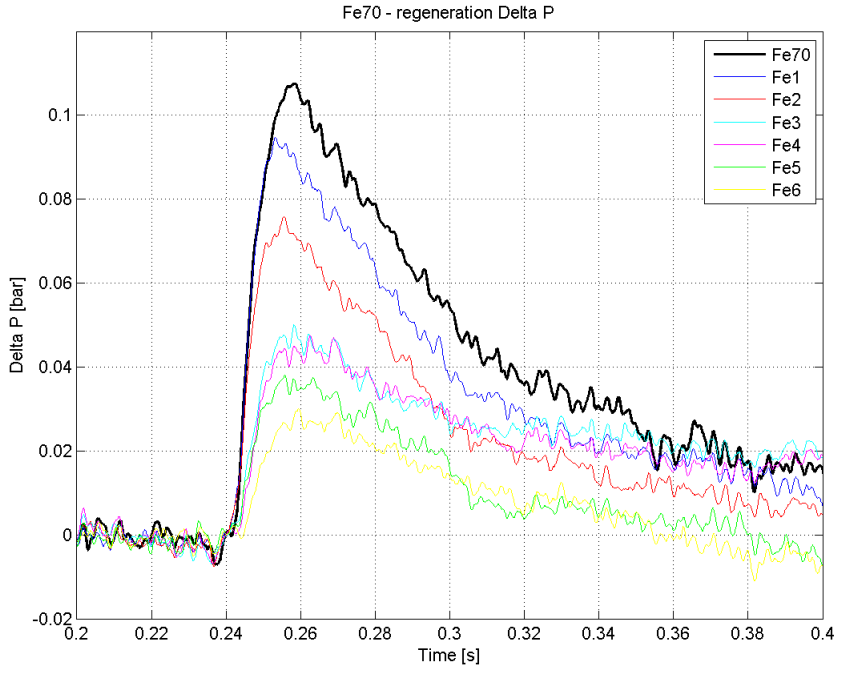

Figure 77: Figure 74: Comparison between ΔP generated by the combustion of Fe70 (APTL) and regenerated particles

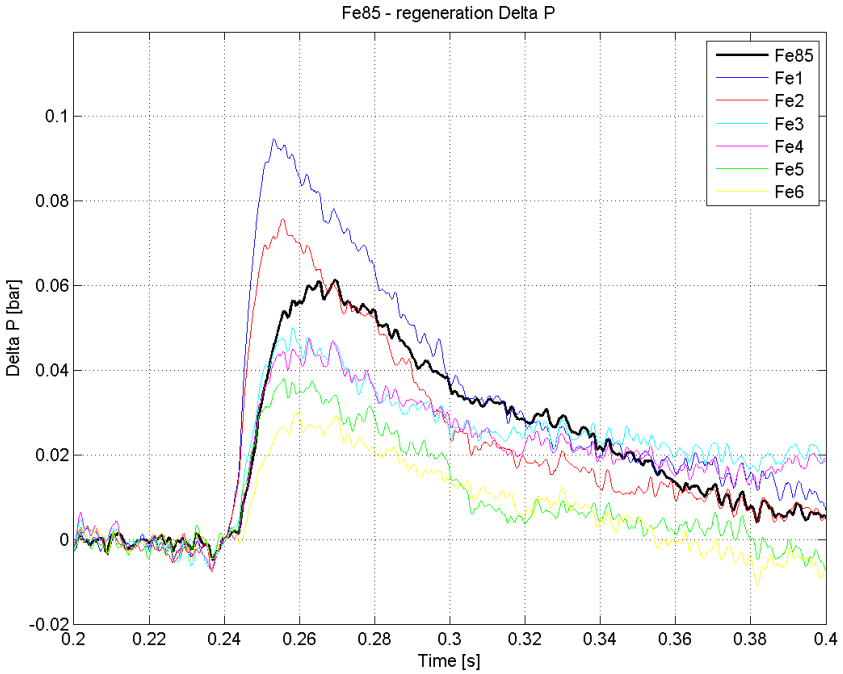

Figure 78: Comparison between ΔP generated by the combustion of Fe85 and regenerated particles

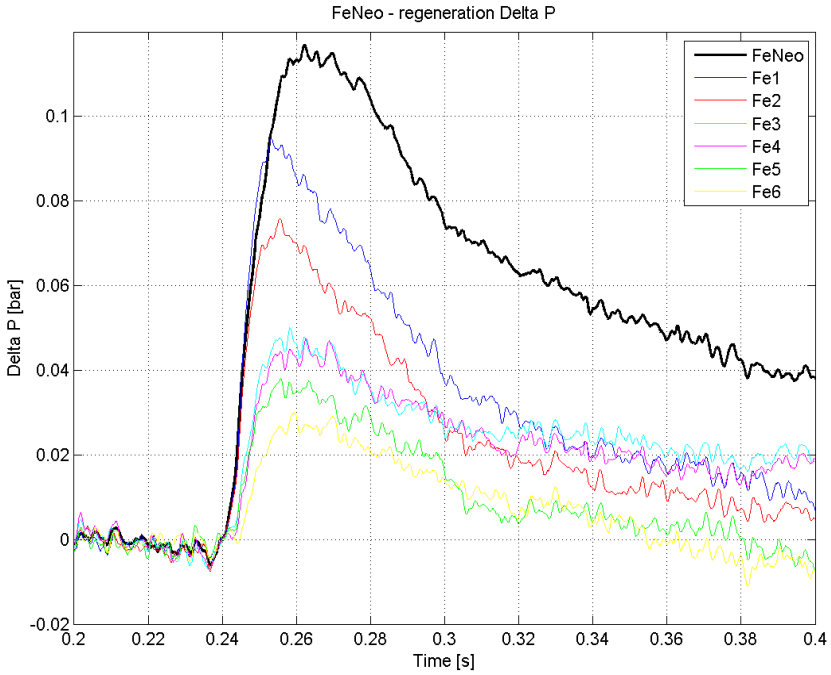

Figure 79: Comparison between ΔP generated by the combustion of Fe70 (Neo) and regenerated particles

These images pointed out that the use of Fe 85nm produced by NEO and Fe70 nm releases a peak higher than the regenerated particles; on the contrary, regarding to Fe25, Fe50 and Fe85 nm, the situation is different and the energy released by the particles is comparable with the regenerated ones.

8.4 Aluminum

8.4.1 Instantaneous and increment pressure

In the case of Aluminum, the nano-particles were regenerated only one time using the aforesaid scheme, so they come from no combusted nanoparticles. The tests are conducted always at 10 bar as initial pressure, but the temperature investigated is both 700 and 750ºC.
In fact, the tests at 700ºC showed that the new aluminum can perfectly burn, instead the commercial ones have problems in the combustion: in particular, both in the case of Al18 and Al85, a lot of tests have not been useful because the combustion didn't take place. In the image below It is possible to see the results, with the evident pressure increment reached by the new aluminum.

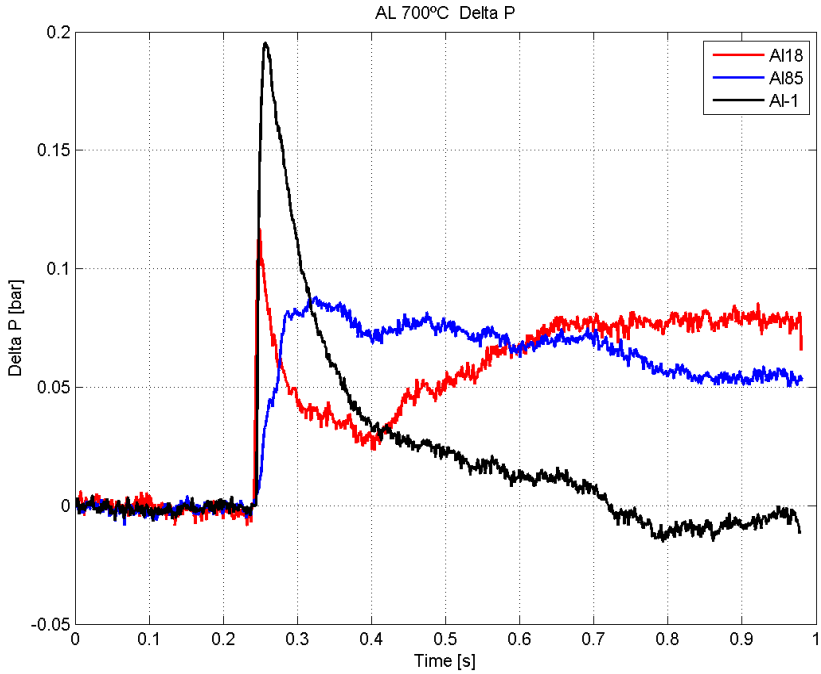

Figure 80: Comparison between ΔP produced by the combustion at 700°C for three different types of Aluminum: Al18, Al85 and Al-1, 'home-made' produced.

As it has just been explained above, the results for Al18 and Al85 should not be reliable because a lot of tests have to be done in order to register combustion phenomena.
For this reason, some tests with the new aluminum are performed also at 750ºC. In these operating conditions, appears that Al 85nm reaches evidently higher values than the same at 700ºC, instead the results of Al18 nm and also of regenerated one are more or less the same for both temperature.

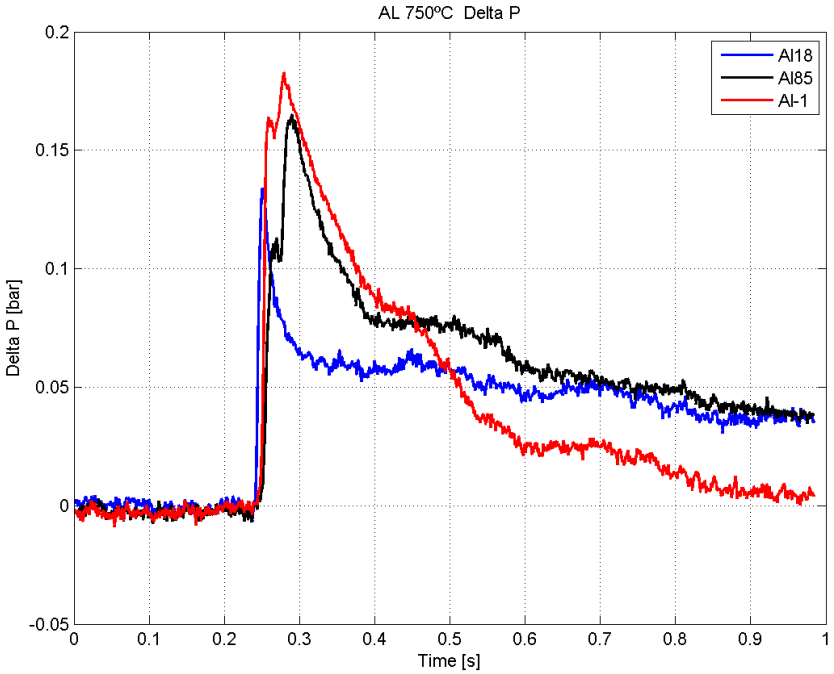

Figure 81: Comparison between ΔP produced by the combustion at 750°C for three different types of Aluminum: Al18, Al85 and Al-1, 'home-made' produced

Regarding these results, it seems that a higher temperature can produce a better combustion for commercial aluminum, instead for the regenerated one, the increment of temperature appears not so fundamental.
This aspect should be certainly investigated in the future, if there will be the possibility to use Aluminum as a metal fuel.

Chapter 9

Conclusions and future developments

In this chapter there is a summary of the achievements obtained in this work and, in general, in the COMETNANO project. Finally, a brief presentation of the possible future developments is reported.

9.1 Conclusions

At the end of this work it is possible to point out the aims reached and the problems found out in the whole during this study on metallic fuel for internal engine combustion.
We can finally make these considerations:

- The aluminum releases a greatest quantity of energy than Iron both in case of volumetric and weight energy (as shown in figure 10); this means that, with the same quantity of nano-particles or with the same volume, it can reach a higher pressure increment;
- Aluminum can burn without problems only with a temperature higher than 700ºC;
- Iron could be the most appropriate and reliable metal for a possible use as metallic fuel because it doesn't find problems in the combustion; on the contrary, for the combustion of commercial aluminum it is necessary create adequate operating conditions, first of all the temperature.
- Regarding iron, among the commercial nano-particles, Iron 50 nm shows the best attitudes: this means that particles with a diameter too small or too big are not suitable for the aim of this project, in accordance with the theory. Rather, the house-made nano-particles, with a diameter of 70nm, result the best ones: however, the different process used to created them

probably affects their structure and makes that one derived from NEO the best.

- Moreover, the combustion qualitative analysis suggests that the combustion of Iron is complete and affects the entire combustion chamber, as can be seen from the images, where the red color represents a complete combustion.
- Regarding emissions, the tests performed, demonstrated that the production of pollutants is small, also because the quantities investigated are little. In fact, with the increase of amount from 30 mg to 70 mg, emission average values raise. In particular, the analysis is concentrated in the presence of NO because the other components of NO_x are so small that the Horiba can't measure them with reliability.
- Another important consideration is the strong relationship between the production of NO and the combustion temperature: in fact, with temperature increase, the NO concentration is evidently higher.
- The combustion of aluminum produces higher values of emissions.
- Regarding the regeneration process, the investigation proved very interesting results: in fact, in the case of Iron, it was demonstrated that, after two regeneration cycles, the energy content of nano-particles evidently decreases so the use of regenerated powder looses its benefits. The causes of this trend must be found in the modification of nano-structuring after some cycles of combustion-regeneration, but also in the possibility that, each time the regeneration process takes place, not all the burnt particles are regenerated: for this reason, the energy content rapidly decreases.
- On the contrary, the Aluminum investigated is generated from no combusted particles, with a process explained in the last chapter: the results show that it performs the best attitudes in the combustion process in comparison with the commercial aluminum, both with an ambient of 700 and 750ºC. However, the results of commercial aluminum are not so reliable because their combustion seemed to be difficult.

9.2 Future developments

This project gave important and interesting information regarding the possibility to use metallic fuel in an internal combustion engine. However, findings are very preliminary and there are not actual evidences regarding the possibility to apply this technique to a real engine. Of course, in general the three years of investigation, and also the last six months, proved that the best choice between the metals is represented by Iron.

However, other studies will be done in order to completely understand the importance of particle diameter and how this parameter can influence the combustion process. Moreover, it was demonstrated that the commercial powders had worse attitudes in comparison with the ones produced by the partners: so it will be important to investigate the reasons of this different behavior and if the production of nano-particles with better characteristics is more convenient than the use of commercial ones.
Another interesting aspect that will be investigated is connected to the regeneration process: in particular, it is necessary to study in deep how the process affects the nano-structuring and how it is possible to eliminate any influences. In fact, the idea of regenerated nano-particles is certainly innovative and allows to reduce the productions of waste material: however, this aspect needs to be improved because if the combustion-regeneration cycle is useful only two times, the benefits of the regeneration are not so evident.
Finally, for the project in general, certainly it is important to continue to investigate the injection and collection system in order to make this work suitable for a real application, because the use of nano-powders as fuel makes it necessary to carry out important changes into the internal combustion engine.

Acronyms and Symbols

ICEs	Internal Combustion Engines
Al	Aluminum
Fe	Ferodium
AlN	Aluminum Nitride
TEM	Transmission Electron Microscopy
CFD	Computational Fluid Dynamics
APPS	Average Primary Particle Size
B	Boron
ASP	Aerosol Spray Pyrolysis
APS	Atmospheric Plasma Spraying
HRR	Heat release rate
XRD	X-ray Diffraction
TGA	ThermoGravimetric Analysis
GHSV	Gas Hourly Space Velocity
NO	Nitrogen Oxides

P	Pressure
T	Temperature
K	Kelvin
ρ_m	Specific density
Q	Heat of combustion
V_m	Volume of the nano-particle
S_m	Nano-particle surface area
T_b	Combustion temperature
f	Geometric factor determined by the shape of the cluster
h_c	Convective heat transfer coefficient
σ	Boltzmann's constant
ε	Emissivity
r	Radius of particle
T_a	Air temperature
E	Activation energy

R	Universal gas constant
P_a	Air Pressure
K_n	Knudsen Number
t	Time
m,n	Effect of the oxidizer pressure and oxide thickness on the oxidation law
h	Thickness of the oxidation film
C	*C*oncentration
w_o	Diffusion of oxygen
D	Diffusion coefficient
v_{ox}	Velocity of oxygen
c	Concentration of oxygen in the oxide shell
cv_{ox}	Convective flux of oxygen
V_o	Oxygen solubility in the oxide shell
$\varepsilon_{\lambda i}$	Spectral emissivity of the particle
c	Speed of light
h	Planck's constant
k_B	Bolzmann's constant
Q_{abs}	Absorption coefficient
C_{abs}	Absorption cross section
d_p	Particle diameter
µm	Micron
Ar	Argon
px	Pixel
Fps	Frame per second
Ppm	Particle per million
ΔP	Pressure Gradient
n_o	Surrounding refractive index
$\vec{x}$	Ray direction in an orthonormal basis ($\vec{x}$,$\vec{y}$)
ε_y	Refractive angle
L	Path length
P_{ins}	Instantaneous Pressure

Bibliography

[1] Internal report available on www.cometnano.org

[2] D.B.Beach, A.J.Rondinone, B.G.Sumpter, S.D. Labinov, R.K.Richards, "*Solid-State Combustion of Metallic Nanoparticles: New Possibilities for an alternative Energy Carrier*", Journal of Energy resources Technology, March 2007, pp. 29-32.

[3] A. Rai, K. Park, L. Zhou, M.R. Zacharia, ''*Understanding the mechanism of aluminium nanoparticle oxidation. Comb.Theory and Modelling'',* 2006, pp.843–859.

[4] P. Puri, V. Yang, "*Multi-Scale Modeling of Nano Aluminum Particle Ignition and Combustion*" Presented at 2007 MURI NEEM Program Review.

[5] Santiago Alberto Molina Alcaide, "*Estudio de la influencia de los parámetros de inyección y la recirculación de gases de escape sobre el proceso de combustión, las prestaciones y las emisiones de un motor diesel de 1.8 litros de cilindrata*", Tesis Doctoral, Valencia, 2003, pp 68-76.

[6] G. Lavoie, J. Heywood, J. Keck, "*Experimental and theoretical study of nitric oxide formation in internal combustion engines*", Combust. Sci. and Technology Vol. 1,1970, pp 313-326.

[7] G.S. Settles, "*Schlieren and shadowgraph tecniques*", Ed. Springer.

[8] J.V. Pastor, R. Payri, J.M. García-Oliver, J.-G. Nerva, "*Schlieren measurements of transient ECN-Spray A penetration under inert and reacting conditions*", SAE international, 2011, 12PFL-0354.

[9] M. A. Trunov, M. Schoenitz, E. L. Dreizin, "*Ignition of Aluminum Powders Under Different Experimental Conditions*", Propellants, Explosives, Pyrotechnics 30 (2005), No. 1. DOI: 10.1002/prep.200400083.

[10] George Karagiannakis, Harry Mandilas, Athanasios Konstandopoulos, Carlo Beatrice, Maurizio Lazzaro, Natale Rispoli, Jose V. Pastor, Edèn ROS, Santiago Molina, "*Determination of Oxidation Characteristics and studies on the feasibility of Metallic nanoparticles combustion under ICE-like conditions*", Sae International, 11 September 2011.

[11] Richard A. Yetter, Grant A. Risha, Steven F. Son, "*Metal Particle combustion and Nanotechnology*", USA, Ed. Elsevier, 2009, pp. 1819-1838.

[12] P.Escot Bocanegra, D. Davidenko, V. Sarou-Kanian, C. Chauveau, I. Gokalp, " *Experimental and numerical studies on the burning of aluminum micro and nanoparticles clouds in air*", Experimental Thermal and Fluid Science, ed. Elsevier, 2010, pp. 299-307.

[13] Mikhaylo A. Trunov, Swati M. Umbrajkar, Mirko Schoenitz, Joseph T. Mang, Edward L. Dreizin, "*Oxidation and melting of Aluminum nanopowders*", Ed. American Chemical Society, 2006, pp. 13094 – 13099.

[14] A. Ermoline, E. L. Dreizin, "*Equations for the Cabrera–Mott kinetics of oxidation for spherical nanoparticles*", Chemical Physics Letters 505 (2011) 47–50. DOI: 10.1016/j.expthermflusci.2009.10.009.

[15] Young-Soon Kwon, Alexander A.Gromov, Alexander P. Ilyin, Elena M. Popenko, Geun-Hie Rim, " *The Mechanism of combustion of superfine aluminum powders*", Combustion and Flame, Ed. Elsevier, 2003, pp. 385-391.

[16] Ying Huang, Grant A. Risha, Vigor Yang, Richard A. Yetter, " *Combustion of bimodal nano/micron-sized aluminum particle dust in air*", The Pennsylvania State University, USA, Science Direct, ed. Elsevier, 2007, pp. 2001-2009.

[17] Ying Huang, grant A. Risha, Vigor Yang, Richard A. Yetter, "*Effect of particle size on combustion of aluminum particle dust in air*", Combustion and Flame, ed. Elsevier, 2009, pp. 5-13.